Constrained Linear and Non-Linear Adaptive Equalization Techniques for MIMO-CDMA Systems

By

Khalid Mahmood

ID # P09052908

This thesis is submitted in partial fulfillment

of the requirements of De Montfort University

for the award of Doctor of Philosophy

Emerging Technologies Research Center (EMTERC)

De Montfort University, Leicester

December, 2013

Declaration

This thesis is a presentation of my original research work. Wherever contributions of others are involved, every effort is made to indicate this clearly, with due reference to the literature, and acknowledgement of collaborative research and discussions.

KHALID MAHMOOD

April 03, 2014

Acknowledgments

In the name of Allah, The Most Gracious, The Most Merciful. All praise and glory is for Allah (SubhanahuWa Ta'aala) who gave me the strength and determination to undertake this work. My utmost gratitude towards De Montfort University for my admittance to this prestigious institute. My heartfelt gratitude and appreciation to my adviser, Dr. Shahshi Paul for his support and guidance. His attention and devotion to my research work, with valuable suggestions, was the impetus that led to the completion of this work. My co-adviser Professor Raouf Hamzaoui also provided valuable feedback which has been incorporated in this research work.

I highly appreciate Dr. Moin Uddin's guidance during my research. I would specially mention my colleague Syed Asad Afatb, for his support and guidance. Asad's contribution towards this research work will never be forgotten. Last but not the least, I would like to thank my wife Unbereen Shafi and my children, Duaa, Ahmad, Raania and little Awad who were very patient with me during my stressful times.

Abstract

Researchers have shown that by combining multiple input multiple output (MIMO) techniques with CDMA then higher gains in capacity, reliability and data transmission speed can be attained. But a major drawback of MIMO-CDMA systems is multiple access interference (MAI) which can reduce the capacity and increase the bit error rate (BER), so statistical analysis of MAI becomes a very important factor in the performance analysis of these systems. In this thesis, a detailed analysis of MAI is performed for binary phase-shift keying (BPSK) signals with random signature sequence in Raleigh fading environment and closed from expressions for the probability density function of MAI and MAI with noise are derived. Further, probability of error is derived for the maximum Likelihood receiver. These derivations are verified through simulations and are found to reinforce the theoretical results. Since the performance of MIMO suffers significantly from MAI and inter-symbol interference (ISI), equalization is needed to mitigate these effects. It is well known from the theory of constrained optimization that the learning speed of any adaptive filtering algorithm can be increased by adding a constraint to it, as in the case of the normalized least mean squared (NLMS) algorithm. Thus, in this work both linear and non-linear decision feedback (DFE) equalizers for MIMO systems with least mean square (LMS) based constrained stochastic gradient algorithm have been designed. More specifically, an LMS algorithm has been developed , which was equipped with the knowledge of number of users, spreading sequence (SS) length, additive noise variance as well as MAI with noise (new constraint) and is named MIMO-CDMA MAI with noise constrained (MNCLMS) algorithm. Convergence and tracking analysis of the proposed algorithm are carried out in the scenario of interference and noise limited systems, and simulation results are presented to com-

pare the performance of MIMO-CDMA MNCLMS algorithm with other adaptive algorithms.

Contents

List of Figures

List of Tables

Nomenclature

$\bar{\lambda}_n^l$	Mean Lagrangian multiplier
$\bar{\mathbf{v}}_n^l$	Expected value of weight error vector
$\bar{\mu}_m^l$	Mean step size
$\bar{\nu}_n^l$	Filtered noise which passes through feed forward filter
ϵ_i	Channel attenuation
$\Gamma(a, x; b)$	Generalized incomplete Gamma function
$\hat{x}_n$	Desired response
κ	Eigenvalue
κ_{max}	Maximum eigenvalue
κ_{min}	Minimum eigenvalue
$\mathbf{v}_n^l$	Weight error vector
$\mathbf{w}_{n(opt)}$	Optimum value of weight
$\mathbf{w}_n^l$	Impulse filter response of the decision feedback equalizer
$\mathbf{w}_n^l$	Weight of the FFF and FBF
$\mathbf{x}_n^l$	Input process

$\mathcal{F}^{-1}$	Inverse Fourier transform
Ω	Symmetric positive definite weighting matrix
$\overline{\vartheta_z}$	Average signal to noise ratio
$\Phi_P(\omega)$	Characteristic function of U_m^l and is the product of N characteristic functions of independent random variables U_m^l
$\Phi_{U_m^l}(\omega)$	Characteristic function of the random variable U_m^l
$\rho_l^{k,j}$	cross-correlation between the signature sequences of subscribers j and k for the l^{th} symbol
σ_ϵ^2	Variance of channel attenuation
$\tilde{R}$	Auto correlation matrix
ϑ_z	Random variable
ξ_∞	Steady state EMSE
A^k	Transmitted amplitude of the k^{th} subscriber
B_n^l	n^{th} MISO feedback filter (FBF)
D_n^l	Combined input to the DFE
$E[h_{mn}]$	Expexted value of channel impulse response
e_{an}^Ω	Weighted a priori error
E_b	Energy per bit
e_n^l	Error between the output of the decision device and the DFE
e_{pn}^Ω	Weighted a posteriori error
$erfc$	Error complement function

$f\left(e_n^l\right)$	General scalar function of the output estimation error
F_n^l	n^{th} MISO feed forward filter (FFF)
$f_{U_m^l}(u)$	PDF of MAI
h_{mn}^l	Envelop of the complex channel for the l^{th} symbol
$H_{mn}^l(t)$	Complex impulse response of Rayleigh channel
$I^{l,k}$	Output of the matched filter
$I^{l,k}$	Random variable
$J\left(\mathbf{w}_n^l\right)$	Cost function to be minimized
M	Number of receiving antenna
M	Taps of feed froward filter (FFF)
N	Number of transmit antenna
Q	Taps of feedback filter (FBF)
$r_m(t)$	Observed signal at the mth receiver
R_{yy}	Auto correlation matrix of input to the FFF
$s_n^{l,k}(t)$	Rectangular signature waveform
T_b	Bit period
T_c	Chip interval
Tr	Trace operator
U_m^l	MAI at the m^{th} receiver for the l^{th} symbol
$w_{m,i}^l$	Desired signal

Z_m^l	$U_m^l + \nu_m$
AWGN	Additive white Gaussian noise
BER	Bit error rate
CDMA	Code division multi access
CF	Characteristic function
CIR	Channel impulse response
CSI	Channel state information
DFE	Decesion feedback equalizer
DS-SSMA	Direct sequence spread spectrum multi access
DSP	Digital signal processor
EMSE	Excess mean square error
ETP	Equal transmitted powers
FBF	Feedforward filter
FDMA	Frequency division multi acces
FFF	Feedforward filter
FIR	Finite impulse response
IGA	Improved Gaussian approximation
ISI	Intersymbol interference
K	Number of subscribers
KFG	Fast Kalman gain

LBER Adaptive least bit error rate

LE Linear equalizer

MAI MUltiple access interference

MBER Minimum bit error rate

MIMO Multiple input-multiple output

ML Maximum Likelihood

MMSE Minimum mean suare error

MNCLMS Multiple access interference plus noise constrained LMS

MSE Mean squared error

MUD Multi user detection

NC-VSLMS Noise constrained variable step size LMS

NCLMS Noise constrained LMS

NLMF Normalized least mean fourth

OFDM Orthognal frequency division multiplexing

PBSK Binary phase-shift keying

PCS Polycyclostationary

pdf Probability density function

PIC Parallel interference cancellation

RLS Recursive least square

SGA Standard Gaussian approximation

SIC Successive interference cancellation

SISO Single input-single output

SNR Signal to noise ratio

SSMA Spread spectrum multi access

TDMA Time division multi acces

UTP Unequal transmitted powers

ZF-DFE zero-forcing decesion feedback equalizer

ACI Adjacent channel interference

BRS Baud rate sampler

CCI Co-channel interference

CP-LMS Complementory pair LMS

FSES Fractionally spaced equalizer

MS-DFE Multi split decesion feedback equalizer

MSD Mean square deviation

SCD Spectral correlation density

SER Ultra wide band

VLMS Variable step size algorithm

Chapter 1

Introduction

There has been a tremendous growth seen in the wireless mobile communication systems since the end of the last century. Communication systems which were once providing the traditional service of voice to a limited number of subscribers are now dealing with increasing numbers of subscribers and a shift of demand from just "voice" to higher data rate services. This led to an exponential increase in system capacity and spectral efficiency requirements. As bandwidth is limited, this demand in high capacity has to be provided by an efficient use of existing frequency bands and channel conditions. One of the techniques, which can provide the required increase in system capacity and enhanced performance is the use of multiple antennas at transmitting as well as at receiving end [1]. This is referred to as multiple-input multiple-output (MIMO) wireless system. MIMO technique is being used in the third generation and beyond mobile systems [2].

MIMO is an antenna technology for wireless communications which utilizes multiple antennas at the source (transmitter) and the destination (receiver) to enhance the communication system performance by increasing the system capacity and spectral efficiency. MIMO configuration can be done in many ways for example a 3×3 MIMO configuration consists of 3 signal transmitting antennas (base Station) with three antennas for receiving signal (mobile terminal). The antennas at each end

of the communications system are combined to minimize errors and optimize data speed.

The object of modern communication system is to provide higher, reliable and secure transmission of data to ever increasing number of subscribers demand. Code division multiple access (CDMA) is one of the communication schemes which allows multiple subscribers to use a single radio channel at the same time with little interference and much higher security. In spite of its numerous advantages, CDMA system suffers from MAI problem which arises due to nonzero cross-correlation in the spreading codes of different subscribers [3]. This can lead to an increased bit error rate (BER). So, statistical analysis of MAI becomes very important factor in analyzing the performance of this system.

Researchers have shown that by combining MIMO techniques with CDMA system higher gains in capacity, reliability and data transmission speed can be attained [4–8]. Such MIMO-CDMA systems have outperformed the SISO-CDMA systems but both are prone to MAI.

In most digital data transmission systems the dispersive linear channel exhibits amplitude and phase distortion. As a result, the received signal is contaminated by ISI. In a system, which transmits a sequence of pulse-shaped information symbols, the time domain full response signaling pulses are smeared by the hostile dispersive channel, resulting in ISI. At the receiver, the linearly distorted signal has to be equalized in order to recover the information.

The equalizers that are utilized to compensate for the ISI can be classified according to their structure, the optimizing criterion and the algorithms used to adapt the equalizer coefficients. On the basis of their structures, equalizers can be classified as linear or decision feedback equalizers.

The learning speed of an adaptive algorithm can be increased if partial knowledge of the channel is incorporated in the design of an adaptive algorithm. Since MAI is a limiting factor in MIMO-CDMA systems, there is a need for deriving the probability

density functions (pdf) of MAI and noise and then use it as a constraint to develop an algorithm for MIMO-CDMA systems.

1.1 Multiple Input-Multiple Output (MIMO) Systems

The need for MIMO systems arrived due to certain performance drawbacks in SISO (single input, single output) technology used in conventional wireless communication systems [9]. In SISO, a single antenna is used at the transmitter, and another single antenna is used at the receiver. In some cases, this creates certain problems with multipath effects. When the transmitted signal is obstructed by hills, buildings or utility wires and towers, the wavefront become scattered, and as such can take numerous paths to reach its destination. This late arrival of scattered portions of the signal creates problems such as fading, cut-out and intermittent reception (picket fencing). Another drawback of SISO can be seen in digital communications systems such as wireless Internet, where the use of this technology has created reduction in data speed as well as increased error propagation. The use of two or more antennas, together with the transmission of multiple signals (one for each antenna) at transmitter and receiver, not only eliminates the problems created by multipath wave propagation,but also can take advantage of this effect and it is achieved by applying an algorithm or a signal processing technique at the receiver to sort out the multiple signals and produce a signal that has the required transmitted data. MIMO technology is finding application in digital communication because of its certain applications in digital television (DTV), wireless local area networks (WLANs), metropolitan area networks (MANs), and mobile communications. A block diagram of MIMO system is shown in figure 1.1.

The MIMO system shown in the figure 1.1 is made up of N transmitting antennas and M receiving antennas. By utilizing the same channel, every receiving

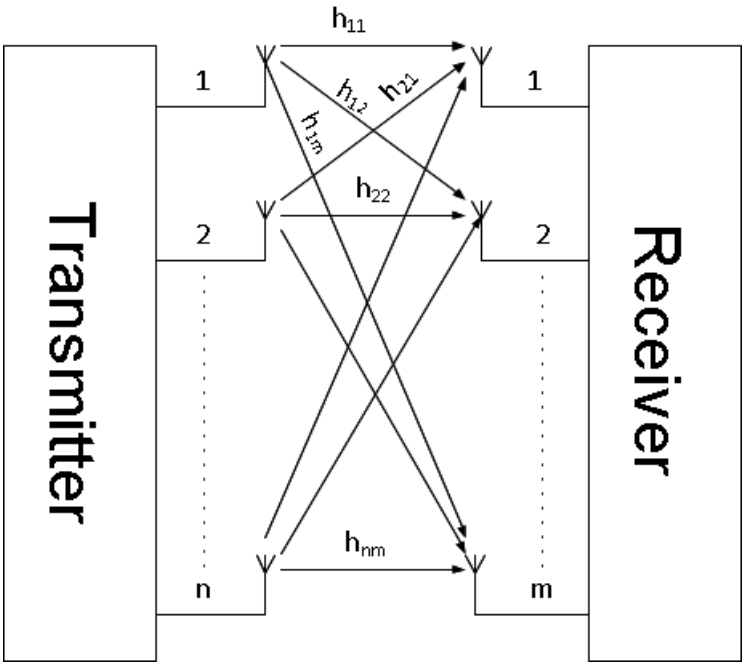

Figure 1.1: A Block Diagram of MIMO Systems

antenna is receiving the direct component as well as the indirect components from the transmitters which are intended for the other receivers. For example, h_{11} represents the direct connection between the transmitter number 1 and the receiver number 1. In this way, a transmission matrix H of $N \times M$ can be shown to be

$$H = \begin{bmatrix} h_{11} & h_{12} & \dots & h_{1n} \\ h_{21} & h_{22} & \dots & h_{2n} \\ \vdots & \vdots & \vdots & \vdots \\ h_{m1} & h_{m2} & \dots & h_{mn} \end{bmatrix} \tag{1.1.1}$$

If $\mathbf{x}$ is considered to be the input vector and $\mathbf{y}$ to be the receiving vector, then the output vector y under additive noise ν would be

$$\mathbf{y} = H\mathbf{x} + \nu \tag{1.1.2}$$

1.2 Code Division Multiple Access (CDMA)

CDMA is one of the communication schemes which allow multiple subscribers to use a single radio channel at the same time with little interference. A block diagram of CDMA system is shown in figure 1.2. Multiple-access capability in CDMA system is accomplished by means of pseudo noise (PN) codes. Every subscriber in this system is allocated a unique code sequence which is being used to encode that subscriber's information signal. At the receiving end, knowing the code sequence of the each subscriber, receiver decodes the received signal and recovers the original signal. Since bandwidth of the code signal is much larger than the bandwidth of the information signal, the encoding process spreads the spectrum whereas despreading is achieved by correlating the received spread signal with a synchronized replica of the spreading code signal. These spreading codes are independent of each other as well as input process.

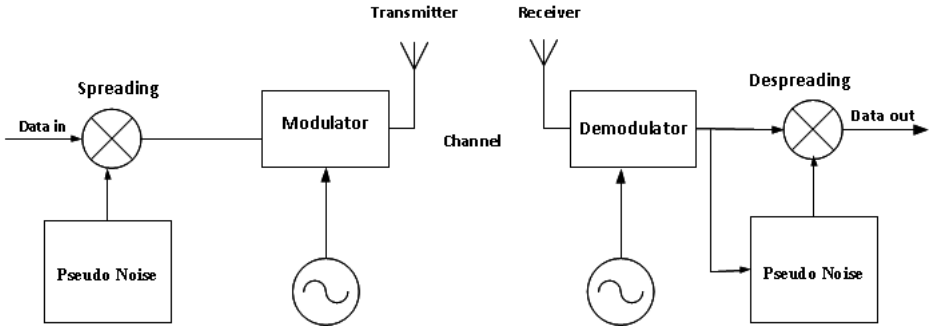

Figure 1.2: A block diagram of CDMA system

Some of the distinguishing features of CDMA systems are

- **Usage of wide bandwidth**: Just like other spread spectrum techniques, CDMA, also utilizes wider bandwidth than is normally required. The use of a wider bandwidth results in the increased security for signal and immunity to interception or jamming.

- **Use of spreading codes:** Bandwidth is increased by spreading the information signal with the help of codes and these codes are independent of the

information signal.

- **Enhanced level of security:** The spreading code must be known at the receiving end to decode the transmitted signal otherwise, it would be very difficult if not impossible to detect the transmitted signal. This feature of CDMA results in very high level of security

- **Multiple access:** Each subscriber is assigned a unique spreading code and these codes are independent of each other. By using these unique codes together with synchronous reception permits multiple subscribers to access the same channel simultaneously.

Some of the advantages of CDMA system are

- CDMA system has the ability of using signals which arrive in the receiver having different time delays. This is refereed to as multipath phenomena. Being narrow band systems, frequency-division multiple access (FDMA) and time division multiple access (TDMA), are not able to discriminate between the multipath signals arrival, and as such need equalization to get rid of the negative effects of multipath. On the other hand due to its wide bandwidth, CDMA systems use multipath signals and combine these signals to get a stronger signal at the receiving end.

- In FDMA and TDMA schemes, maximum number of subscribers is fixed and once that maximum number of subscribers is reached, new subscribers may not be accommodated,where as CDMA system may allow more subscribers with some background noise.

- Less timing organization as compared to TDMA, ISI as well as co-channel interference (CCI) are not as severe as is the case in TDMA [10].

- To maintain a required temporal order among symbols, a complicated system organization must be employed in TDMA, but such a complicated system is

not required in CDMA [10].

1.3 MIMO-CDMA Systems

Researchers have shown that by combining MIMO techniques with CDMA system, higher gains in capacity, reliability and data transmission speed can be attained [4–8]. This is realized by the spatial diversity of multiple antennas at the transmitting end as well as at the receiving end resulting in added degrees of freedom when complex channel gains between different transmitting and receiving antenna pairs are adequately uncorrelated. MIMO-CDMA systems are more robust to MAI as compared to SISO DS-CDMA. In fact MIMO-CDMA is a promising communication scheme allowing faster data speed multimedia services and web browsing [11]. Combining MIMO and CDMA can further improve the system transmission rate over the traditional CDMA system [12]. A block diagram of a typical MIMO-CDMA is given in figure 1.3 .

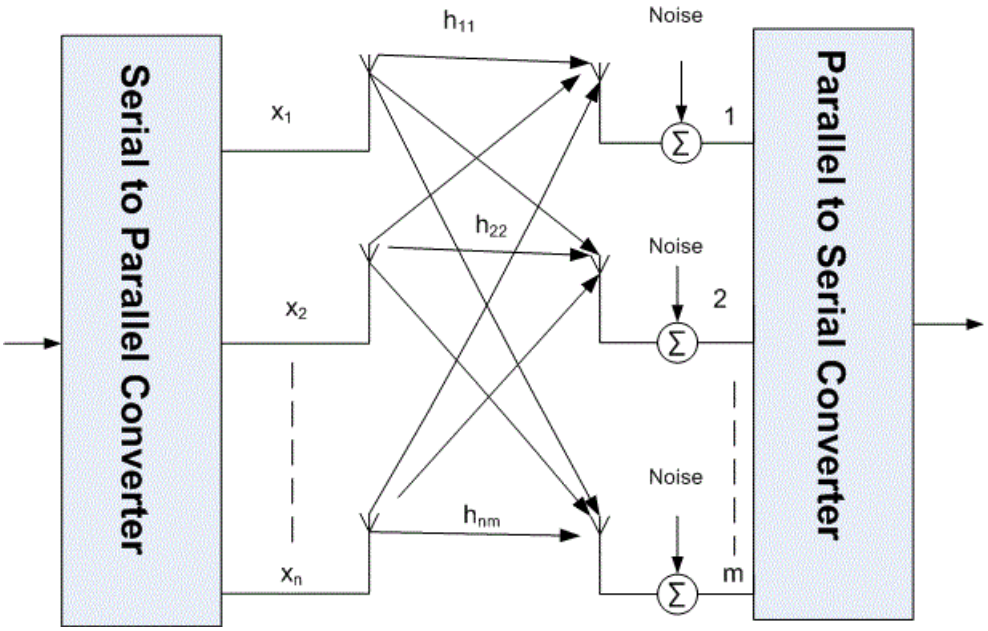

Figure 1.3: Block diagram of MIMO-CDMA system

1.4 Adaptive Equalization Techniques

All signals while passing through a channel undergo a certain amount of time dispersion since frequency response of that channel does not have constant magnitude and linear phase. Due to this phenomena, tails of adjacent pulses interfere with the measurement of current pulse (ISI) which can lead to an incorrect decision by the receiver. Equalization techniques are used to avoid this problem. Equalization is the process of adjusting the relative phases of different frequencies in order to achieve a constant group delay.

The equalizers that are utilized to compensate for the ISI can be classified according to their structure, the optimizing criterion and the algorithms used to adapt the equalizer coefficients. On the basis of their structures, the equalizers can be classified as linear or non linear (decision feedback) equalizers.

Equalizers can also be distinguished on the basis of the criterion used to optimize their coefficients. The optimization is governed by the performance criteria used. For example, when applying the mean square error (MSE) criterion, the equalizer is optimized such that the mean squared error between the distorted signal and the actual transmitted signal is minimized. A range of adaptive algorithms can be invoked, in order to provide the equalizer the means of adapting its coefficients to the time-varying dispersive channels.

1.4.1 Linear Equalization (LE)

In most digital data transmission systems the dispersive linear channel encountered exhibits amplitude and phase distortion due to which the received signal is affected by ISI. Systems in which a sequence of pulse-shaped information symbols are transmitted, the time domain full response signaling pulses are distorted by the hostile dispersive channel which leads to the inter symbol interference. At the receiver, the linearly distorted signal has to be equalized to recover the information. Linear

equalizers are used to mitigate the effect of ISI by learning the behavior of the channel and inverse its effect. linear equalizer (LE) can be termed as inverse modeling filter in broader sense due to the fact that linear equalizer works as inverse of a channel. Linear equalizers are used in the communication systems, where ISI is not severe [13]. As can be seen in the figure it consists of a feed forward filter which is fed only with present and future received signal samples, implying that no latency is inflicted. As a result of this, the feed forward filter eliminates only the pre-cursor ISI, but not the post-cursor ISI [14].

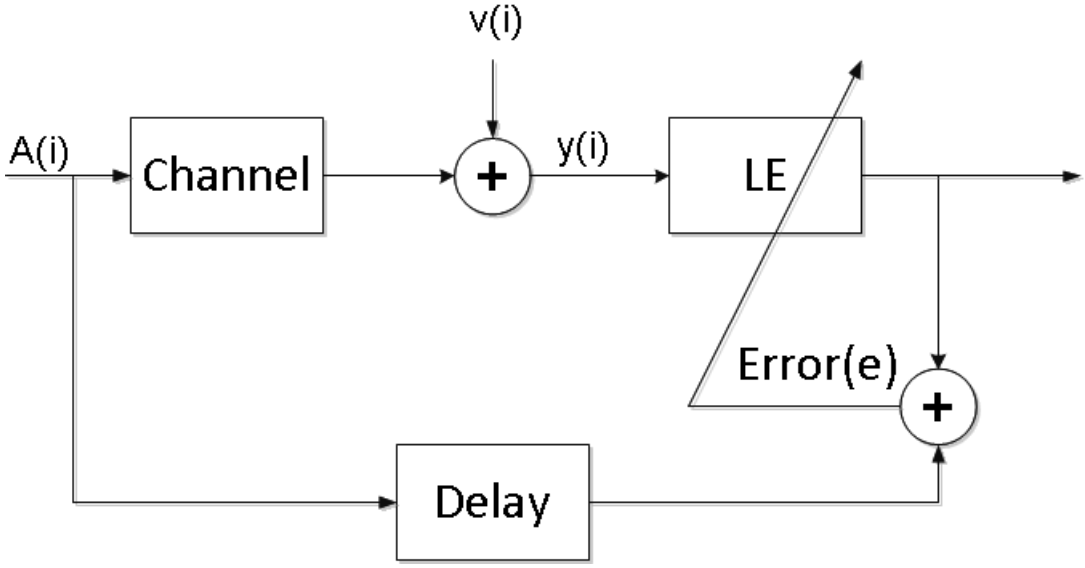

Figure 1.4: Block diagram of Linear Transverse Equalizer

1.4.2 Decision Feedback Equalization (DFE)

The development of the DFE was initiated by the idea of using previous detected symbols to compensate for the ISI in a dispersive channel. DFE offers the potential for improved performance over the LE while maintaining comparable complexity. Reliable transmission of information at the highest possible data rates is the desired goal of digital communication system. However one of the most important obstacle in achieving this goal of maximum efficiency is ISI caused by the communication channel [15]. ISI refers to the effect of neighboring symbols on the current symbol

and if not mitigated properly it can lead to high BER in the recovery of the transmitted sequence at the receiver.Various methods have been developed to enhance the performance of the communication systems by reducing the effects of the ISI. Linear equalization is one of the methods employed but a major problem with linear equalization is that it doesn't takes in to account the fact that the transmitted sequence has a "finite alphabet" structure. To overcome this drawback of linear equalization, DFE was proposed [15]. DFE uses previous decisions to improve the equalizer performance. Almost all the techniques proposed for equalization make some assumptions about the underlying characteristics of the disturbance signals and the structure of the communication channel model. In many cases where true information about the channel is not available, algorithms have to be used for the correct estimation of the model parameters. For example, in mobile communications the channel parameters are normally estimated by using the training sequences. The time variations in these parameters also necessitate the need for tracking them . The errors due to tracking is another point of concern. These concerns bring forward, the question of robustness, that is, whether the small variations from the true model, and small disturbances, can cause large degradations in the performances of the algorithms using these parameters.

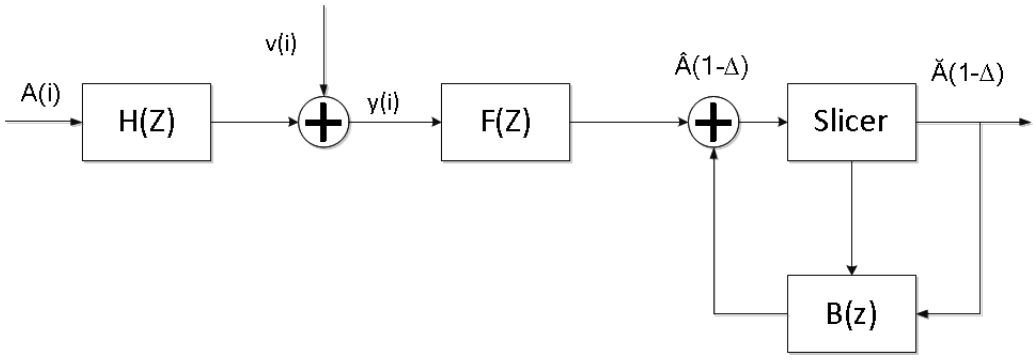

Figure 1.5: Block diagram of Decision Feedback Equalizer

Figure 1.5 shows a simplified block diagram of a DFE where the forward filter and the feedback filter can each be a linear filter, such as transverse filter.The nonlinear characteristic of the DFE is due to the nonlinear characteristic of the

detector which is used to provide input to the feedback filter.The basic idea of a DFE is that if the values of the symbols previously detected are known, then ISI caused by these symbols can be mitigated at the output of the forward filter by subtracting previous symbol values with appropriate weighting. The feed forward and feedback tap weights can be adjusted simultaneously to fulfill a criterion such as minimizing the MSE. The advantage of a DFE structure is the feedback filter,which is additionally working to remove ISI, operates on noiseless quantized levels resulting in an output which is free of channel noise.

1.5 Literature Review

1.5.1 Statistical Analysis of Multiple access Interference (MAI) in MIMO-CDMA Systems

In spite of its numerous advantages, a major drawback of MIMO-CDMA systems is MAI which can reduce the capacity as well as BER resulting in a degraded communication system, so statistical analysis of MAI becomes very important factor to analyze the performance of these systems .

In CDMA systems, each subscriber is assigned a unique orthogonal spreading code. These orthogonal codes should ideally provide perfect isolation from the other subscribers to maintain error free communication between respective subscribers but in reality the orthogonality between these codes is very difficult to preserve due to asynchronism and channel delay spread at the receiving end. Asynchronism and channel delay spread exist on the up link while channel delay spread can be seen on the down link of the channel. Correlation receiver cannot perfectly separate the signals for the multiple subscribers. This phenomena leads to what is called MAI causing a system performance degradation, which may render the system useless for even moderate subscriber loads with equal power received from each subscriber.

Most of the research work has been done on the characterization of SISO-CDMA

systems and was based on approximate derivations,such as, standard Gaussian approximation (SGA) [16] , improved Gaussian approximation (IGA) [17] and simplified IGA (SIGA) [18]. Central limit theorem was applied in SGA to get an approximate sum of an additive white Gaussian noise process (AWGNP). This method is widely used because of its ease of application but a major drawback of SGA is that it overestimates the system performance and this problem becomes severe when the number of subscribers is less [17]. The Standard Hermite polynomial error correction method [19] was employed to improve the accuracy of SGA. The conditional characteristic function of MAI and bounds on the error probability were derived for binary direct-sequence spread-spectrum multiple access (DS/SSMA) systems. This method was named the improved Gaussian approximation (IGA) [20]. In case when the number of subscriber is small, IGA has outperformed the SGA [17] but the increased computational complexity is a major limitation of this method. IGA was further simplified and was named simplified IGA (SIGA) [21]

Another approach is to perform the BER of a spread spectrum multiple access (SSMA) system without the knowledge or assumption about MAI. Most of these techniques are basically an extension of previously studied ISI. Some of these techniques include moment space method [22], characteristic function method [23], moments method [24], and the approximate Fourier series method [25]. It has been noted that these techniques are superior to the central limit theorem based techniques in approximating BER but with higher computational costs. SNR of Rician fading channels at the correlator receiver's output was performed [26]. The BER performance of DS-CDMA system in frequency non selective Rayleigh fading channel for deterministic sequences using SGA approach was evaluated by [27], whereas [23] utilized the characteristic function (CF) technique to assess the performance of SSMA scheme in an AWGN environment. The characteristic function (CF) method to evaluate the performance of DS-SSMA scheme on multiptah fading channels with multipath ISI was applied in [28] but MAI was ignored. An approximate Fourier se-

ries technique [25,29] was utilized to evaluate the BER performance of selective and non selective Rayleigh fading environment. System degradation caused by imperfect chip and phase synchronization were also assessed in this technique.

For a given signal to noise ratio, BER dependency on number of subscribers was analyzed by [30]. A closed form expression for the characteristic function of MAI for asynchronous operation in Rayleigh fading environment was derived. Conditional characteristic function of MAI together with bounds on probability error rate for DS-SSMA scheme were also obtained [30]. Average probability of error at correlation receiver's output for binary as well as quaternary synchronous and asynchronous DS-SSMA schemes which use random signature sequence was derived in [31]

Probability density function of MAI for synchronous down link CDMA scheme in an AWGN case was derived and the results were then used to derive the conditional probability density function of MAI , inter carrier interference and noise in multi carrier CDMA scheme provided that fading environment was known [32].

A new unified approach to MAI analysis in fading environmrents was presented [33], assuming that the channel phase is either known or has perfectly been estimated. Random behavior of the channel fading was also included to get the realistic results for the pdf of MAI together with noise.

Due to the computational complexities in the statistical analysis of MAI in MIMO-CDMA systems, considerable work is not found in the literature. So instead of accurate statistical analysis of MAI, researchers have either used some strong assumptions for example, Gaussian assumption for interference in MIMO system [34] or suboptimal approaches to detect the subscriber without involving the need for MAI statistics such as successive interference cancellation (SIC) [35] and parallel interference cancellation (PIC). MAI was analyzed and approximated as Gaussian distribution [36] for fading channel in MIMO case. In contrast to the existing works, an exact characterization of MAI in Rayleigh fading environment is developed for MIMO-CDMA systems in this thesis. Consequently, explicit closed-form expression

for both the probability density functions (pdfs) of MAI and MAI plus noise is derived for Rayleigh fading channel.

1.5.2 Equalization in Multiple Input Multiple Output (MIMO) Systems

Multiple input multiple output (MIMO) communication schemes offer the potential for significant increases in spectral efficiency over their single-input single output counterparts by enabling simultaneous transmission of independent data streams. MIMO schemes also offer the potential for significant performance gains in a variety of other metrics. Standard transceiver architectures for these schemes include linear precoding and equalization, and the combination of linear precoding and DFE, which offers the potential for improved performance over the linear approach while maintaining comparable complexity.

Equalization of wireless MIMO frequency-selective channels is a challenging task mainly due to the fact that the respective MIMO equalizers should cope with inter symbol as well as inter stream interference. When the channel is static and has already been estimated by the receiver, a well established solution would be to apply a multicarrier technique, such as a MIMO orthogonal-frequency-division multiplexing (OFDM) system [37]. Even though MIMO OFDM systems offer simplicity in analysis and receiver design, they still suffer from drawbacks related to implementation (peak to average power ratio), identifiability (spectral nulls), and sensitivity to carrier synchronization [38]. Another drawback is that uncoded OFDM has no significant performance gain as the delay spread of the channel increases [39], i.e., uncoded OFDM does not exploit multipath diversity. On the other hand, single-carrier (SC) modulation is a well-proven technology in many existing wireless and wire line applications and has been extensively used in practice. Thus, alternative SC approaches for the design of batch MIMO decision feedback equalizers (DFEs) have been proposed [40, 41].

However, in MIMO systems with relatively long bursts and under time varying conditions, the involved channel impulse responses change within a burst and, as expected, batch MIMO DFEs fail to equalize the channel. On the other hand, if a MIMO OFDM system is employed, the frame size should be made short and thus cyclic prefix overhead becomes overwhelming [38]. Therefore, to achieve effective channel equalization in such cases, adaptive methods are required. Both a minimum bit error rate (MBER) design [42,43] and the standard minimum mean-square error (MMSE) design [44, 45] and [46] have been invoked for implementing adaptive MIMO DFEs. The respective equalizers are updated either by using gradient Newton methods or by employing stochastic gradient techniques. The main problems appearing in adaptive MIMO equalization, i.e., the increased filter size and the colored noise caused by inter stream interference, slow down significantly the performance of stochastic gradient algorithms. On the other hand, the computational requirements of MIMO RLS algorithms increase significantly. In some adaptive schemes with convergence properties close to RLS but of lower computational cost were proposed in [47]. But still the computational complexity is very high compared to the LMS type algorithms.

For scenarios in which accurate channel state information (CSI) is available at both the transmitter and the receiver, there is a well established framework that unifies the design of linear transceivers under many design criteria [48]. A counterpart for the design of systems with DFE has recently emerged [49–51]. This framework was also extended to MIMO systems with pre-interference subtraction at the transmitter in [51]. However, in many scenarios, such as frequency division duplex systems, obtaining accurate CSI at the transmitter may require a considerable amount of feedback to the transmitter. An approach that allows the designer to limit the required amount of the feedback is to quantize the transmitter design. In these limited feedback schemes [52] , the receiver uses its CSI to choose the best transmitter design from a code book of available designs, and then feeds back the

index of this precoder to the transmitter. This strategy has been considered for beam forming schemes [53–56], unitary precoding with linear equalization [57] and unitary precoding for orthogonal space time block codes [58, 59]. For zero-forcing DFE schemes, a limited feedback scheme in which the receiver feeds back the order of interference cancellation was proposed in [60,61]. A limited feedback scheme for systems with a (general) linear precoder at the transmitter and zero-forcing DFE at the receiver was presented in [51].

From the theory of constrained optimization, it is found that the learning speed of any adaptive filtering algorithm can be increased by adding a constraint to it as in the case of the normalized LMS (NLMS) [62] and the normalized least-mean-fourth (NLMF) [63] algorithms. In an LMS-type algorithm that exploits the knowledge of the channel noise variance for identification and tracking of finite impulse response (FIR) channels, called noise constrained LMS (NCLMS) algorithm, was proposed in [64] . Recently an LMS based constrained adaptive algorithm was designed for CDMA systems which exploit the knowledge of both MAI and noise variances [65]. The novelty of this constraint resides in the fact that the MAI variance was never used as a constraint before. Motivated by this, it is proposed to design both linear and non-linear (DFE) equalizers for MIMO systems using the framework of [65].

1.6 Drawbacks in Previous Techniques: A motivation for the proposed work

There are several drawbacks in the techniques discussed above which are enumerated as follows:

- Although MIMO OFDM systems offer simplicity in analysis and receiver design, they still suffer from drawbacks related to implementation (peak to average power ratio), identifiability (spectral nulls), and sensitivity to carrier synchronization [38].

- Uncoded OFDM has no significant performance gain as the delay spread of the channel increases [38] i.e., uncoded OFDM does not exploit multipath diversity.

- Minimum bit error rate (MBER) DFE [42] can promise a better bit error rate performance but due to its reliance on BER cost function which provides very irregular surface is highly susceptible to divergence [66].

- The computational requirements of MIMO RLS algorithms increase significantly [47].

- Performance of CSI based DFEs depends on the accurate estimate of channel information [48]. This is problematic due to the time-varying nature of wireless channels.

- A major drawback of MIMO-CDMA systems is MAI which can reduce the capacity and increase BER, so statistical analysis of MAI becomes very important factor in the performance analysis of these systems . Statistical analysis of MAI in MIMO-CDMA is quite complicated and most of the researchers have used suboptimal approach to detect the subscriber without involving the need for MAI statistics such as successive interference cancellation (SIC) and parallel interference cancellation (PIC). Lack of research in the characterization of MAI in MIMO-CDMA has provided a motivation to perform a complete statistical analysis and find the closed form solution to the probability density functions (pdf's) of MAI and MAI plus noise in Rayleigh channel environment.

- If partial knowledge of the channel is available, it can be used to enhance the system performance. Moreover, CDMA systems suffer from MAI and noise, consequently, there is a dire need to design a multiuser detector which would deal with the MAI and noise. In previous research work, MAI has been used as part of interfering noise, and was assumed to be an unstructured

white Gaussian noise. [33] used MAI and noise to form a new constraint and used it in developing an algorithm named MAI plus noise constrained LMS (MNCLMS) algorithm. MNCLMS was shown to have outperformed the other algorithms which were constrained on noise only but [33]'s work is related to SISO-CDMA systems.

1.7 Thesis Objective

Thus, in the light of the above discussion it is apparent that there is a need for designing new adaptive equalization techniques which can overcome the above mentioned drawbacks. The learning speed of an adaptive filtering algorithm can be increased by adding a constraint to it [62]. Recently an LMS based constrained adaptive algorithm is designed for CDMA systems based on the knowledge of MAI and noise variances [65]. The novelty of this constraint resides in the fact that the MAI variance was never used as a constraint before. Motivated by this, it is proposed to design both linear and non-linear (DFE) equalizers for MIMO systems using the framework of [65].

The objectives of the proposed work are as follows:

1. To design a linear transverse and non-linear equalizer (DFE) for MIMO systems based on constrained optimization technique employing the framework of [65].

2. Constraints will be imposed on both MAI and noise variances. For this, the statistical characterization of MAI and MAI plus noise in MIMO CDMA systems will be analyzed.

3. Performance analysis (transient, steady-state, and tracking) of the proposed adaptive algorithms will be carried out in the scenario of interference and noise limited systems.

4. Extensive simulations will be presented to corroborate the theoretical findings.

1.8 Thesis Organization

After the introductory chapter, a comprehensive analysis of MAI for MIMO synchronous CDMA system using BPSK signal with random signal sequences in fading environments such as Rayleigh is presented in chapter 2 with simulation results to support the analytical results.

Chapter 3 deals with the investigation of optimum coherent reception in the presence of multiple access interference and BER is derived for the Rayleigh channel.Simulation results shown at the end of chapter 3 show the close agreement to the analytical findings. In chapter 4, various types of DFE are discussed. In chapter 5, two types of MIMO receivers have been proposed: One with linear adaptive equalization and the other with MIMO DFE. For both receivers, a new constrained algorithm is proposed. Convergence analysis, transient analysis and tracking analysis of the constrained algorithm are performed in chapter 6. Simulation results are presented to validate the analysis. Chapter 7 deals with the conclusion, contributions and recommendations for the future work.

1.9 Peer Reviewed Published Work and Conference Publications

1. "Design of MAI constrained decision feedback equalizer for MIMO CDMA system," Mahmood, K.; Moinuddin, M.; Asad, S.M.; Paul, S., Wireless Communications and Signal Processing (WCSP), 2011 International Conference on , vol., no., pp.1,5, 9-11 Nov. 2011

2. “Statistical Analysis of Multiple Access Interference in Rayleigh Fading Environment for MIMO CDMA Systems”, Mahmood, K.; Moinuddin, M.; Azzedine Zerguine; Asad, S.M.; Paul,S., submitted to ICASSP2014 - SPCOM

Chapter 2

Statistical Analysis of multiple access interference (MAI) and noise in MIMO-CDMA systems

2.1 Introduction

In an ideal scenario, MIMO-CDMA system offers a great improvement in overall system capacity [67]– [68]. But in practice, this achievement is limited due to the presence of MAI. MAI reduces the capacity and increases the BER of the MIMO systems resulting in the degradation of the system. Thus, a complete statistical analysis of MAI is vital in the design and performance analysis of these systems.

Due to computational complexities in the statistical analysis of MAI in MIMO-CDMA systems, there is no substantial research work in the literature. Thus, either some strong assumptions are used, for example, Gaussian assumption for interference in MIMO system [69, 70] or suboptimal approaches are employed to detect the subscriber without involving the need for MAI statistics such as successive interference cancellation (SIC) [71] and parallel interference cancellation (PIC) [72]. In contrast to the existing research, an exact characterization of MAI in Rayleigh

fading environment is developed for MIMO-CDMA systems in this thesis. Consequently, explicit closed-form expressions for both the probability density function (pdfs) of MAI and MAI plus noise is derived for Rayleigh fading channel assuming that the channel phase is either estimated or known at the receiving end.

2.2 Probability Density Function (pdf) of MAI Plus Noise in Flat Fading Environment

In this section, closed form expressions for pdf of MAI and MAI plus noise for flat fading channel (Rayleigh) has been derived under the assumption that the channel phase is either known or has perfectly been estimated.

2.2.1 System Model

A block diagram of a MIMO-CDMA system with N transmit and M receive antennas is considered as shown in figure 2.1. Consider a flat-fading channel whose complex impulse response between the nth transmitter and mth receiver for the lth symbol is

$$H_{mn}^{l}(t) = h_{mn}^{l} e^{j\phi_l} \delta(t) \tag{2.2.1}$$

where h_{mn}^{l} is the envelope and ϕ_n is the phase of the complex channel for the lth symbol. Assuming that the receiver is able to perfectly track the phase of the channel, the detector in the mth receiver observes the signal

$$\begin{aligned} r_m(t) &= \sum_{n=1}^{N} \sum_{l=-\infty}^{\infty} \sum_{k=1}^{K} A^k b_n^{l,k} s_n^{l,k}(t) h_{mn}^{l} \\ &\quad + \nu_m(t), \qquad m = 1, 2, \ldots M \end{aligned} \tag{2.2.2}$$

where K represents the number of users, $s_n^{l,k}(t)$ is the rectangular signature waveform with random signature sequence of the k^{th} subscriber defined in the $(l-1)T_b \leq$

$t \leq lT_b$, T_b and T_c are bit period and the chip interval, respectively, related by $N_c = T_b/T_c$, $\left\{b_n^{l,k}\right\}$ is the input bit stream of the k^{th} subscriber, h_{mn}^l is the l^{th} channel tap between the m^{th} transmitter and the n^{th} receiver ($h_{mn}^l = 1$ for the additive white Gaussian noise (AWGN) channel), A^k is the transmitted amplitude of the k^{th} subscriber and ν_m is the additive white Gaussian noise with zero mean and variance $\sigma_{\nu_m}^2$ at the m^{th} receiver. The cross-correlation between the signature sequences of subscribers j and k for the l^{th} symbol is $\rho_l^{k,j} = \int_{(l-1)T_b}^{lT_b} s_n^k(t)\, s_n^j(t)\, dt = \sum_{i=1}^{N_c} c_{l,i}^k c_{l,i}^j$, where $\left\{c_{l,i}^k\right\}$ is the normalized spreading sequence (so that the auto correlations of the signature sequences are unity) of subscriber k for the l^{th} symbol. The receiver consists of a matched filter at the front end which is matched to the signature waveform of the desired user.

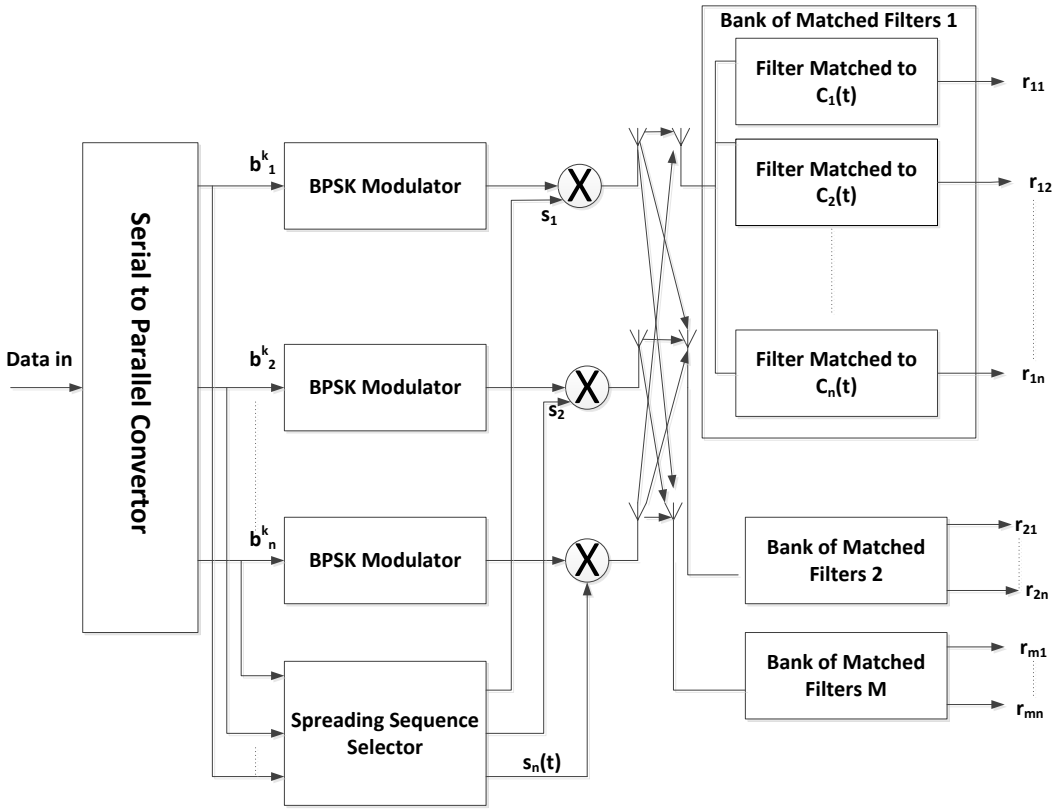

Figure 2.1: Block Diagram of MIMO-CDMA Transmitter and Receiver

In this analysis, the desired subscriber is subscriber 1. Thus, the matched filter's output for the l^{th} symbol at the m^{th} receiver can be written as follows:

$$H_{mn}^{l}(t) = h_{mn}^{l} e^{j\phi_l} \delta(t) \tag{2.2.3}$$

For a Rayleigh fading channel, the pdf of h_{mn}^{l} will be

$$f_{h_{mn}^{l}}(x) = \frac{x}{\sigma_h^2} \exp\left(-\frac{x^2}{2\sigma_h^2}\right), \quad \text{for} \quad x > 0, \tag{2.2.4}$$

where σ_h^2 represents the variance of the Rayleigh channel. Assuming that the receiver is able to perfectly track the phase of the channel, the detector in the m^{th} receiver observes the signal

$$\begin{aligned} r_m(t) &= \sum_{n=1}^{N} \sum_{l=-\infty}^{\infty} \sum_{k=1}^{K} A^k b_n^{l,k} s_n^{l,k}(t) h_{mn}^{l} \\ &\quad + \nu_m(t), \qquad m = 1, 2, \ldots M \end{aligned} \tag{2.2.5}$$

The cross-correlation between the signature sequences of subscribers j and k for the l^{th} symbol is

$$\rho_l^{k,j} = \int_{(l-1)T_b}^{lT_b} s_n^k(t) s_n^j(t) dt = \sum_{i=1}^{N_c} c_{l,i}^k c_{l,i}^j \tag{2.2.6}$$

The receiver consists of a matched filter at the front end which is matched to the signature waveform of the desired subscriber. In our analysis, the desired subscriber is subscriber 1. Thus, the matched filter's output for the l^{th} symbol at the m^{th} receiver can be written as follows:

$$\begin{aligned} y_m^l &= \int_{(l-1)T_b}^{lT_b} r_m(t) s_m^{l,1}(t) dt \\ &= \sum_{n=1}^{N} A^1 b_n^{l,1} h_{mn}^{l} + U_m^l + \nu_m, \quad m = 1, 2, \ldots M, \end{aligned} \tag{2.2.7}$$

where ν_m is the additive noise at the m^{th} receiver and U_m^l is the MAI at the m^{th} receiver for the l^{th} symbol in the presence of the fading channel h_{mn}^l and is given by

$$U_m^l = \sum_{n=1}^{N} \sum_{k=2}^{K} A^k b_n^{l,k} \rho_n^{k,1} h_{mn}^l, \qquad m = 1, 2, \ldots M \tag{2.2.8}$$

which can also be expressed as follows

$$U_m^l = \sum_{n=1}^{N} I_{mn}^{l,k} h_{mn}^l, \qquad m = 1, 2, \ldots M \tag{2.2.9}$$

where the random variable $I^{l,k} = \sum_{k=2}^{K} A^k b^{l,k} \rho^{k,1}$ is shown to follow Gaussian behavior in [33], that is, $I^{l,k} \sim \mathcal{N}(0, \sigma_I^2)$ where $\sigma_I^2 = \dfrac{A^2 (K-1)}{N_c}$. For the sake of tractability of analysis, we have assumed the same behavior for random variable $I^{l,k}$ in MIMO scenario.

Equation (2.2.6) shows that the cross-correlation $\rho^{k,l}$ is in the range $(-1, +1)$ and can be set up by the following relation [33],

$$\rho^{k,l} = \frac{N_c - 2d}{N_c}, \quad d = 0, 1 \ldots N_c \tag{2.2.10}$$

where d is a binomial random variable with an equal probability of success and failure and its mean and variance are $E(d) = \frac{Nc}{2}$ and $\sigma_d^2 = \frac{N_c}{4}$. Since the channel taps are independent from the spreading sequences and the data sequences, the interferer's components $A^k b_n^{l,k} \rho_n^{k,1} h_{mn}^l$ therefore, are independent of each other and have zero mean.

Equation (2.2.7) can be written compactly as

$$y_m^l = \sum_{n=1}^{N} A^1 b_n^{l,1} h_{mn}^l + Z_m^l, \quad m = 1, 2, \ldots M, \tag{2.2.11}$$

where , $Z_m^l = U_m^l + \nu_m^l$

2.3 Probability Density Function (pdf) of Multiple Access Interference (MAI)

In order to find the pdf of random variable $p_n^l = I_{mn}^{l,k} h_{mn}^l$, the independence of $I_{mn}^{l,k}$ and h_{mn}^l can be applied as follows

$$\begin{aligned} f_P(p) &= \int_{-\infty}^{\infty} \frac{1}{|x|} f_I\left(\frac{p}{x}\right) f_{h_{mn}^l}(x)\, dx, \qquad x > 0 \\ &= \int_0^{\infty} \frac{1}{x} \frac{1}{\sqrt{2\pi\sigma_I^2}} \exp\left(-\frac{p^2}{2x^2\sigma_I^2}\right) \frac{x}{\sigma_h^2} \exp\left(-\frac{x^2}{2\sigma_h^2}\right) dx, \end{aligned}$$

which is found to be

$$f_P(p) = \frac{1}{2\sigma_I\sigma_h} \exp\left(-\frac{|p|}{\sigma_h\sigma_I}\right) \tag{2.3.1}$$

Thus, the characteristic function of the random variable p_n^l can be evaluated as

$$\begin{aligned} \Phi_{P_m^l}(\omega) &= E\left[e^{iwP}\right] \\ &= \frac{1}{2\sigma_I\sigma_h} \int_{-\infty}^{\infty} \exp(i\omega p) \exp\left(-\frac{|p|}{\sigma_h\sigma_I}\right) dp \\ &= \frac{1}{\omega^2\sigma_{P_n^l}^2 + 1} \end{aligned}$$

where $\sigma_{P_n^l}^2 = \sigma_I^2\sigma_h^2$. Since the interferers are independent but not identical, therefore from (2.2.9), it can be observed that the characteristic function of U_m^l will be the product of N characteristic functions of independent random variables P_n^l, that is,

$$\Phi_{U_m^l}(\omega) = \prod_{n=1}^{N} \Phi_{P_n^l}(\omega) = \prod_{n=1}^{N} \frac{1}{\omega^2\sigma_{P_m^l}^2 + 1} \tag{2.3.2}$$

Where $\Phi_{U_m^l}(\omega)$ is the characteristic function of U_m^l and is the product of N characteristic functions of independent random variables P_n^l

Inverse Fourier transform of the above characteristic function, $\Phi_{U_m^l}(\omega)$ will yield

$$\begin{aligned} f_{U_m^l}(u) &= \mathcal{F}^{-1}\left[\Phi_{U_m^l}(\omega)\right] \\ &= \frac{1}{2\pi}\int_{-\infty}^{\infty}\exp\left(-i\omega U_m^l\right)\prod_{n=1}^{N}\frac{1}{\omega^2\sigma_{P_n^l}^2+1}d\omega \end{aligned} \tag{2.3.3}$$

The above integral is evaluated in Appendix A which gives the following expression for the pdf of U_m^l:

$$f_{U_m^l}(u) = \frac{1}{2}\sum_{n=1}^{N}\frac{C_n e^{-\frac{|u|}{\sigma_{P_m^l}}}}{\sigma_{P_n^l}} \tag{2.3.4}$$

where C_n is defined in (A.2). The pdf of MAI in (2.3.4) shows that the MAI experienced at any receiving antenna will be a sum of Laplacian distributed random variables. It can be seen that by setting $N = 1$ in the above, the pdf of MAI will reduce to single Laplacian random variable which is consistent with the result in [33].

2.4 Probability Density Function (pdf) of Multiple Access Interference (MAI) and Noise

In order to find the pdf of MAI and noise, equation (2.3.4) is being utilized. Z_m^l is considered to be a random variable resulting in MAI and noise

Thus, the pdf of random variable Z_m^l can be evaluated by the convolution of the pdfs of U_m^l and ν_m^l as follows

$$\begin{aligned} f_{Z_m^l}(z) &= f_{U_m^l}(\omega) * f_{\nu_m^l}\left(\nu_m^l\right) \\ &= \int_{-\infty}^{\infty} f_{U_m^l}(t)\, f_{\nu_m^l}(u-t)\, dt \\ &= \sum_{j=1}^{N}\frac{C_n}{2\sigma_{P_n^l}}\beta_n \end{aligned} \tag{2.4.1}$$

where $*$ is the the convolution operator and β_n is the integral defined as

$$\beta_n = \frac{1}{\sqrt{2\pi}\sigma_{\nu_m^l}} \int_{-\infty}^{\infty} e^{-\frac{|t|}{\sigma_{P_m^l}} - \frac{\left(u_m^l - t\right)^2}{2\sigma^2_{\nu_m^l}}} dt \tag{2.4.2}$$

which can be solved by using completing square method and by employing the definition of error complement function erfc(x) [73] and it is found to be:

$$\begin{aligned} \beta_n &= \frac{e^{\frac{\sigma^2_{\nu_m^l}}{2\sigma^2_{P_j}}}}{2} \left[e^{\frac{-p}{\sigma_{U_m^l}}} \operatorname{erfc}\left(\frac{\sigma_{\nu_m^l}}{\sqrt{2}\sigma_{P_n^l}} - \frac{Z_m^l}{\sqrt{2}\sigma_{\nu_m^l}} \right) \right. \\ &\quad \left. + e^{\frac{U_m^l}{\sigma_{P_n^l}}} \operatorname{erfc}\left(\frac{\sigma_{\nu_m^l}}{\sqrt{2}\sigma_{P_n^l}} + \frac{Z_m^l}{\sqrt{2}\sigma_{\nu_m^l}} \right) \right] \end{aligned} \tag{2.4.3}$$

The pdf $f_{Z_m^l}(z)$ can be set as

$$f_{Z_m^l}(z) = \frac{1}{2\sqrt{\pi}} \sum_{n=1}^{N} \frac{C_n}{\sigma_{P_m^l}} \exp\left(\frac{\sigma^2_{\nu_m^l}}{2\sigma^2_{P_n^l}} \right) \Gamma\left(\alpha, \frac{\sigma^2_{\nu_m^l}}{2\sigma^2_{P_n^l}}; \frac{\left(Z_m^l\right)^2}{4\sigma^2_{P_n^l}} \right) \tag{2.4.4}$$

where $\Gamma(\alpha, x; b)$ is the generalized incomplete gamma function defined as [74] defined as

$$\Gamma(a, x; b) := \int_x^{\infty} t^{a-1} \exp(-t - b/t)\, dt. \tag{2.4.5}$$

for $\alpha = \frac{1}{2}$, the Generalized Incomplete Gamma Function can be written as

$$\Gamma\left(\frac{1}{2}, x; b\right) = \frac{\sqrt{\pi}}{2} \left[\exp\left(-2\sqrt{b}\right) \operatorname{erfc}\left(\sqrt{x} - \sqrt{b/x}\right) + \exp\left(2\sqrt{b}\right) \operatorname{erfc}\left(\sqrt{x} + \sqrt{b/x}\right) \right] \tag{2.4.6}$$

where $\operatorname{erfc} x = \frac{2}{\pi} \int_x^{\infty} exp\left(-t^2\right) dt$ is error complement function . Equation (2.4.4) can expressed as

$$f_{Z_m^l}(z) = \frac{1}{2\sqrt{\pi}} \sum_{n=1}^{N} \frac{C_n}{\sigma_{P_n^l}} \exp\left(\frac{\sigma^2_{\nu_m^l}}{2\sigma^2_{P_n^l}} \right) \Gamma\left(\frac{1}{2}, \frac{\sigma^2_{\nu_m^l}}{2\sigma^2_{P_n^l}}; \frac{\left(Z_m^l\right)^2}{4\sigma^2_{P_n^l}} \right) \tag{2.4.7}$$

2.5 Simulation Results

This section deal with the simulation as well as numerical results to validate the theoretical results derived. The effect of different parameters on the pdf of MAI and MAI and noise is also investigated in this section namely the effect of number of transmitting as well as receiving antennas, length of pseudo noise (PN) sequence and number of subscribers in the system.

The simulation setup consists of two different scenarios consisting of of 2×2 and 4×4 MIMO systems. The CDMA system uses random signature sequences. The SNR used for all simulations is 20dB. The Rayleigh channel is chosen to be flat slow fading.

Figure 2.2 shows the effect on the pdf of MAI as the system's diversity increases. As can be seen, the variance of MAI increases with an increase in diversity. This is consistent with theoretical predictions that the severity of interference would increase in the presence of such diversity. The effect of the length of signature sequence on the pdf of MAI can be seen in figure 2.3. The MIMO system in this case is 4×4. This is also consistent with results reported in [33]. As can be noticed, the variance of MAI decreases with an increase in the length of the signature sequence.

Table 2.1 shows the comparison of analytical and experimental variances in each case which demonstrates the correctness of the theoretical analysis. As mentioned earlier in the analysis that the MIMO-MAI is a sum of Laplacian distributed random variables, it is therefore prudent to inspect the kurtosis of the MIMO-MAI. Table 2.1 lists the kurtosis of MAI which is gradually decreasing as the signature length increases. The increase in the signature sequence length would result in MAI in AWGN to be Gaussian whereas effecting the MAI under the fading environment at the same time.

The effect of interference, i.e, MAI and noise on a system's performance is depicted in Figure 2.4 . It is intuitive to predict that the system will be severely degraded by the increase in the number of subscribers. As the number of sub-

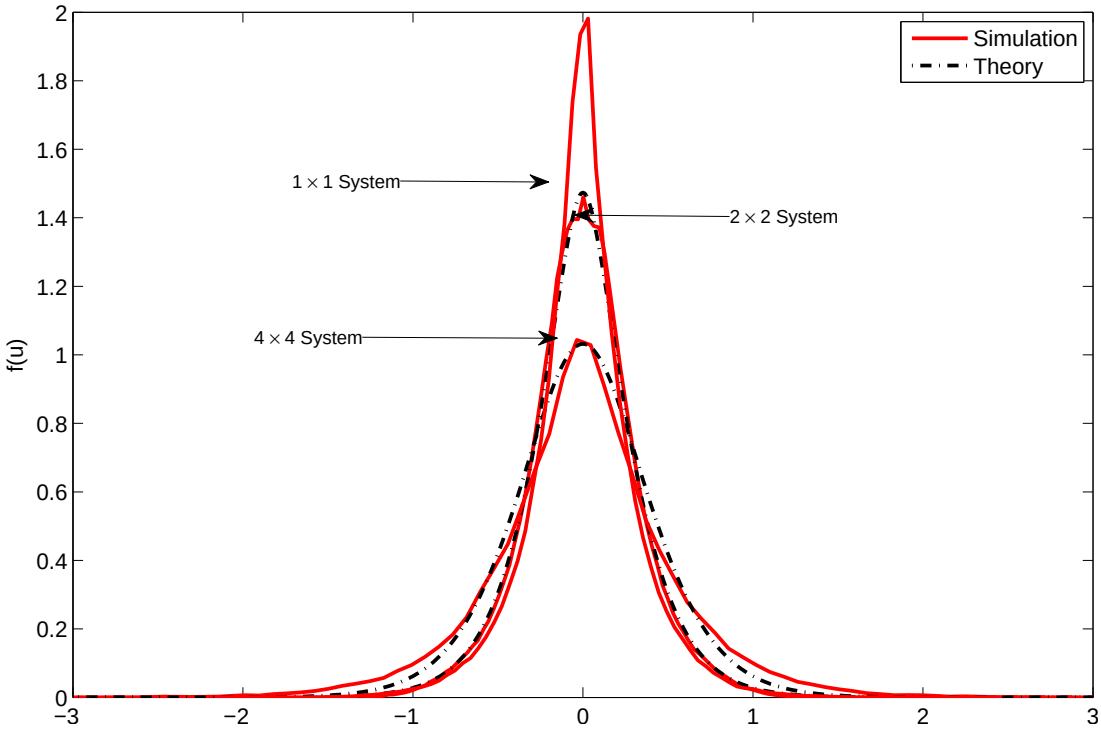

Figure 2.2: pdf of MAI for different scenarios of transmit and receive antennas.

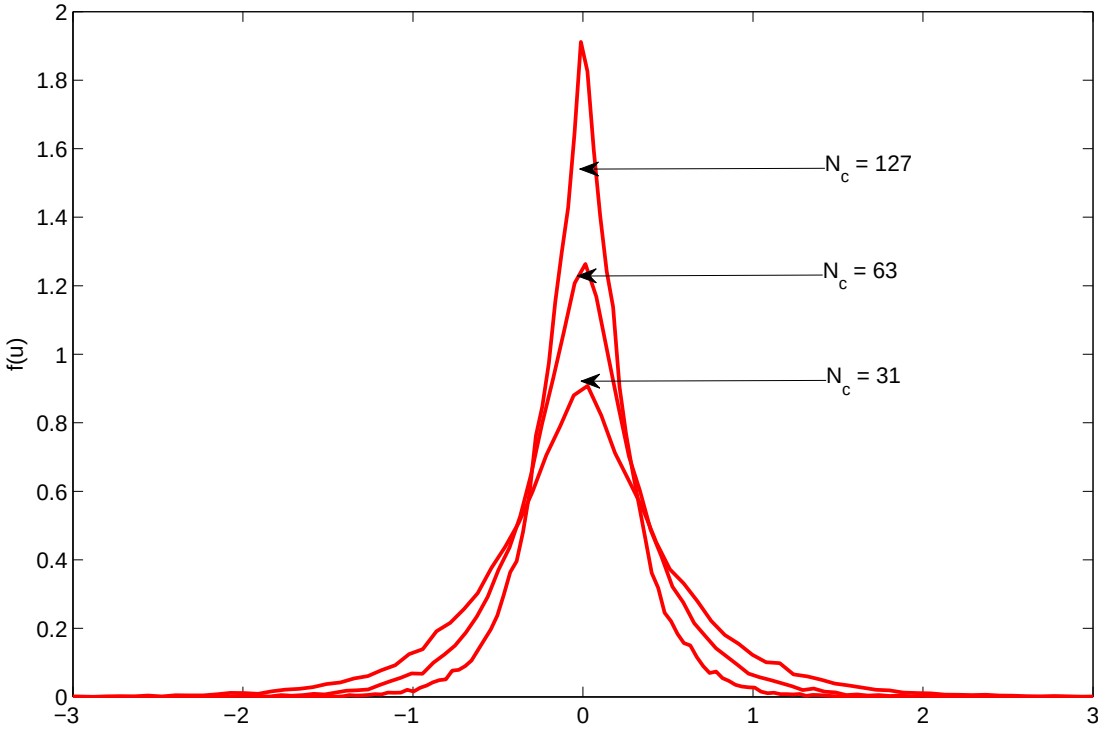

Figure 2.3: pdf of MAI under various length of PN sequences.

Table 2.1: Kurtosis and variance of MAI in a 4×4 MIMO system with $K = 4$.

	$N_c = 31$	$N_c = 63$	$N_c = 127$
Experimental Kurtosis of MAI	5.11	5.12	5.03
Experimental Variance	0.3833	0.1926	0.0946
Analytical Variance	0.387	0.19	0.0945

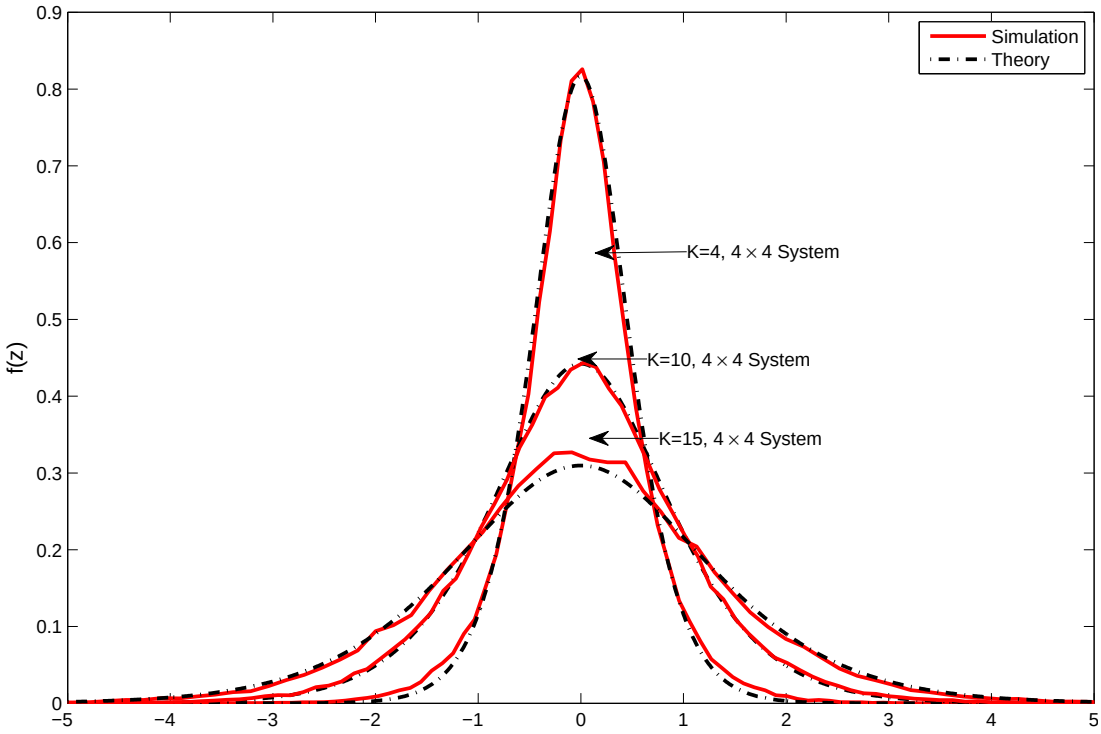

Figure 2.4: pdf of MAI-plus-noise under different number of users in the system.

scribers is increasing, the power of the MAI experienced by the desired subscriber is also increasing as shown in Figure 2.4. Table 2.2 lists the experimental kurtosis of MAI and noise under different capacity and diversity scenarios to test its Gaussianity. In all the cases, the kurtosis decreases with increase in the system user capacity. Particularly for the 2×2 MIMO case, the MAI-plus-noise acts more like Gaussian as kurtosis of Gaussian distribution is 3.

Table 2.2: Experimental Kurtosis of MAI-plus-noise under different system's capacity.

MIMO System	2×2	4×4
$K = 4$	3.77	4.63
$K = 10$	3.3	4.02
$K = 15$	3.18	3.9

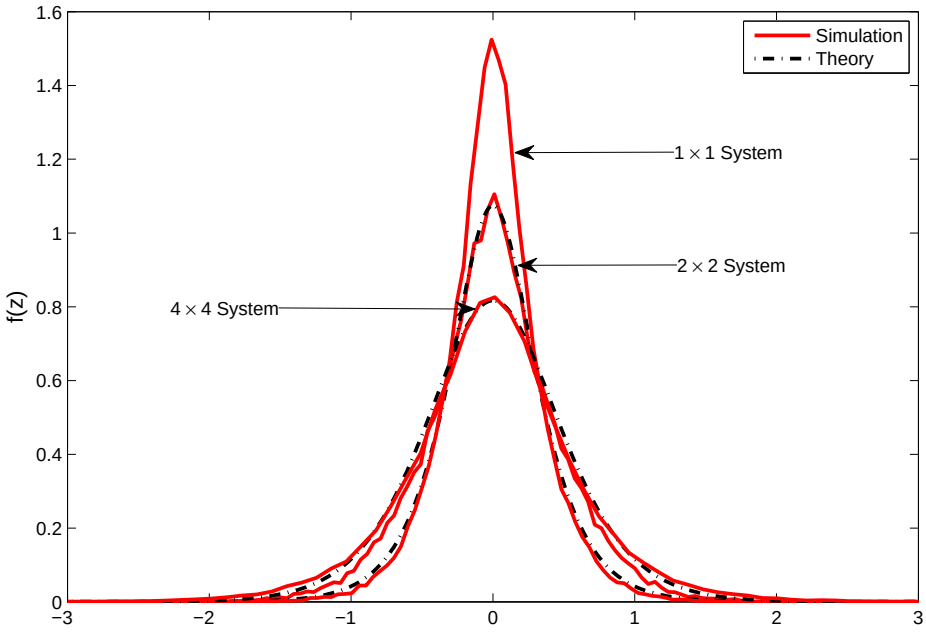

Figure 2.5: pdf of MAI-plus-noise for different scenarios of transmit and receive antennas.

Figure 2.5 shows the effect of diversity on the pdf of MAI-plus-noise. Even though a MIMO-CDMA system will provide higher data rates with increase in reliability, the system will be severely degraded by the limiting factors such as MAI and MAI

plus noise. The results shown above motivate the fact that any receiver design for such a system will have to take MAI plus noise in to account in order to have optimum reception.

2.6 Remarks

In this chapter, a thorough statistical analysis of MAI and MAI-plus-noise for MIMO-CDMA systems has been performed in the presence of Rayleigh fading channel. The analysis results in a new closed-form expressions for the pdf of MAI and MAI and noise. It is found that the pdf of MAI and noise is a function of number of subscribers, number of antennas, spreading code length, channel variance and noise variance. Moreover, the effect of these parameters on the pdf of MAI is investigated in simulations. The simulation results have shown a close agreement with the theoretical findings.

Chapter 3

BER Performance of MIMO-CDMA Systems Based on Characterization of Multiple-Access Interference (MAI)

3.1 Introduction

This chapter deals with the design of an optimum receiver in the presence of MAI plus noise for Rayleigh environment. Probability of error is derived for the maximum likelihood receiver. Simulation results shown at end of the chapter, support the analytical finding. Design as well as characteristics of optimum receivers in the presence of AWGN for different modulation methods have been extensively covered in literature. It is reported in the literature that AWGN channels optimum detector is comprised of a correlation demodulator or a matched filter followed by an optimum decision rule, is based on maximum aposteriori probability (MAP) criterion for the case when a priori probabilities of the transmitted signal are unequal. Maximum likelihood (ML) criterion is used in case when a priori probabilities of the

transmitted signal are equal. Decisions based on any of the criteria used depends on the conditional probability function (pdf) of the received vector at the output of the matched filter or the correlator. In this analysis, maximum likelihood (ML) criterion is utilized.

3.2 BER Performance

BER is the number of bits in error with respect to the total number of bits received at a particular receiver. BER performance is considered to be very important criteria for CDMA systems as it determines the quality of transmission as well as amount of data to be transmitted per unit of bandwidth. Since all subscribers contribute to the interference levels at the receiving side , the BER of each subscriber increases when more subscribers try to access the channel. Subsequently, maximum number of subscriber is determined by the amount of interference which can be accepted [75].

At the front end of the optimum receiver, a matched filter is attached which is matched to the desired subscriber. The desired subscriber in this analysis is the subscriber 1. The matched filter's output for the l^{th} symbol at the m^{th} receiver can be written as follows:

$$\begin{aligned} y_m^l &= \int_{(l-1)T_b}^{lT_b} r_m(t)\, s_m^{l,1}(t)\, dt \\ &= \sum_{n=1}^{N} A^1 b_n^{l,1} h_{mn}^l + U_m^l + \nu_m^l, \quad m = 1, 2, \ldots M, \end{aligned} \tag{3.2.1}$$

In equation (3.2.1) , the first term represents the desired subscriber, the second term represents MAI plus noise, whereas the third term represents the additive Gaussian noise

The pdf of MAI-plus-noise was found to be

$$f_Z(z) = \frac{1}{\sqrt{2}} \sum_{j=1}^{N} \frac{C_n}{\sigma_{U_m^l}} \exp\left(\frac{\sigma_{\nu_m^l}^2}{2\sigma_{U_m^l}^2}\right) \Gamma\left(\frac{1}{2}, \frac{\sigma_{\nu_m^l}^2}{2\sigma_{U_m^l}^2}; \frac{\left(Z_m^l\right)^2}{4\sigma_{U_m^l}^2}\right) \tag{3.2.2}$$

The output of the matched filter matched to the signature waveform of the desired subscriber for the lth symbol can be written as

$$y_m^l = w_{m,i}^l + Z_{m,i}^l \qquad i = 1, 2 \quad \text{(for BPSK signals)} \tag{3.2.3}$$

$w_{m,i}$ in equation (3.2.3) is the desired symbol in a MIMO system. If E_b represents the energy per bit then $w_{m,i}$ is either $+N\alpha_i\sqrt{E_b}$ or $-N\alpha_i\sqrt{E_b}$ for BPSK signals. Moreover as the received signal is given by

$$\begin{aligned} y_m^l &= \int_{(l-1)T_b}^{lT_b} r_m(t)\, s_m^{l,1}(t)\, dt \\ &= \sum_{n=1}^{N} A^1 b_n^{l,1} h_{mn}^l + z_m^l + \nu_m, \quad m = 1, 2, \ldots M, \end{aligned} \tag{3.2.4}$$

where $\sum_{n=1}^{N} A^1 b_n^{l,1} h_{mn}^l$ represents the desired signal, the channel taps α^l are no longer Rayleigh fading but rather a sum of Rayleigh fading. This can be seen as

$$\sum_{n=1}^{N} A^1 b_n^{l,1} h_{mn}^l = A^1 b^{l,1} \sum_{n=1}^{N} h_{mn}^l \tag{3.2.5}$$

Since it is ass that same data is being transmitted from each transmitting antenna (a type of diversity that can be justified). So $\alpha^l = \sum_{n=1}^{N} h_{mn}^l$ that is sum of Rayleigh fading.

In the derivation of BER, the pdf of $\left(\alpha^l\right)^2$ is required as can be seen in equation (3.2.12) for which we need the pdf of α^l. The pdf of α^l is obtained from [76, Eq.

4a-4b] as

$$f_{\alpha^l}(t) = \frac{\alpha^{2N-1} e^{-\frac{\alpha^2}{2b}}}{2^{N-1} b^N (N-1)!}, \tag{3.2.6}$$

$$b = \frac{\sigma^2}{N} \left[(2N-1)!!\right]^{1/N} \tag{3.2.7}$$

where $(2N-1)!! = (2N-1)(2N-3)\cdots 3.1$ and $\alpha^l = x/\sqrt{N}$, x is the normalized Rayleigh random variable and N is the number of transmitters. For BPSK signaling, the conditional pdf $p\left(y_m^l | w_{m,1}^l\right)$ can be obtained by using (2.4.4) as

$$p\left(y_m^l | w_{m,1}^l\right) = \frac{1}{2\sqrt{\pi}} \sum_{n=1}^{N} \frac{C_n}{\sigma_{U_m^l}} \exp\left(\frac{\sigma_{\nu_m^l}^2}{2\sigma_{U_m^l}^2}\right) \Gamma\left(\frac{1}{2}, \frac{\sigma_{\nu_m^l}^2}{2\sigma_{U_m^l}^2}; \frac{\left(y_m^l - N\alpha_i\sqrt{E_b}\right)^2}{4\sigma_{U_m^l}^2}\right) \tag{3.2.8}$$

For the case when $w_{m,1}^l$ and $w_{m,2}^l$ have equal a priori probabilities, then according to ML criterion, the optimum test statistic is the likelihood ratio $\left(\Lambda = p\left(y_m^l | w_{m,1}^l\right) / p\left(y_m^l | w_{m,2}^l\right)\right)$. Now assuming that the channel attenuation (α^l) is deterministic, therefore any error occurred is only due to the MAI-plus noise $(Z_{m,i}^l)$. It is shown in [33] that the MAI-plus noise term has a zero mean and a zero skewness which shows its symmetric behavior about its mean. Consequently, the conditional pdf $p\left(y_m^l | w_{m,1}^l\right)$ with deterministic channel attenuation will also be symmetric resulting in the threshold for the ML optimum receiver to be its mean value, that is, zero. Finally, the probability

of error given $w_{m,1}^l$ is transmitted is found to be

$$\begin{aligned} P\left(e|w_{i,1}\right) &= \int_{-\infty}^{0} p\left(y_m^l|w_{m,1}^l\right) dy_m^l \\ &= \frac{1}{2\sqrt{\pi}} \sum_{n=1}^{N} \int_{-\infty}^{0} \frac{C_n}{\sigma_{U_m^l}} \exp\left(\frac{\sigma_{\nu_m^l}^2}{2\sigma_{U_m^l}^2}\right) \\ &\times \Gamma\left(\frac{1}{2}, \frac{\sigma_{\nu_m^l}^2}{2\sigma_{U_m^l}^2}; \frac{\left(y_m^l - N\alpha_i\sqrt{E_b}\right)^2}{4\sigma_{U_m^l}^2}\right) dy_m^l \qquad (3.2.9) \\ &= \frac{1}{2} \sum_{n=1}^{N} C_n \exp\left(\frac{\sigma_\eta^2}{2\sigma_I^2\sigma_\alpha^2}\right) \\ &\times \int_{\sigma_\eta^2/2\sigma_I^2\sigma_\alpha^2}^{\infty} e^{-t} \text{erfc}\left(\sqrt{\frac{\alpha^2 N^2 E_b}{4\sigma_I^2\sigma_\alpha^2 t}}\right) dt \qquad (3.2.10) \end{aligned}$$

In order to get the pdf of $\left(\alpha^l\right)^2$, we apply a transformation to the random variable α^l. This can be as follows:

A new variable γ_z set up as

$$\gamma_z = \frac{\alpha_i^2 N^2 E_b}{4\sigma_I^2\sigma_\alpha^2 t} \qquad (3.2.11)$$

The mean of γ_z i.e. $\overline{\gamma_z} = E\left[\gamma_z\right]$ can be found as

$$\overline{\gamma_z} = E\left[\gamma_z\right] = \frac{E\left[\alpha_i^2\right] N^2 E_b}{4\sigma_I^2\sigma_\alpha^2 t} = \frac{2bNN^2E_b}{4\sigma_I^2\sigma_\alpha^2 t} = \frac{bN^3E_b}{2\sigma_I^2\sigma_\alpha^2 t} \qquad (3.2.12)$$

From 3.2.11

$$\alpha_i = \frac{2}{N}\sqrt{\frac{\gamma_z\sigma_I^2\sigma_\alpha^2 t}{E_b}} \qquad (3.2.13)$$

To summarize

$$f_{\gamma_z}\left(\gamma_z\right) = \left.\frac{f_{\alpha_i}\left(\alpha_i\right)}{\left|d\gamma_z/d\alpha_i\right|}\right|_{\alpha_i = \frac{2}{N}\sqrt{\frac{\gamma_z\sigma_I^2\sigma_\alpha^2 t}{E_b}}} \qquad (3.2.14)$$

$$\frac{d\gamma}{d\alpha} = \frac{\alpha_i N^2 E_b}{2\sigma_I^2\sigma_\alpha^2 t} = \frac{2}{N}\sqrt{\frac{\gamma_z\sigma_I^2\sigma_\alpha^2 t}{E_b}} \times \frac{N^2 E_b}{2\sigma_I^2\sigma_\alpha^2 t} \qquad (3.2.15)$$

The pdf of Mai-plus-noise and subsequently the BER are evaluated in Appendix B.

The BER can therefore be setup as follows:

$$\begin{aligned} P(e) &= \frac{1}{2}\sum_{j=1}^{N} C_j 2^{1-N} \exp\left(\frac{\sigma_\eta^2}{2\sigma_I^2\sigma_\alpha^2}\right)\left(\frac{\sigma_I^2\sigma_\alpha^2}{bN^2E_b}\right)^N \frac{\Gamma(2N)}{\Gamma(N+1)} \\ &\times \int_{\sigma_\eta^2/2\sigma_I^2\sigma_\alpha^2}^{\infty} e^{-t}t^N {}_2F_1\left(N, N+\frac{1}{2}; N+1, -\frac{2\sigma_I^2\sigma_\alpha^2 t}{bN^2E_b}\right) dt \end{aligned} \quad (3.2.16)$$

The integral in equation (3.2.16) is given by

$$\int_{\sigma_\eta^2/2\sigma_I^2\sigma_\alpha^2}^{\infty} e^{-t}t^N {}_2F_1\left(N, N+\frac{1}{2}; N+1, -\frac{2\sigma_I^2\sigma_\alpha^2 t}{bN^2E_b}\right) dt \quad (3.2.17)$$

There is no closed form solution for the above integral so the result were evaluated through numerical integration.

3.3 Simulation Results

Figure 3.1 shows the performance of CDMA systems in flat Rayleigh fading environment. As can be seen that BER performance is worsening when the number of subscriber is increasing. It is also worth noting that at a certain signal to noise ratio, BER is not changing. As shown the proposed analytical results are closely matched with the experimental one. Figure shows BER plotted against number of subscribers for the 20dB SNR and a 2×2 MIMO system. It can be seen that the analytical results are closely matched with the experimental one.

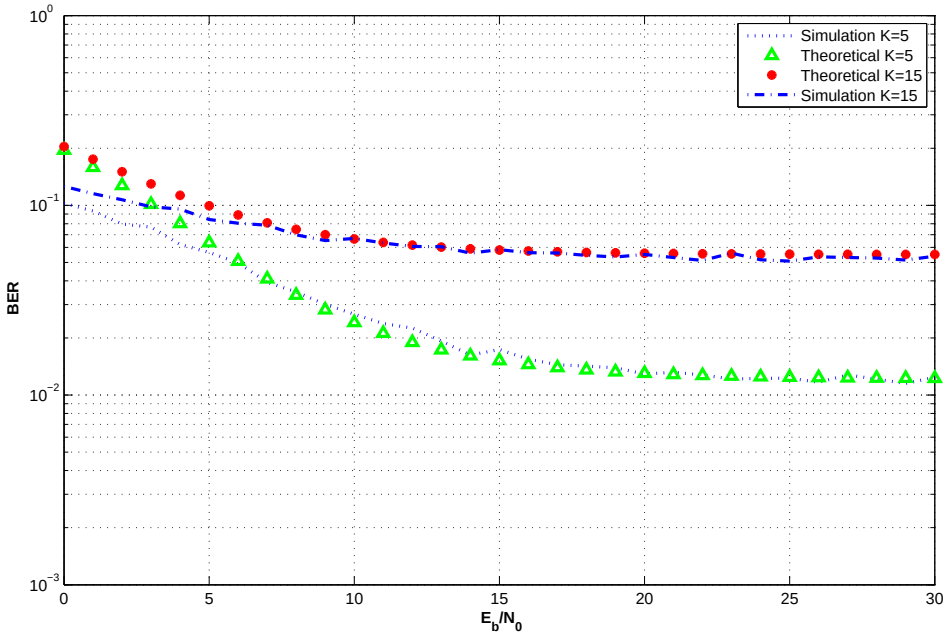

Figure 3.1: Experimental and analytical results of probability of bit error in flat Rayleigh fading environment versus SNR.

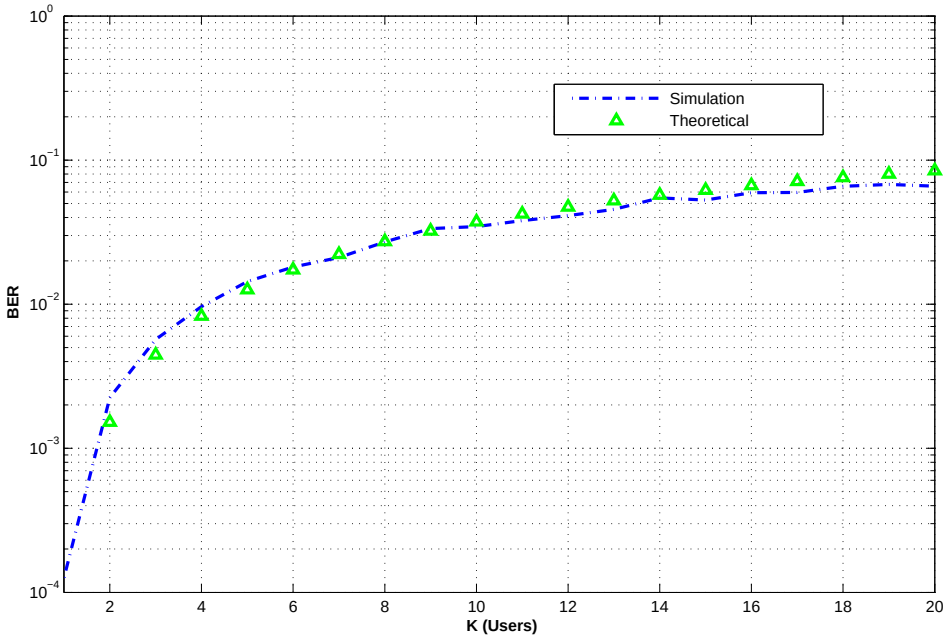

Figure 3.2: Experimental and analytical results of probability of bit error in flat Rayleigh fading environment versus number of subscriber.

Chapter 4

Multiple Input Multiple Output Decision Feedback Equalization

4.1 Introduction

This chapter deals with the construction of the DFE and its advantages. Some alternative decision feedback equalizer structures will also be discussed. Some of the constrained optimization techniques which are being applied to different applications of adaptive filtering such as MIMO-DFE receivers will also be elaborated in this chapter.

4.2 Decision Feedback Equalization (DFE)

In most digital data transmission systems the dispersive linear channel encounters amplitude and phase distortion. As a result, the received signal is affected by ISI. Systems in which a sequence of pulse-shaped information symbols are transmitted, the time domain full response signaling pulses are distorted by the hostile dispersive channel which leads to the inter symbol interference. At the receiver, the linearly distorted signal has to be equalized to recover the information. Equalizers employed at the receiving end for ISI compensation can be classified according to their

structure, the optimizing criterion and the algorithms used to adapt the equalizer coefficients. On the basis of their structures, the equalizers can be classified as linear or decision feedback equalizers. Various methods have been developed to enhance the performance of the communication systems by reducing the effects of the ISI. Linear equalization is one of the methods employed but a major problem with linear equalization is that it doesn't takes in to account the fact that the transmitted sequence has a "finite alphabet" structure.

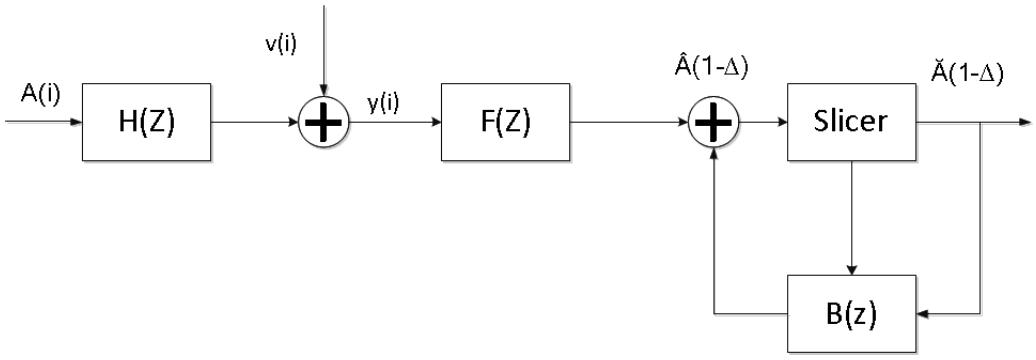

Figure 4.1: Block diagram of Decision Feedback Equalizer

Figure 4.1 shows a simplified block diagram of a DFE where the forward filter and the feedback filter can each be a linear filter, such as transverse filter. The nonlinear characteristic of the DFE is due to the nonlinear characteristic of the detector which is used to provide input to the feedback filter. The basic idea of a DFE is that if the values of the symbols previously detected are known, then ISI caused by these symbols can be mitigated at the output of the forward filter by subtracting previous symbol values with appropriate weighting. The forward and feedback tap weights can be adjusted simultaneously to fulfill a criterion such as minimizing the MSE. The advantage of a DFE structure is the feedback filter,which is additionally working to remove ISI, operates on noiseless quantized levels resulting in an output which is free of channel noise.

4.3 Some Alternative Decision feedback equalizer Structures

4.3.1 Frequency Shift Decision Feedback Equalizer (FRESH-DFE)

Frequency Shift Decision Feedback Equalizer (FRESH-DFE) [77] is a decision feedback equalization technique in which the feed forward filter (FFF) is replaced by a number (bank) of frequency shift adaptive filters to optimize the performance of DFE in a cyclostationary environment. A cyclostationary process is a random signal process that has been subjected to some form of repetitive operation such as sampling, scanning, or multiplexing will usually exhibit statistical parameters that vary periodically with time. In many cases, the repetitive operation is introduced intentionally to put the signal in a format that is easily manipulated and preserves the time-position integrity of the events that the signal is representing. FRESH filter basically is designed to extract data carrying waveform, but it can also be employed to extract the data if its output is sampled at the baud rate. Such FRESH filter technique could be equivalent to a linear Fractionally Spaced Equalizer (FSES) (with an unlimited number of equalizer taps) if the frequency shifts equal to the baud rate and its harmonics. The Decision Feedback Equalizer (DFE) is shown to have better performance in a cyclostationary environment and this is due to the fact that DFE utilizes FSE as its forward filter. DFE exploits the information of the baud rate and its harmonics. The feedback filter (FBF) is used to mitigate the residual IS1 caused by earlier symbols. When compared to the FSE, performance of the DFE is much better, especially in cases where there is high noise and interference. [78] and [77] have shown that FRESH-DFE can achieve better MSE and better Symbol Error Rate (SER) compared to the DFE.

The structure of FRESH-DFE is divided in three parts namely, Conjugate-Linear

(LCL) FRESH filter [78], followed by a baud rate sampler (BRS) and a feedback filter (FBF). Conjugate-Linear filter uses the information of the interference cyclic frequencies at 0, m/T_{in} and $2f_l + k/T_{in}$, BRS uses the information of the symbol rate $1/T$ as well as its harmonics whereas feedback filter (FBF) mitigates the residual IS1 caused by earlier symbols. Even though the input is assumed to be continues in time, it can be represented by an oversampled discrete version. To be able to recover Spectral Correlation density (SCD) of a continues time signal from its discrete-time counterpart, the sampling rate must be greater than twice the Nyquist rate [79]. The higher the sampling rate the better is the performance of the FRESH-DFE. In an environment where inter symbol interference (ISI) is high, FRESH-DFE outperforms the DFE but the complexity increases.

4.3.2 FRESH-DFE: A New Structure for Interference Cancellation

Main causes of poor system performance in the digital cellular system are Fading, shadowing, frequency selectivity and interference but among them ISI and interference particularly lower the performance of any cellular system. Many techniques such as the use of micro and macro diversity against fading and shadowing respectively and equalization against frequency selectivity and interference have been employed to mitigate the adverse effect caused by ISI, co-channel interference (CCI) and adjacent channel interference (ACI). Most of these techniques utilize adaptive filters to alleviate the influence of time variant effects in digital communications. In some cases interference is removed by serial, parallel, or hybrid interference cancelers especially in the case of multiuser CDMA [78, 80, 81]. [82] has used DFE to increase the capacity of CDMA system which uses short spreading sequences. [83] has shown several interference erasure techniques. [84] and [85] have used what is called cyclostationary properties to get rid of interference in a cellular system that uses carriers with certain frequency offsets. Although DFE techniques offer con-

siderable performance gains in systems operating over impaired channels but still more research has to be done to further reduce the effect of interference. A major drawback in a DFE structures found in literature [86–88] assume that digital signals are wide-sense stationary processes but as shown by [89–91] digitally modulated signals exhibit what is called "cyclostationary properties". These cyclostationary properties have been effectively used in digital communications to get rid of interference [82,92–94]. By using the cyclostationary properties of a digitally modulated signal [77] has proposed a new structure of DFE to optimize the performance of DFE under the assumption that the input to the receiver is composed of a quasi-periodic digitally modulated signal of interest and other interfering signals, possibly all mutually differing in carrier frequencies and/or symbol rates. Simulation results carried out in [77] show that the proposed receiver realizes significant improvement over the system that uses conventional DFE. The results also indicate that the performance improvement is much better at lower signal to interference ratio.

4.3.3 Multi Split Decision Feedback Equalizers

Due to the rapid changes in the characteristics of a channel, quick convergence of the equalizer taps to the optimum value is extremely important. However faster convergence will increase the computational cost and as such becomes a conflicting parameter compared to the quick convergence. To overcome this problem, split adaptive techniques were developed which were shown to have quick convergence rate with a small increase in complexity [95–97]. One of the advantages of a Split processing technique is that it provides stability and quicker convergence at the expense of a moderate increase in computational complexity. This idea of multi-split (MS) adaptive filtering is extended to the DFE by [98] to develop a new technique called multi split DFE (MS-DFE) in which split processing is achieved by continuously splitting both the forward filter and the feedback filter with each splitting symmetry and anti symmetry conditions are imposed separately conditions on the impulse responses of

filters by using appropriate and distinct sets of linear constraints. These filters are connected in parallel. Adaptive algorithms such as the LMS, LMS-DCT and RLS algorithms are employed to update the tap coefficients of the equalizer. MS-LMS and MS-IUS algorithms are used when dealing with multi-splitting techniques.

The main problems appearing in adaptive MIMO equalization, i.e., the increased filter size and the colored noise caused by inter stream interference, slow down significantly the performance of stochastic gradient algorithms. On the other hand, the computational requirements of MIMO RLS algorithms increase significantly. In [47], some adaptive schemes with convergence properties close to RLS but of lower computational cost are proposed. But still there computational complexity is very high compared to the LMS type algorithm. For scenarios in which accurate CSI is available at both the transmitter and the receiver, there is a well established framework that unifies the design of linear transceivers under many design criteria [48]. A counterpart for the design of systems with DFE has recently emerged [49–51, 99]. This framework was also extended to MIMO systems with pre-interference subtraction at the transmitter in [99]. However, in many scenarios, such as frequency division duplex systems, obtaining accurate CSI at the transmitter may require a considerable amount of feedback to the transmitter. An approach that allows the designer to limit the required amount of the feedback is to quantize the transmitter design. In these limited feedback schemes [52], the receiver uses its CSI to choose the best transmitter design from a code book of available designs, and then feeds back the index of this precoder to the transmitter. This strategy has been considered for beam forming schemes (e.g., [53–56, 100–102]), unitary precoding with linear equalization (e.g., [58]) and unitary precoding for orthogonal space time block codes [58], [59]. For zero-forcing DFE schemes, a limited feedback scheme in which the receiver feeds back the order of interference cancellation was proposed in [60, 61]. In [51], a limited feedback scheme for systems with a (general) linear precoder at the transmitter and zero-forcing DFE at the receiver is designed.

4.4 Constrained Adaptive Algorithms

The performance of an adaptive algorithm can be improved if the partial knowledge of the channel is incorporated into the algorithm design [103, 104]. Inspired by this idea, an algorithm for the tracking and identification of FIR channels incorporating the variance of the channel noise has been proposed [103]. It was named noise constrained least mean squares (NCLMS) algorithm. NCLMS is a variable step size algorithm (VSLMS) and is a popular modification of LMS algorithm in which step size rule arises from the constraint i.e noise variance. An advantage of the NCLMS algorithm is that it has the same computational complexity as the LMS but with superior performance. NCLMS has been applied to the tracking time constant and time varying channels [64]. A complementary pair LMS (CP-LMS) is developed which could solve the problem of selecting appropriate update step size in LMS algorithm [105]. CP-LMS algorithm is comprised of two adaptive filters which are operating in parallel with different update step sizes with one filter re-initializing the other with the better coefficient estimates. A variable step size for both filters of CP-LMS, which uses the noise variance is implemented in NC-VSLMS algorithm.

Though NCLMS outperforms the VSLMS algorithm in the constant channel environment, the performance will degrade with mismatch.While developing NCLMS, it is assumed that noise variance is known to the receiver. Since it is very strong assumption, an adaptive error constrained LMS has been presented [106]. This algorithm is developed by using a constrained optimization technique called augmented Lagrangian [107] to estimate the variance of the noise. Recently an LMS based constrained adaptive algorithm is designed for CDMA systems which exploit the knowledge of both MAI and noise variances [65]. The novelty of this algorithm resides in the fact that MAI variance was never used as a constraint before. But this algorithm is developed for single input single output CDMA system.

4.5 Constrained optimization techniques

Constrained optimization techniques have been applied to different applications of adaptive filtering such as MIMO-DFE receivers. Few of these techniques are discussed in this chapter.

4.5.1 Constrained MMSE-DFE

As mentioned earlier, the error propagation associated with DFE effects its performance. Several techniques have been devised to mitigate this constraint. One such technique is constrained MMSE-DFE [108] which imposes an inequality norm constraint on the tap energy of the FBF. Therefore, the constraint on the FBF is given as

$$tr\left\{\mathbf{B}^H\mathbf{B}\right\} \leq \xi, \tag{4.5.1}$$

where ξ is the energy threshold. This results in the constraint MMSE solution for the FFF and FBF, respectively as

$$\mathbf{F}_{op}(\lambda) = \left(\mathbf{H}_1\mathbf{H}_1^H + \lambda\mathbf{H}_2\mathbf{H}_2^H + \sigma_z^2\mathbf{I}\right)^{-1}\mathbf{H}_1\mathbf{1}_1, \tag{4.5.2}$$

$$\mathbf{B}_{op}(\lambda) = \mathbf{H}_2^H\mathbf{F}_{op}(\lambda), \tag{4.5.3}$$

where $\mathbf{H}_1$ and $\mathbf{H}_2$ are the sub-matrices of $\mathbf{H}$ and $\mathbf{1}_1 = [\mathbf{0}\,\mathbf{0}\,\ldots\,\mathbf{0}\,\mathbf{I}_M]^T$ is a $(DM \times M)$ matrix; $\mathbf{0}$ is a $(M \times M)$ matrix of all zeros. The choice of the value of the multiplier λ, governs the behavior of the constrained DFE. When $\lambda = 0$, it results in the conventional DFE. This assumes the ideal operation of the FBF, i.e., the post-cursor ISI is canceled by the FBF. When $\lambda = 1$, it results in the MMSE linear equalizer. This assumes that the FFF will mitigate not only the precursor ISI but the post-cursor ISI as well. Severe error propagation can be dealt with by choosing λ very close to 1.

4.5.2 Cyclic MMSE

A property of modulated signals is that they are polycyclostationary (PCS) in nature meaning modulated signals have correlation functions which are time poly-periodic. This property of PCS together with MMSE is used to improve the equalization of modulated signals [109]. The DFE structure is built from the received signal that are possibly shifted by its cyclic frequencies. This structure is particularly beneficial for OFDM where the DFE has been shown exhibit improved BER performance in the presence of narrow band and wide band interference.

4.5.3 Limited Feedback ZF-DFE

Precoding is one technique used in digital communication to suppress the channel impairments to the transmitted symbol. If CSI is available to the transmitter, the data can be precoded before transmission to minimize the channel effects on the symbols. This is equivalent as stating that the data is weighted at the transmitter such that the signal power is maximized at the receiver output, i.e.,

$$\mathbf{x} = \mathbf{P}\mathbf{b}, \tag{4.5.4}$$

where $\mathbf{P}$ is the precoding matrix. The approach devised in [51] presents a design framework for a limited low-rate feedback of the CSI to the transmitter with a zero-forcing DFE. This approach assumes perfect CSI at the receiver. The optimum zero-forcing DFE solution obtained can be written as

$$\mathbf{F} = \mathbf{C}\left(\mathbf{H}\mathbf{P}\right)^{\dagger}, \tag{4.5.5}$$

$$\mathbf{B} = diag\left(\mathbf{L}_{11}, \ldots \mathbf{L}_{KK}\right)\mathbf{L}^{-1} - \mathbf{I}, \tag{4.5.6}$$

where $\mathbf{C} = \mathbf{I} + \mathbf{B}$, $\mathbf{L}$ is a lower triangular matrix resulting from the Cholesky decomposition of $\sigma_z^2\left(\mathbf{P}^H\mathbf{H}^H\mathbf{H}\mathbf{P}\right)^{-1} = \mathbf{L}\mathbf{L}^H$ and $(.)^{\dagger}$ is the pseudo-inverse.

4.5.4 Adaptive Channel Aided DFE

Another approach devised in [110] uses a basic property of the DFE, i.e., the post-cursors of the channel response convolved with the FFF is canceled by the FBF. This approach results in effectively mitigating the propagation errors. The LMS algorithm is used to estimate the channel response and subsequently the optimum solution of the FBF. It incorporates the channel estimator in the DFE structure. The update equation for the MIMO DFE can be written as

$$\mathbf{f}_{nm,k+1} = \mathbf{f}_{nm,k} + \mu_f \mathbf{y}_{nm,k} e_k^*, \tag{4.5.7}$$

where μ_f is the learning rate of the algorithm and e_k^* is the error. If the coefficients of the channel estimator is denoted by $\mathbf{q}$ then the LMS update equation for the estimator is given as

$$\mathbf{q}_{nm,k+1} = \mathbf{q}_{nm,k} + \mu_q \mathbf{b}_{nm,k} e_k^*, \tag{4.5.8}$$

where μ_q is the learning rate of the algorithm and $\mathbf{b}_k$ is the FFF decision. It is shown in [110] that this is essentially a system identification problem where $\mathbf{q}_{nm,opt} = h_{nm}^*$. With the optimum solution $\mathbf{q}_{nm,opt}$, the optimum solution for the FBF is given as

$$\mathbf{b}_{nm,opt} = \text{post}\left\{\mathbf{q}_{nm,opt} \otimes \mathbf{f}_{nm,opt}\right\}, \tag{4.5.9}$$

where $\otimes$ indicates convolution and post $\{.\}$ denotes the post-cursor-taking operation.

4.5.5 Adaptive Conjugate Gradient Decision Feedback Equalizer

The complexity involved in the design of the DFE is the main issue addressed in [47]. The proposed idea applied an adaptive modified conjugate gradient algorithm to derive an equalizer with identical convergence, improved tracking capabilities but with a problem of higher computational load as compared to RLS algorithm. Two updat-

ing strategies of the equalizers filters based on the Galerkin projection are utilized to reduce the complexity. It has been shown that SISO adaptive algorithms based on conjugate gradient methods are numerically steady. Another advantage is that their convergence properties are comparable to the RLS and their computational cost is between RLS and LMS algorithms. The main motivation for this approach was that no work has been done for developing MIMO adaptive equalization algorithms based on CG method. The MIMO DFE solution using the least squares criterion can be computed as the minimum of the cost function

$$J\left(\mathbf{w},\Phi\left(k\right),\mathbf{r}_{i}\left(k\right)\right)=\frac{\mathbf{w}^{H}\Phi\left(k\right)\mathbf{w}}{2}-Re\left\{\mathbf{w}^{H}\mathbf{r}_{i}\left(k\right)\right\} \tag{4.5.10}$$

with respect to $\mathbf{w}$. Matrix $\Phi\left(k\right)$ stands for the exponentially time-averaged input data auto correlation and $\mathbf{r}_{i}\left(k\right)$ is the cross correlation vector. The modified CG method for the MIMO DFE minimizes the cost function in (4.5.10) by iteratively updating the vector $\mathbf{W}$ as

$$\mathbf{W}\left(k\right) \;=\; \mathbf{W}\left(k-1\right)+\mathbf{U}\left(k\right)\mathbf{A}\left(k\right), \tag{4.5.11}$$

where the columns of $\mathbf{U}\left(k\right)$ are the search direction for each M systems and $\mathbf{A}\left(k\right)$ is a $M\times M$ diagonal matrix having the ith step size, $\alpha_{i}\left(k\right)$ given by

$$\alpha_{i}\left(k\right)=\frac{\mathbf{u}_{i}^{H}\left(k\right)\mathbf{t}_{i}\left(k\right)}{\mathbf{u}_{i}^{H}\left(k\right)\Phi\left(k\right)\mathbf{u}_{i}\left(k\right)},\qquad i=1,\ldots,M \tag{4.5.12}$$

The search direction is updated as

$$\mathbf{U}\left(k+1\right)=\mathbf{G}\left(k\right)+\mathbf{U}\left(k\right)\beta\left(k\right), \tag{4.5.13}$$

where $\mathbf{G}\left(k\right)$ is the gradient of the system given by

$$\mathbf{G}\left(k\right)=\mathbf{T}\left(k\right)-\Phi\left(k\right)\mathbf{U}\left(k\right)\mathbf{A}\left(k\right), \tag{4.5.14}$$

where $\mathbf{T}(k)$ is defined as

$$\mathbf{T}(k) = \lambda \mathbf{G}(k-1) + \mathbf{y}(k)\,\mathbf{e}^{H}(k). \tag{4.5.15}$$

The search direction vectors for the next update can be computed as

$$\mathbf{U}(k+1) = \mathbf{G}(k) + \mathbf{U}(k)\,\beta(k), \tag{4.5.16}$$

where the ith diagonal element of the matrix $\beta(k)$ can be computed as

$$\beta_i(k) = \frac{(\mathbf{g}_i(k) - \mathbf{g}_i(k-1))^{H}\,\mathbf{g}_i(k)}{\mathbf{g}_i^{H}(k-1)\,\mathbf{g}_i(k-1)}, \tag{4.5.17}$$

where $\mathbf{g}_i(k)$ is the ith column of the gradient matrix $\mathbf{G}(k)$. Now all the linear systems are constantly updated by the modified conjugate gradient algorithm. This is computationally complex. Using the Galerkin projections, an approximate solution can be obtained by updating through just one seed system j at each instant, while the other systems are updated through the projections, i.e., they use the search direction of the seed system as

$$\mathbf{w}_i(k) = \mathbf{w}_i(k-1) + \mathbf{u}_j(k)\,\alpha_i(k), \tag{4.5.18}$$

where the step size $\alpha_i(k)$ is selected as

$$\alpha_i(k) = \frac{\mathbf{u}_j^{H}(k)\,\mathbf{t}_i(k)}{\mathbf{u}_j^{H}(k)\,\Phi(k)\,\mathbf{u}_i(k)}, \quad i = 1, \ldots, M \tag{4.5.19}$$

and $\mathbf{u}_j(k)$ is the search direction of the seed system. This scheme although reduces the complexity but at the expense of the small performance degradation.

4.5.6 MBER Space-Time Decision Feedback Equalization Assisted Multiuser Detection for Multiple Antenna Aided Space-Division Multiple Access (SDMA) Systems

In the CDMA system, users are separated by a unique user-specific spreading code, whereas in an SDMA system users are separated by a unique user-specific channel impulse response (CIR) found at the receiver antennas. CIR in this case can be termed as a user-specific CDMA signatures and are non orthogonal to each other. This property is not considered a serious limitation as orthogonal spreading codes become non-orthogonal due to the convolution process by the CIR. However, due to this property of the CIRs, an efficient multiuser receiver would be required for separating the users in the SDMA system. One of the popular SDMA-receiver designs is to employ the minimum mean square error (MMSE) multi user detection (MUD) [111]. However, in CDMA and an adaptive beam forming-based MUD cases, perhaps a better option is to choose detector's coefficients by directly minimizing the system's bit error (BER) [112, 113]. For the single-user single-antenna system, the minimum BER (MBER) has been shown to be less susceptible to the error propagation (EP) due to decision feedback errors compared to the MMSE DFE [112]. For the base station employing multiple transmit antennas, an MBER multiuser transmission scheme has been proposed [114], while for the multiple antenna assisted receiver, an MBER rake receiver is proposed based on the adaptive minimum bit error rate (AMBER) criterion [115]. Theoretically MBER ST-DFE-MUD, which is unachievable in practice. The adaptive least bit error rate (LBER) aided ST-DFE-MUD can practically be implemented and can also be characterized in terms of its steady-state BER as well as convergence performance [42]. The MBER ST-DFE-MUD design shows a better BER performance as compared to the standard MMSE design [42]. Another advantage of this technique is that, unlike MMSE design, whose performance decreases considerably due to decision feedback errors

in the presence of multiuser feedback loops, the MBER ST-DFE-MUD is robust to the error propagation (EP). An adaptive implementation of the MBER ST-DFE-MUD is considered based on a stochastic gradient learning algorithm referred to as the LBER technique. LBER ST-DFE-MUD consistently outperforms not only the least mean square (LMS) based ST-DFE-MUD but also has a lower computational complexity than the latter in the case of the BPSK modulation scheme [42]

4.5.7 Fast Techniques for Computing Finite-Length MIMO MMSE Decision Feedback Equalizers

In broadband applications, data is normally transmitted in packets, These packets are made up of a predetermined training sequence followed by random data. An efficient equalization scheme in this scenario can be based on a DFE.

A major concern regarding the success of an equalization scheme is the complexity required for computing the optimal DFE filters. Algorithms for finding the optimal tap coefficients of a MMSE-DFE are based on the Cholesky factorization approach [116]. The approach used in [117] used the generalized Schur algorithm [118] for fast Cholesky decomposition of the matrices involved in both feedback and feed forward filters computation. An alternative approach for computing the optimal DFE coefficients in MIMO DFE is based on formulating the MMSE- DFE as a linear estimation problem [119], as opposed to the constrained linear estimation cost function [117]. But since using the DFE cost function as a linear estimation problem provides same general result, the usefulness of its corresponding optimal expressions has not been fully appreciated. This approach provides more compact formulas than the ones resulting from the constrained formulation of [116] and this can be achieved via a simple observation,that the expression of the resulting feed forward filter (FFF) corresponds exactly to the definition of the Kalman gain matrix encountered in regularized RLS problems in which fast recursions are ready to be used. Subsequently FFF can be efficiently and effectively computed through

fast Kalman gain (FKG) update, whereas the feedback filter (FBF) is achieved through fast and reliable MIMO convolution techniques. The alternative approach for computing the optimal DFE coefficients in MIMO DFE based on formulating the MMSE- DFE as a linear estimation problem has number of advantages when compared to the previously employed techniques namely

1. Significantly reduced computational complexity, for the same channel and DFE filters length and noise statistics. By linear estimation, the complexity of the corresponding formulas depends strongly on and can achieve additional computational gains.

2. The new DFE tap computation uses simplified structured recursions, suitable for a control-flow implementation, making it much simpler than the method used in [117], as the [117] relies on the use of non-structured recursive equations, while often requiring the use of a digital signal processor (DSP).

Chapter 5

Proposed MIMO Receivers

5.1 Introduction

Since MAI is a limiting factor in MIMO-CDMA systems, it is imperative to study the effect of MAI on the system performance. It has been reported in the literature that the learning ability of an adaptive algorithm can be increased if a constraint is added to it. In this chapter, a MIMO-CDMA constrained LMS algorithm is developed to be implemented for the two types of MIMO receivers i.e one with the linear adaptive equalization and the other with MIMO decision feedback equalization. The proposed algorithm is equipped with the knowledge of the number of subscribers, spreading sequence (SS) length, additive noise variance as well as the variance of MAI plus noise (new constraint). A distinguishing feature of this algorithm is that MAI variance has never been used as a constraint though MAI plus noise was used by [65] to develop an algorithm named MAI and noise constrained (MNCLMS) but MNLMS algorithm is applicable to SISO CDMA systems whereas in this work, an algorithm is being developed for MIMO- CDMA systems. A Robbins - Monroe algorithm [**?**] is utilized to minimize the conventional mean-square error criterion incorporating MAI and noise as a new constraint. This scheme will result in MAI and noise constrained LMS (MNCLMS) algorithm in the MIMO-CDMA systems. The

proposed algorithm is a variable step size algorithm as the step size rule is applicable placing the constraints on MAI and noise. By using the proposed, algorithm,the performance of both receivers will be analyzed.

5.2 Motivation

Adaptive algorithms such as least LMS and RLS do not use models for channel coefficients and or noise. Whereas model based algorithms use various types of models such as random walk, auto-regressive etc for coefficients and the additive white Gaussian noise. Model parameters are known or are jointly estimated with the channel. Adaptive algorithms can be inferred to as model based algorithms with model parameters choice dependent on data [120]. It has been reported in the adaptive filtering literature that practically it is possible to improve the performance of the adaptive algorithm if the partial knowledge of the channel is available provided that the computational cost of an algorithm is not increased tremendously. According to the noise constrained LMS algorithm [64]

$$\mathbf{w}_{n+1} = \mathbf{w}_n + \mu_n^l e_n \mathbf{X}_n \tag{5.2.1}$$

$$\mu_{n+1} = 2\mu_n^l(1 + \gamma\lambda_n) \tag{5.2.2}$$

$$\lambda_{n+1} = \lambda_n + \beta\left[(\frac{1}{2}e_n^2 - \sigma_{\nu_m^l}^2) - \lambda_n\right] \tag{5.2.3}$$

λ, α and β are positive constants. This algorithm is a variable step size LMS algorithm because the step size rule is applicable due to the constraint on the noise variance. The computational cost of the aforementioned algorithm is the same as of LMS but the convergence rate of the noise constrained LMS algorithm is much

faster than the LMS due to its three independent parameters.

MAI is the major limiting factor in the system performance of a multisubscriber environment, it is required to design a multi receiver scheme which will mitigate the effect of MAI and additive noise. Previous research work treated MAI as part of interfering noise. This assumption is not practically correct which led this work to use MAI as an additional constraint by using structured information contained in it. It is also believed that by using the combined information of MAI and the interfering noise to form into a single constrained will result in an algorithm which would outperform the noise only constrained algorithm. It should be noted that using MAI alone as a constraint is not a viable choice since noise is an undeniable physical constraint and as such cannot be ignored while developing such algorithms.

As NCLMS algorithm is noise constrained only, a new effective constrained algorithm is developed by incorporating MAI variance in addition to the the noise variance in the algorithm resulting in a generalized MAI plus noise constrained LMS (MNCLMS) adaptive algorithm. Since the proposed algorithm is generalized, this algorithm is able to deduce MAI constrained algorithm, noise constrained algorithm and zero constrained noise algorithm as special cases.

5.3 Algorithm Development

5.3.1 MIMO-CDMA MNCLMS Constrained Algorithm for Linear Equalizer (LE)

The desired subscriber's component can be written as

$$b_m^l = \left[\left(\mathbf{h}_{m1}^l\right)^T \left(\mathbf{h}_{m2}^l\right)^T \ldots \left(\mathbf{h}_{mn}^l\right)^T \right] \left[\left(\mathbf{x}_1^l\right)^T \left(\mathbf{x}_2^l\right)^T \ldots \left(\mathbf{x}_N^l\right)^T \right]^T \tag{5.3.1}$$

In (5.3.1), $\mathbf{h}_{m1}^l = \left[h_{m1}^l \, h_{m1}^{l-1} \ldots h_{m1}^{l-L+1}\right]^T$ is the time varying impulse response of

the channels and is an $L \times 1$ vector, whereas $\mathbf{x}_n^l = \left[x_n^l \, x_n^{l-1} \, \ldots x_n^{l-L+1}\right]^T$ is an $L \times 1$ vector. The filter impulse response of the linear equalizer which consists of a feed forward filter is given by

$$\mathbf{w}_n^l = \left[\left(F_n^l\right)^T\right] \tag{5.3.2}$$

In (5.3.2), F_n^l is the n^{th} MISO feed forward filter (FFF) with dimension of $ML \times 1$, where L is the taps of feed forward filter and M is the number of receivers.

The mean-squared error to be minimized is given by

$$J\left(\mathbf{w}_n^l\right) = \left[e_n^l\right]^2 \tag{5.3.3}$$

Where e_n^l is the error between the output of the decision device and the linear filter and can be written as

$$e_n^l = \hat{x}_n - \mathbf{w}_n^l D_n^l \tag{5.3.4}$$

D_n^l is the combined input to the LE and is given by

$$D_n^l = \left[\left(\mathbf{y}_n^l\right)^T\right] \tag{5.3.5}$$

and is of the order of $(ML \times 1)$. $\mathbf{y}_n^l = \left[\left(\mathbf{y}_1^l\right)^T \; \left(\mathbf{y}_2^l\right)^T \quad \left(\mathbf{y}_{\mathrm{M}}^l\right)^T\right]^T$ is the input to the feed forward filter (FFF) of dimension $ML \times 1$ and is a collection of vectors consisting of y_m^l given by $\mathbf{y}_m^l = \left[y_m^l \; y_m^{l-1} \quad y_m^{l-L+1}\right]^T$.

and

$$\hat{\mathbf{x}}_n = \mathbf{w}_o^T D_n^l = \mathbf{x}_n^l + \bar{\nu}_n^l \tag{5.3.6}$$

or

$$\mathbf{x}_n^l = \mathbf{w}_o^T D_n^l - \bar{\nu}_n^l \tag{5.3.7}$$

$\bar{\nu}_n^l$ is the filtered noise which passes through feed forward filter and is composed of MAI and noise.

Minimization of the cost function in (5.3.3) over $\mathbf{w}_n^l$ will give the optimal value at time l. In other words, $\mathbf{w}_{opt} = H_{mn}^l$(of size $1 \times NL$ matrix) with $\hat{J}(opt) = \sigma^2_{\bar{\nu}_n^l}$ represents the minimum mean squared error (MSE).It is shown in the literature that knowledge of $\sigma^2_{\bar{\nu}_n^l}$ [64] is quite helpful in the selecting the search direction for an adaptive algorithm in multiuser case similar to the MNCLMS algorithm in single user environment.

Now, it is desired to minimize $J(\mathbf{w}_n^l)$ over $\mathbf{w}_n^l$ subject to the constraint $J(\mathbf{w}_n^l) = \sigma^2_{\bar{\nu}_n^l}$. The Lagrangian of this would be

$$J_1(\mathbf{w}_n^l, \lambda_n^l) = J(\mathbf{w}_n^l) + \lambda_n^l \left[J(\mathbf{w}_n^l) - \sigma^2_{\bar{\nu}_n^l} \right] \tag{5.3.8}$$

As critical values of λ_n^l are not unique in our case, so we are using an augmented Lagrangian to get rid of this issue by defining the under mentioned cost function

$$J_2(\mathbf{w}_n^l, \lambda_n^l) = J(\mathbf{w}_n^l + \gamma \lambda_n^l \left[J(\mathbf{w}_n^l) - \sigma^2_{\bar{\nu}_n^l} \right] - \gamma_n \lambda_n^2 \tag{5.3.9}$$

Solution to (5.3.9) is given by using the method used in [64] and is shown to be

$$\mathbf{w}_n^{l+1} = \mathbf{w}_n^l + \mu_n^l e_n^l D_n^l \tag{5.3.10}$$

where μ_n^l is the positive step size and is

$$\mu_n^l = \mu_n \left(1 + \gamma_n \lambda_n^l\right) \;\; m = 1, 2, \ldots, M \tag{5.3.11}$$

$$\lambda_n^{l+1} = \lambda_n + \beta_n \left[\frac{1}{2} (e_n^{l^2} - \sigma^2_{\nu_n^l}) - \lambda_n^l \right] \;\; m = 1, 2, , \ldots, M \tag{5.3.12}$$

As channel taps are independent from the spreading sequences and the data sequences, the interferer's components are also independent of each other with zero mean.

The variance of MAI for an equal power can be set up as

$$U_m^l = A^2 \left(\frac{K-1}{N_C} \right) \sum_{n=1}^{N} E\left[h_{mn}^2\right] \tag{5.3.13}$$

whereas the variance of MAI in the unequal transmitted power is given by

$$U_m^l = \frac{\sum_{k=2}^{k} (A^k)^2}{N_C} \sum_{n=1}^{N} E\left[h_{mn}^2\right] \tag{5.3.14}$$

In (6.4.14) and (5.3.14) $E\left[h_{mn}^2\right]$ is the second moment of $E\left[h_{mn}\right]$.

5.3.2 MIMO-CDMA MNCLMS Constrained Algorithm for Decision Feedback Equalizer (DFE)

Desired subscriber's component can be expressed as

$$b_m^l = \left[\left(\mathbf{h}_{m1}^l\right)^T \left(\mathbf{h}_{m2}^l\right)^T \ldots \left(\mathbf{h}_{mn}^l\right)^T \right]^T \left[\left(\mathbf{x}_1^l\right)^T \left(\mathbf{x}_2^l\right)^T \ldots \left(\mathbf{x}_N^l\right)^T \right]^T \tag{5.3.15}$$

In the equation above, $h_{mn} = \left[h_{mn}^l \, h_{mn}^{l-1} \ldots h_{mn}^{l-L+1}\right]^T$is the time varying impulse response of the channels and is an $L \times 1$ vector, whereas $\mathbf{x}_n^l = \left[x_n^l \, x_n^{l-1} \ldots x_n^{l-L+1}\right]^T$is an $L \times 1$ vector.The impulse filter response of the decision feedback equalizer which consists of a feed forward and a feedback filter is given by

$$\mathbf{w}_n^l = \left[\left(F_n^l\right)^T \quad , - \left(B_n^l\right)^T \right]^T \tag{5.3.16}$$

In 5.3.16, F_n^l is the n^{th} MISO feed forward filter (FFF) with dimension of $ML \times 1$

and B_n^l is the n^{th} MISO feedback filter (FBF) of $NQ \times 1$ dimension, whereas L and Q are the taps of FFF and FBF respectively.

The mean-squared error to be minimized is given by

$$J\left(\mathbf{w}_n^l\right) = \left[e_n^l\right]^2 \tag{5.3.17}$$

Where e_n^l is the error between the output of the decision device and the DFE and can be written as

$$e_n^l = \hat{x}_n - \mathbf{w}_n^l D_n^l \tag{5.3.18}$$

D_n^l is the combined input to the DFE and is given by

$$D_n^l = \left[\left(\mathbf{y}_n^l\right)^T \qquad \left(\mathbf{x}_n^l\right)^T\right]^T \tag{5.3.19}$$

and is of the order of $(ML + NQ) \times 1)$. It should be noted that

$$\mathbf{y}_n^l = \left[\left(\mathbf{y}_1^l\right)^T \ \left(\mathbf{y}_2^l\right)^T \quad \left(\mathbf{y}_{\mathrm{M}}^l\right)^T\right]^T$$

is the input to the feed forward filter (FFF) of dimension $ML \times 1$ and is a collection of vectors consisting of y_m^l given by

$$\begin{aligned} \mathbf{y}_m^l &= \left[y_m^l \ y_m^{l-1} \quad y_m^{l-L+1}\right]^T \\ \mathbf{x}_n^l &= \left[\left(\mathbf{x}_1^l\right)^T \qquad \left(\mathbf{x}_N^l\right)^T\right]^T \end{aligned}$$

$\mathbf{x}_n^l$ is the input to FBF of dimension $NQ \times 1$, whereas $\mathbf{x}_N^l = \left[x_n^l \ \mathbf{x}_n^{l-1} \quad \mathbf{x}_n^{l-Q+1}\right]^T$ and

$$\hat{\mathbf{x}}_n = \mathbf{w}_o^T D_n^l = \mathbf{x}_n^l + \bar{\nu}_n^l \tag{5.3.20}$$

or

$$\mathbf{x}_n^l = \mathbf{w}_o^l D_n^l - \bar{\nu}_n^l \tag{5.3.21}$$

$\bar{\nu}_n^l$ is the filtered noise which passes through feed forward filter and is composed of MAI and noise.

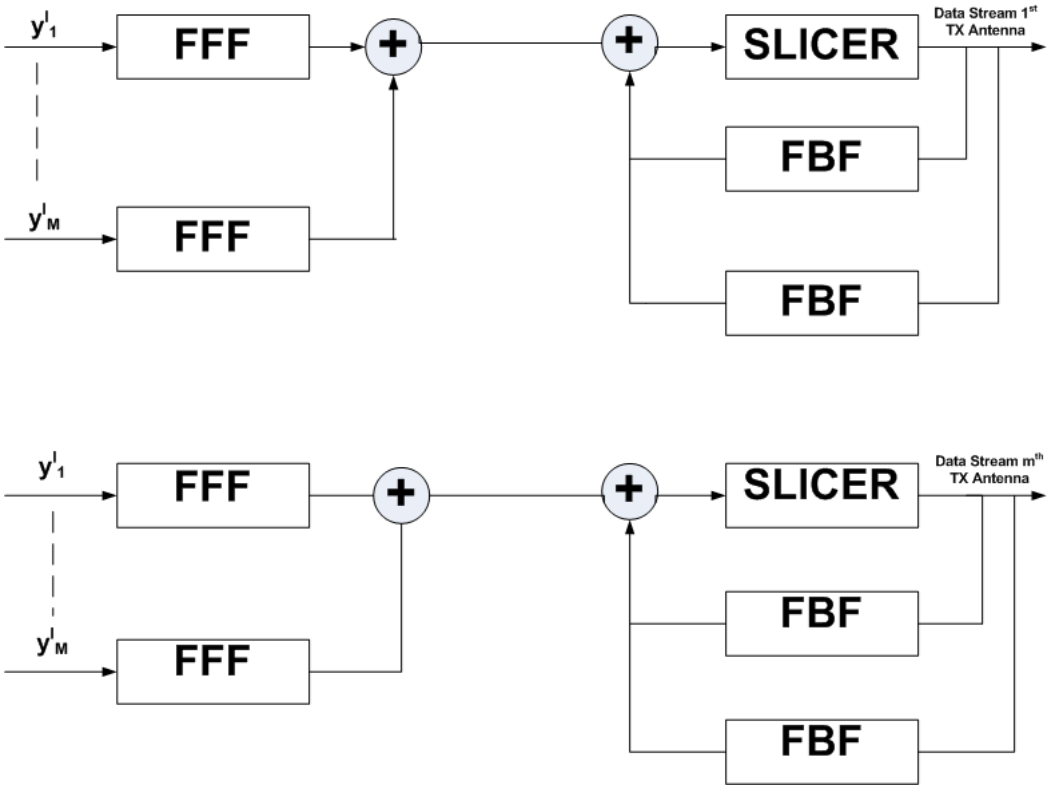

Figure 5.1: MIMO-DFE at single antenna

Minimization of the cost function in equation (5.3.17) over $\mathbf{w}_n^l$ will give the optimal value at time l. In other words, $\mathbf{w}_{opt} = H_{mn}^l$(of size $1 \times NL$ matrix) with $\hat{J}(opt) = \sigma_{\bar{\nu}_n^l}^2$ represents the minimum MSE. It is shown in the literature that knowledge of $\sigma_{\bar{\nu}_n^l}^2$ [64] is quite helpful in the selecting the search direction for an adaptive algorithm in multiuser case similar to the MNCLMS algorithm in single subscriber environment.

Now, it is desired to minimize $J(\mathbf{w}_n^l)$ over $\mathbf{w}_n^l$ subject to the constraint $J(\mathbf{w}_n^l) = \sigma_{\bar{\nu}_n^l}^2$. The Lagrangian of this would be

$$J_1(\mathbf{w}_n^l, \lambda_n^l) = J(\mathbf{w}_n^l) + \lambda_n^l \left[J(\mathbf{w}_n^l) - \sigma^2_{\bar{\nu}_n^l} \right] \tag{5.3.22}$$

As critical values of λ_n^l are not unique in our case, so We are using an augmented Lagrangian to get rid of this issue by defining the under mentioned cost function

$$J_2(\mathbf{w}_n^l, \lambda_n^l) = J(\mathbf{w}_n^l + \gamma \lambda_n^l \left[J(\mathbf{w}_n^l) - \sigma^2_{\bar{\nu}_n^l} \right] - \gamma_n \lambda_n^2 \tag{5.3.23}$$

Solution to (5.3.23) is given by using the method used in [64] and is shown to be

$$\mathbf{w}_n^{l+1} = \mathbf{w}_n^l + \mu_n^l e_n^l D_n^l \tag{5.3.24}$$

where μ_n^l is the positive step size and is

$$\mu_n^l = \mu_n \left(1 + \gamma_n \lambda_n^l\right) \;\; m = 1, 2, \ldots, M \tag{5.3.25}$$

$$\lambda_n^{l+1} = \lambda_n + \beta_n \left[\frac{1}{2} (e_n^{l^2} - \sigma^2_{\bar{\nu}_n^l}) - \lambda_n^l \right] \;\; m = 1, 2, , \ldots, M \tag{5.3.26}$$

5.4 Generalized MIMO MAI and Noise-Constrained LMS Algorithm

Based on the MAI variance analysis, the proposed MAI and noise constrained LMS (MNCLMS) algorithm as was defined in equations (5.3.24) , (5.3.25) and (5.3.26) is being modified to include the MAI variance.

So for equal transmitted power (EPT) the algorithm will look like

$$\lambda_n^{l+1} = \lambda_n^l + \beta_n \left\{ \frac{1}{2} \left(\left(e_n^l\right)^2 - \frac{A^2(k-1) \sum_{n=1}^{N} E([h]}{N_C} - \sigma^2_{\bar{\nu}_n^l} \right) \right\} - \lambda_n^l \tag{5.4.1}$$

And for unequal transmitted power (UTP), MNCLMS would be

$$\lambda_n^{l+1} = \lambda_n^l + \beta_n \left\{ \frac{1}{2} \left(\left(e_n^l\right)^2 - \frac{\sum_{k=2}^{k} (A^K)^2 \sum_{n=1}^{N} E([h]}{N_C} - \sigma^2_{\nu_n^l} \right) \right\} - \lambda_n^l \tag{5.4.2}$$

5.5 Computational Complexity of the Proposed Algorithms

Computational cost of an algorithm is an important aspect of any algorithm. Higher computational cost can render an algorithm useless. A trade off between computational cost and the performance is possible, i.e, if the increased cost results in considerable performance gain, then higher cost can be ignored. In this section, we present the computational costs of few algorithms. As can be seen in table 5.1 and table 5.2, computational cost of the proposed algorithms is higher when compared to [65] but MNCLMS is for SISO- CDMA case, whereas, the proposed algorithm is for MIMO- CDMA case. This algorithm can be used for run-time applications like channel estimation, tracking and channel equalization. MIMO systems are being used in modern wireless standards.

Table 5.1: Computational complexity per iteration for different algorithms for real valued data in terms of the real multiplications, real additions and real divisions

Algorithm	$\times$	$+$
LMS	$2L+1$	L
RLS	L^2+5L+1	L^2+3L
MNCLMS [121]	$2L+1$	$2L+6$
MIMO-MNCLMS(LE)	$2ML+8$	$2ML+4$

Table 5.2: Computational complexity per iteration for different algorithms for real valued data in terms of the real multiplications, real additions and real divisions

Algorithm	$\times$	$+$
LMS	$2L+1$	$2L$
RLS	L^2+5L+1	L^2+3L
MNCLMS [121]	$2L+1$	$2L+6$
MIMO-MNCLMS(DFE)	$2\left(ML+NQ\right)+8$	$ML+NQ+4$

Chapter 6

Convergence Analysis, Transient Analysis and Tracking Analysis of the MNCLMS Algorithms in The Presence of MAI and Noise

6.1 Introduction

In this chapter, convergence analysis, transient analysis and tracking analysis of the MNCLMS algorithms will be performed in the presence of MAI and noise for linear as well as decision feedback equalizers. Performance of the proposed MNCLMS algorithms for LE and DFE will be presented at the end of the chapter by comparing it with other algorithms such as ZNCLMS, NCLMS and the MCLMS.

6.2 Convergence Analysis of the MNCLMS Algorithms in the Presence of MAI and Noise

This section deals with the convergence analysis of the proposed MNCLMS algorithm in the presence of noise plus MAI. Following independent assumptions [122] are being used while performing the convergence analysis.

A1: The input process $\left\{\mathbf{x}_n^l\right\}$ is an i.i.d random variable with correlation matrix of R_{xx}

A2: The noise sequence is zero mean i.i.d. sequence, Gaussian random variable with variance $\sigma^2_{\nu_n^l}$ and is independent of the input process

A3: MAI in AWGN environment represented by U_l^m is zero mean i.i.d Gaussian random variable with variance $\sigma^2_{U_m^l}$ and is independent of both the input process as well as the noise.

A4: For any fixed time say l, step size μ_n^l and weight vector $\mathbf{v}_n^l$ are thought to be statistically independent.

The above mentioned assumptions are justified as follow

For assumption 1, we did not placed a strong condition, i.e we are not assuming that the input process should be Gaussian.

Assumption 2 termed as independent assumption, is also commonly used in the literature

Gaussian appropriation of MAI in AWGN is well known and has been used numerous forms [123]. As MAI is independent of the noise process, assumption 3 can be validated. In this way, MAI plus noise is also independent of the input process.

Generally μ_n^l and $\mathbf{v}_n^l$ are dependent but if the parameters are chosen in such a way that steady-state variance of μ_n^l and or $\mathbf{v}_n^l$ is small, assumption 4 can be justified.

$\mathbf{x}_k$ and $\mathbf{x}_n$ are also independent as both are uncorrelated for $n \neq k$.Thus the input vector $\mathbf{x}_n$ and the weight error vector (defined later)$\mathbf{v}_n^l$ are also independent [124].

6.3 Convergence in the Mean for Linear Equalizer (LE)

Weight update equation of the proposed algorithm is given by

$$\mathbf{w}_n^{l+1} = \mathbf{w}_n^l + \mu_n^l e_n^l D_n^l \tag{6.3.1}$$

Where $n = 1, 2....., N$ represents the n^{th} stream.

If $\mathbf{w}_{n(opt)}$ is said to be the optimum value of weight, then the weight error vector $\mathbf{v}_n^l$ can be defined as

$$\mathbf{v}_n^l = \mathbf{w}_{n(opt)} - \mathbf{w}_n^l \tag{6.3.2}$$

Subtracting $\mathbf{w}_{n(opt)}$ from both side of (5.3.24) results in

$$\mathbf{v}_n^{l+1} + \mathbf{w}_{n(opt)} = -\mathbf{w}_n^l + \mathbf{w}_{n(opt)} - \mu_n^l e_n^l D_n^l$$

$$\mathbf{v}_n^{l+1} = \mathbf{v}_n^l - \mu_n^l e_n^l D_n^l \tag{6.3.3}$$

The desired response of the decision device $\left(\tilde{\mathbf{x}}_n^l\right)$can be expressed as

$$\tilde{\mathbf{x}}_n^l = \mathbf{w}_{(opt)}^T D_n^l \tag{6.3.4}$$

The error is then given by

$$e_n^l = \mathbf{w}_{(opt)}^T - (\mathbf{w}_n^l)^T \tag{6.3.5}$$

For $n = 1, 2, \ldots N$.

(6.3.5) can be compactly written as

$$e_n^l = \left(\mathbf{v}_n^l\right)^T D_n^l = \left(D_n^l\right)^T \mathbf{v}_n^l \tag{6.3.6}$$

Now the recursion of the weight error vector can be shown to be

$$\mathbf{v}_n^{l+1} = \mathbf{v}_n^l - \mu_n^l D_n^l \left(D_n^l\right)^T \mathbf{v}_n^l \tag{6.3.7}$$

$$\mathbf{v}_n^{l+1} = \left\{\mathbf{I} - \mu_n^l D_n^l \left(D_n^l\right)^T\right\} \mathbf{v}_n^l \tag{6.3.8}$$

Taking expectation on both sides of (6.3.8) with the assumptions made earlier, will yield

$$\bar{\mathbf{v}}_n^l = \left[\mathbf{I} - \bar{\mu_n^l} E\left\{D_n^l \left(D_n^l\right)^T\right\}\right] \bar{\mathbf{v}}_n^l \tag{6.3.9}$$

$\bar{\mu}_n^l = E\left[\mu_n^l\right]$ is the mean step size and $\bar{\mathbf{v}}_n^l = E\left[\mathbf{v}_n^l\right]$ is the weight error vector in the equation above. Whereas

$$E\left[D_n^l \left(D_n^l\right)^T\right] = E\left[\left(\mathbf{y}_n^l\right)^T\right] \left[\left(\mathbf{y}_n^l\right)^T\right]^T$$

or

$$\tilde{R} = E\left[\left(\mathbf{y}_n^l\right)^T\right]^T \left[\left(\mathbf{y}_n^l\right)^T\right] \tag{6.3.10}$$

6.3.1 Auto-correlation Structure of MIMO-CDMA Linear Equalizer (LE)

$\tilde{R}$ is the correlation matrix of the input process i.e, $\tilde{R} = E\left[D_n^l \left(D_n^l\right)^T\right]$ and is given by

$$\tilde{R} = R_{D_n^l D_n^l} \tag{6.3.11}$$

6.3.2 Eigenvalues of Linear Equalizer (LE)

The value of $\bar{\mu}_n$is bounded in the range

$$0 < \bar{\mu}_n < \frac{2}{\kappa_{max}} \tag{6.3.12}$$

where κ_{max} is the maximum eigenvalue of the input correlation matrix $\tilde{R}$. By using a strong but simpler condition for convergence of the mean weight error vector [125] can be written as

$$\mu_{max} < \frac{2}{\kappa_{max}} \tag{6.3.13}$$

6.4 Convergence in the Mean for Decision Feedback Equalizer (DFE)

Weight update equation of our proposed algorithm is given by

$$\mathbf{w}_n^{l+1} = \mathbf{w}_n^l + \mu_n^l e_n^l D_n^l \tag{6.4.1}$$

If $\mathbf{w}_{n(opt)}$ is said to be the optimum value of weight, then the weight error vector $\mathbf{v}_n^l$can be defined as

$$\mathbf{v}_n^l = \mathbf{w}_{n(opt)} - \mathbf{w}_n^l \tag{6.4.2}$$

Subtracting $\mathbf{w}_{n(opt)}$ from both side of (5.3.24) results in

$$\mathbf{v}_n^{l+1} + \mathbf{w}_{n(opt)} = -\mathbf{w}_n^l + \mathbf{w}_{n(opt)} - \mu_n^l e_n^l D_n^l$$

$$\mathbf{v}_n^{l+1} = \mathbf{v}_n^l - \mu_n^l e_n^l D_n^l \tag{6.4.3}$$

If the DFE is optimum then, the desired response of the decision device $\left(\tilde{\mathbf{x}}_n^l\right)$can be expressed as

$$\tilde{\mathbf{x}}_n^l = \mathbf{w}_{(opt)}^T D_n^l \tag{6.4.4}$$

The error is then given by

$$e_n^l = \mathbf{w}_{(opt)}^T - (\mathbf{w}_n^l)^T \tag{6.4.5}$$

For $n = 1, 2, \ldots N$.

(6.4.5) can be compactly written as

$$e_n^l = \left(\mathbf{v}_n^l\right)^T D_n^l = \left(D_n^l\right)^T \mathbf{v}_n^l, \tag{6.4.6}$$

Now the recursion of the weight error vector can be shown to be

$$\mathbf{v}_n^{l+1} = \mathbf{v}_n^l - \mu_n^l D_n^l \left(D_n^l\right)^T \mathbf{v}_n^l \tag{6.4.7}$$

$$\mathbf{v}_n^{l+1} = \left\{\mathbf{I} - \mu_n^l D_n^l \left(D_n^l\right)^T\right\} \mathbf{v}_n^l \tag{6.4.8}$$

Taking expectation on both sides of (6.4.8) with the assumptions made earlier, will yield

$$\bar{\mathbf{v}}_n^{l+1} = \left[\mathbf{I} - \bar{\mu}_n^l E\left\{D_n^l \left(D_n^l\right)^T\right\}\right] \bar{\mathbf{v}}_\mathbf{n}^\mathbf{l} \tag{6.4.9}$$

$\bar{\mu}_n^l = E\left[\mu_n^l\right]$ is the mean step size and $\bar{\mathbf{v}}_n^l = E\left[\mathbf{v}_n^l\right]$is the weight error vector in the equation above and

$$E\left[D_n^l \left(D_n^l\right)^T\right] = E\left[\left(\mathbf{y}_n^l\right)^T \quad \left(\mathbf{x}_n^l\right)^T\right]\left[\left(\mathbf{y}_n^l\right)^T \quad \left(\mathbf{x}_n^l\right)^T\right]^T$$

or

$$\tilde{R} = E\left[\left(\mathbf{y}_n^l\right)^T \quad \left(\mathbf{x}_n^l\right)^T\right]^T\left[\left(\mathbf{y}_n^l\right)^T \quad \left(\mathbf{x}_n^l\right)^T\right] \tag{6.4.10}$$

6.4.1 Auto-correlation Structure of Decision Feedback Equalizer (DFE)

$\tilde{R}$ is the correlation matrix of the input process i.e, $\tilde{R} = E\left[D_n^l \left(D_n^l\right)^T\right]$ and is given by

$$\tilde{R} = \begin{bmatrix} R_{yy} & R_{yx} \\ R_{xy} & R_{xx} \end{bmatrix} \tag{6.4.11}$$

Now (6.4.9) looks like

$$\bar{\mathbf{v}}_n^{l+1} = \left(I - \bar{\mu}_n^l \tilde{R}\right)\bar{\mathbf{v}}_\mathbf{n}^\mathbf{l} \tag{6.4.12}$$

R_{yy} in (6.4.11) refers to the auto-correlation matrix of $\mathbf{y}_m^l$ i.e input to the feed forward filter and is composed of

$$R_{yy} = R_{b_n} + R_{U_m^l} + R_{\bar{\nu_n^l}} \tag{6.4.13}$$

$R_{\bar{\nu_n^l}} = \sigma^2_{\bar{\nu_n^l}} I$ and $R_b = E_{b_n} I$, since noise and data sequence are both i.i.d. Now, $R_{U_m^l} = \sum_{n=1}^{N} \sigma^2_{1_n} I \sigma^2_{hn} I$. (6.4.13) can be written as

$$R_{yy} = E_b I + \sum_{n=1}^{N} \sigma^2_{1_n}\sigma^2_{hn} I + \sigma^2_{\bar{\nu_n^l}} I \tag{6.4.14}$$

The second term of (6.4.14) represents the MAI because it is an independent but is not identical and I is an $ML \times ML$ identity matrix.

6.4.2 Eigenvalues of Decision Feedback Equalizer (DFE)

To find the eign value of $\tilde{R}$, we are transforming it according to the following

$$\begin{bmatrix} R_{yy} & R_{yx} \\ R_{xy} & R_{xx} \end{bmatrix} = \begin{bmatrix} c & b \\ b^T & Q \end{bmatrix} \tag{6.4.15}$$

where, $c = E_b + \sigma^2_{\nu^l_n} + \sum_{n=1}^{N} \sigma^2_{U^l_m}$ and is a scalar, Q is a sub matrix of $\tilde{R}$ given as $Q = \tilde{R}(2 : ML + NQ, 2 : ML + NQ)$. First row and first column of $\tilde{R}$ are left out. $b = [0_1 \ldots 0_{ML-1}, x_1, \ldots x_{NQ-1}]$, and $b^T b = \|b\|^2$

As there is no closed form expression for determining the eigenvalues of the correlation matrix defined in equation (6.4.11). A method to bound the eigenvalues of positive-definite Toeplitz matrices can be found in [126] and its application to the correlation matrix given in (6.4.11) can be found in [127] and are given by

$$\kappa_{max} \leq \kappa \leq \kappa_{min} \tag{6.4.16}$$

where

$$\kappa_{min} = \frac{E_b + \sigma^2_{\nu^l_n} + \sum_{n=1}^{N} \sigma^2_{U^l_n} + \eta_1}{2} + \sqrt{\frac{\left(E_b + \sigma^2_{\nu^l_n} + \sum_{n=1}^{N} \sigma^2_{U^l_m}\right)^2}{4} + \|b\|^2}$$

$$\kappa_{max} = \frac{E_b + \sigma^2_{\nu^l_n} + \sum_{n=1}^{N} \sigma^2_{U^l_m} + \eta_{p-1}}{2} + \sqrt{\frac{\left(E_b + \sigma^2_{\nu^l_n} + \sum_{n=1}^{N} \sigma^2_{U^l_m} - \eta_{p-1}\right) + \|b\|^2}{4}}$$

where η_1 is any lower bound on the minimal eigenvalue and η_{p-1} is any upper bound on maximal eigenvalue of Q respectively.

If $L \geq 1$ and $Q \geq 2$, then

$$\kappa_{max} \approx E_b + (ML + 1) \sum_{n=1}^{N} \sigma^2_{U^l_m} + \sigma^2_{\nu^l_m} \tag{6.4.17}$$

and

$$\kappa_{min} = \frac{2E_b + \sigma^2_{\nu^l_n} - \sqrt{4\left(E_b\right)^2 + \left(\sigma^2_{\nu^l_n}\right)^2}}{2} \tag{6.4.18}$$

Since, $\bar{\mu}^l_n = E\left[\mu_n\right]$ is the mean step size and $\bar{\lambda}_n = E\left[\lambda_n\right]$, the value of $\bar{\mu}^l_n$ is bounded in the range

$$0 < \bar{\mu}^l_n < \frac{2}{\kappa_{max}} \tag{6.4.19}$$

Where κ_{max} is given by (6.4.17).

6.5 Transient Analysis of the Proposed Algorithm

Transient analysis of an adaptive algorithm is very important to observe the convergence behavior of an adaptive algorithm and to derive steady-state expressions for different error performance measures, such as EMSE and mean-square deviation (MSD). Basically, transient analysis is the observation of the time-evolution of the adaptive algorithms when there are variations in the signal statistics; or in other words to study the learning mechanism of an adaptive algorithm. Energy conservation method is used to carry out the transient analysis [128].

6.5.1 Error Measures

Transient analysis of an adaptive algorithm deals with the time evaluation of of $E\left[\left|e^l_n\right|^2\right]$and $E\left[\|\mathbf{v}^l_n\|^2\right]$, where $\mathbf{v}^l_n$ is the weight error vector and is given by

$$\mathbf{v}^l_n = \mathbf{w}^l_{n(opt)} - \mathbf{w}^l_n \tag{6.5.1}$$

For some symmetric positive definite weighting matrix Ω ,We define, weighted a priori and a posteriori estimation errors as

$$e^{\Omega}_{an} = \left(\mathbf{v}^l_n\right)^T \Omega D^l_n \tag{6.5.2}$$

and

$$e_{pn}^{\Omega} = \left(\mathbf{v}_n^{l+1}\right)^T \Omega D_n^l \tag{6.5.3}$$

For the case when, $\Omega = I$, the weighted a priori and a posteriori estimation errors defined above will be reduced to a standard a priori and a posteriori estimation errors, respectively, i.e

$$e_{an}^{l} = \left(D_n^l\right)^T \mathbf{v}_n^l \tag{6.5.4}$$

and

$$e_{pn}^{l} = \left(D_n^l\right)^T \mathbf{v}_n^{l+1} \tag{6.5.5}$$

It will be elaborated later in that different choices of Ω will yield different performance measures for the evaluation of an adaptive filter.

Since,

$$e_n^l = \mathbf{x}_n^l - \left(\mathbf{w}_n^l\right)^T D_n^l = \left(\mathbf{w}_{(opt)}\right)^T - \bar{\nu_n^l} - \left(\mathbf{w}_n^l\right)^T D_n^l$$

$$e_n^l = \left(\mathbf{v}_n^l\right)^T D_n^l - \nu_n^l = e_{an}^l - \bar{\nu_n^l} \tag{6.5.6}$$

Also, by using (6.5.3) and and (6.4.3) it can be shown that

$$e_{pn}^{\Omega,l} = e_{an}^{\Omega,l} - \mu_n^l \|D_n^l\|_{\Omega}^2 e_n^l \tag{6.5.7}$$

6.5.2 Performance Measures

The EMSE of the proposed algorithm is given by

$$EMSE = E\left[\left|e_{an}^l\right|^2\right] \tag{6.5.8}$$

and steady state EMSE is

$$E\left[\left|e_{an}^l\right|^2\right] = \xi_{\infty} \tag{6.5.9}$$

6.5.3 Fundamental Weighted Energy Relation

The fundamental weighted-energy conservation relation [128] is used in this section to develop the framework for the transient analysis of the proposed MNCLMS algorithm. (6.5.7) can be expressed as

$$e_n^{\Omega,l} = \frac{e_n^{\Omega,n} - e_{pn}^{\Omega,l}}{\mu_n^l \left\| D_n^l \right\|_\Omega^2} \tag{6.5.10}$$

By using (6.4.3) and (6.5.10) ,the following equation can be established

$$\bar{\mathbf{v}}_n^{l+1} = \mathbf{v}_n^l - \frac{D_n^l}{\left\| D_n^l \right\|_\Omega^2} \left[e_{an}^{\Omega,l} - e_n^{\Omega,l} \right] \tag{6.5.11}$$

The fundamental weighted-energy conservation relation can be shown as

$$\mathbf{v}_n^{l+1} + \frac{1}{\left\| D_n^l \right\|_\Omega^2} \left| e_{an}^{\Omega} \right|^2 = \left\| \mathbf{v}_n^l \right\|_\Omega^2 + \frac{1}{\left\| D_n^l \right\|_\Omega^2} \left| e_{pn}^{l,\Omega} \right|^2 \tag{6.5.12}$$

6.5.12 describes, how the weighted energies of the error quantities evolve with time. Different choices of Ω will yield different performance measures for the evaluation of an adaptive filter [128].

6.5.4 Time Evolution of the Weighted Variance

This section deals with derivation of time evolution of the weighted variance for the proposed MNCLMS algorithm using the fundamental weighted-energy conservation relation equation (6.5.12). Substituting (6.5.7) into (6.5.12) and taking expectation on both sides will result in

$$E\left[\left\| \mathbf{v}_n^{l+1} \right\|_\Omega^2 \right] = E\left[\left\| \mathbf{v}_n^l \right\|_\Omega^2 \right] - 2\bar{\mu_n^l} E\left[e_{an}^{l,\Omega} e_n \right] + \overline{(\mu_n^l)^2} E\left[\left\| D_n^l \right\|_\Omega^2 e_n^2 \right] \tag{6.5.13}$$

where $\overline{(\mu_n^l)^2}$ is $E[(\mu_n^l)^2]$. Next, the expectations in the second and third terms on the right hand side of equation (6.5.13) is evaluated by using the following as-

sumption

A5): For any constant matrix Ω and for all l, e_{an}^{l} and e_{an}^{Ω} are jointly Gaussian.

This assumption seems reasonable for longer filters using the central limit theorem [65, 129, 130]. So, $E\left[e_{an}^{l,\Omega}e_n\right]$ can be simplified as

$$\begin{aligned} E\left[e_{an}^{l,\Omega}e_n\right] &= E\left[\left(D_n^l\right)^T\Omega\mathbf{v}_n^l\left(D_n^l\right)^T I\mathbf{v}_n^l\right] = E\left[\left(\mathbf{v}_n^l\right)^T\left(\Omega\left(D_n^l\right)\left(D_n^l\right)^T I\right)\mathbf{v}_n^l\right] \\ &= E\left[\left\|\mathbf{v}_n^l\right\|^2_{\Omega E\left[\left(D_n^l\right)\left(D_n^l\right)^T\right]}\right] = E\left[\left\|\mathbf{v}_n^l\right\|^2_{\Omega\tilde{R}}\right] \end{aligned} \tag{6.5.14}$$

Now, $E\left[\left\|D_n^l\right\|_\Omega^2 e_n^2\right]$ is being solved by using the following assumption

A6):The adaptive filter is long enough so that $\left\|D_n^l\right\|_\Omega^2$and e_n^2 are uncorrelated [128].

This assumption is more realistic when the filter length gets longer [128]. As MAI plus noise is independent of D_n^l, expectation $E\left[\left\|D_n^l\right\|_\Omega^2 e_n^2\right]$ can be simplified as

$$E\left[\left\|D_n^l\right\|_\Omega^2 e_n^2\right] = E\left[\left\|D_n^l\right\|_\Omega^2\right]E\left[e_n^2\right] = E\left[\left\|D_n^l\right\|^2\right]\left(E\left[\left(e_{an}^l\right)^2\right] - \sigma^2_{\bar{\nu_n^l}}\right) \tag{6.5.15}$$

Now using (6.5.14) and (6.5.15) and, (6.5.13) can be written as

$$E\left[\left\|\mathbf{v}_n^{l+1}\right\|_\Omega^2\right] = E\left[\left\|\mathbf{v}_n^l\right\|_\Omega^2\right] - 2\bar{\mu}_n^l E\left[\left\|\mathbf{v}_n^l\right\|^2_{\Omega\tilde{R}}\right] + \overline{(\mu_n^l)^2}E\left[\left\|D_n^l\right\|_\Omega^2\right]\left(\xi_n^l - \sigma^2_{\bar{\nu_n^l}}\right) \tag{6.5.16}$$

(6.5.16) shows the time evaluation or the transient behavior of the weighted variance $E\left[\left\|\mathbf{v}_n^l\right\|_\Omega^2\right]$ for any constant weight matrix Ω. Different performance measures can be achieved by the proper choice of the weight matrix Ω.

6.5.5 Constructing the Learning Curves for the Excess Mean Square Error (EMSE)

Learning curves for the EMSE can be constructed by using $EMSE = E\left[\left(e_{an}^{l}\right)^{2}\right] = E\left[\left\|\mathbf{v}_{n}^{l}\right\|_{\tilde{R}}^{2}\right]$. If $\Omega = I, \tilde{R}, \ldots, \tilde{R}^{N-1}$, a set of relations can be obtained. Now by using the Cayley-Hamilton theorem, following can be established

$$\Omega = -p_0 I - p_1 \tilde{R} - \ldots - p_{N-1}\tilde{R}^{N-1} \tag{6.5.17}$$

where

$$p(x) \triangleq det\left(xI - \tilde{R}\right) = p_0 + p_1 x + \ldots + p_{N-1}x^{N-1} + x^{N} \tag{6.5.18}$$

is the characteristic polynomial of $\tilde{R}$.Consequently,

$$\begin{aligned} E\left[\left\|\mathbf{v}_{n}^{l+1}\right\|_{\tilde{R}^{N-1}}^{2}\right] &= E\left[\left\|\mathbf{v}_{n}^{l}\right\|_{\tilde{R}^{N-1}}^{2}\right] + 2\bar{\mu_{n}^{l}}\left(p_0 E\left[\left\|\mathbf{v}_{n}^{l}\right\|_{I}^{2}\right] + p_1 E\left[\left\|\mathbf{v}_{n}^{l}\right\|_{\tilde{R}}^{2}\right] + \ldots \right. \\ &\quad \left. + p_{N-1}E\left[\left\|\mathbf{v}_{n}^{l}\right\|_{\tilde{R}^{N-1}}^{2}\right]\right) \\ &\quad + \overline{(\mu_{n}^{l})^{2}}E\left[\left\|D_{n}^{l}\right\|_{\tilde{R}^{N-1}}^{2}\right]\left(\xi_{n}^{l} + \sigma_{\nu_{n}^{l}}^{2}\right) \end{aligned} \tag{6.5.19}$$

So,

$$\Upsilon_{n}^{l} = \begin{bmatrix} 1 & -2\bar{\mu_{n}^{l}} & 0 & \cdots & 0 & 0 \\ 0 & 1 & -2\bar{\mu_{n}^{l}} & 0 & \cdots & 0 \\ \vdots & 0 & 1 & -2\bar{\mu_{n}^{l}} & \cdots & \vdots \\ 0 & 0 & 0 & 1 & -2\bar{\mu_{n}^{l}} & 0 \\ 0 & 0 & \cdots & 0 & 1 & -2\bar{\mu_{n}^{l}} \\ 2\bar{\mu_{n}^{l}}p_0 & 2\bar{\mu_{n}^{l}}p_1 & 2\bar{\mu_{n}^{l}}p_2 & \cdots & 2\bar{\mu_{n}^{l}}p_{N-2} & 1 + 2\bar{\mu_{n}^{l}}p_{N-1} \end{bmatrix} \tag{6.5.20}$$

And

$$\varpi_n^l = \begin{bmatrix} E\left[\left\|\mathbf{v}_n^l\right\|_I^2\right] \\ E\left[\left\|\mathbf{v}_n^l\right\|_{\tilde{R}}^2\right] \\ \vdots \\ E\left[\left\|\mathbf{v}_n^l\right\|_{\tilde{R}_{N-1}}^2\right] \end{bmatrix} \tag{6.5.21}$$

Similarity

$$\mathrm{Þ}_n^l = \begin{bmatrix} E\left[\left\|D_n^l\right\|_I^2\right] \\ E\left[\left\|D_n^l\right\|_{\tilde{R}}^2\right] \\ \vdots \\ E\left[\left\|D_n^l\right\|^2\right] \end{bmatrix} \tag{6.5.22}$$

By combining 6.5.20 , 6.5.21 and 6.5.22 ,

$$\varpi_n^{l+1} = \Upsilon_n^l \varpi_n^l + \overline{(\mu_n^l)^2}\left(\xi_n^l + \sigma_{\nu_n^l}^2\right)\mathrm{Þ}_n^l \tag{6.5.23}$$

6.6 Steady-State Analysis of the MNCLMS Algorithms

Steady-state analysis of an adaptive filter is performed to study the behavior of steady-state EMSE and MSD. Steady-state performance measures is also obtained by analyzing (6.5.13) when $l \to \infty$ which is presented in the next section i.e

$$\lim_{l\to\infty} E\left[\left\|\mathbf{v}_n^{l+1}\right\|_\Omega^2\right] = \lim_{l\to\infty} E\left[\left\|\mathbf{v}_n^l\right\|^2\right] \tag{6.6.1}$$

So at steady-state (6.5.16) will become

$$2\bar{\mu}_n^\infty \lim_{l\to\infty} E\left[\left\|\mathbf{v}_n^l\right\|_{\Omega\tilde{R}}^2\right] = \overline{(\mu_n^\infty)^2} \lim_{l\to\infty} E\left[\left\|D_n^l\right\|_\Omega^2\right]\left(\xi_n^\infty + \sigma_{\nu_n^l}^2\right) \tag{6.6.2}$$

Where $\bar{\mu}_n^\infty$, $\overline{(\mu_n^\infty)^2}$and ξ_n^∞ are steady-state values of $\bar{\mu}_n^l$, $\overline{(\mu_n^l)^2}$and ξ_n^l respectively.

Now using (5.3.25) and (5.3.26) it can be shown that

$$\left(\bar{\mu}_n^l\right)^2 = \overline{\left(\mu_n^l\right)^2}\left(2\gamma\lambda_n^l + \gamma^2\left(\bar{\lambda}_n^l\right)^2\right) \tag{6.6.3}$$

$$\begin{aligned}\left(\lambda_n^{l+1}\right)^2 &= (1-\beta)^2\left(\lambda_n^l\right)^2 + \beta(1-\beta)\bar{\lambda}_n^l\xi_n^l + \frac{\beta^2}{4}\left[E\left[\left|e_n^l\right|^4\right]\right. \\ &\quad \left. -2\sigma_{\nu_n^l}^2\left(\xi_n^l + \sigma_{\nu_n^l}^2\right) + \sigma_{\nu_n^l}^4\right]\end{aligned} \tag{6.6.4}$$

(6.6.4) can be written compactly as

$$\left(\lambda_n^{l+1}\right)^2 = (1+\beta)^2\overline{\left(\lambda_n^l\right)^2} + \beta(1-\beta)\bar{\lambda}_n^l\xi_n^l + \frac{\beta}{2}\xi_n^l\sigma_{\nu_n^l}^2 \tag{6.6.5}$$

If we define mean Lagrangian multiplier as $\bar{\lambda}_n^l = E\left[\lambda_n^l\right]$, it can be shown that at steady-state

$$\bar{\lambda}_n^l = \frac{\xi_n^\infty}{2} \tag{6.6.6}$$

Similarly, if $\bar{\mu}_n^l = E\left[\mu_n^l\right]$, it can be shown that

$$\bar{\mu}_n^\infty = \mu\left(1 + \gamma\frac{\xi_n^\infty}{2}\right) \tag{6.6.7}$$

(6.6.3) can be expressed as

$$\overline{\left(\mu_n^\infty\right)^2} = \mu^2\left[1 + 2\gamma\lambda_n^\infty + \gamma^2\left(\lambda_n^\infty\right)^2\right] \tag{6.6.8}$$

(6.6.5) is written as

$$\overline{\left(\lambda_n^\infty\right)^2} = \frac{1}{(2-\beta)}\left[\frac{(1-\beta)}{2}\left(\xi_n^\infty\right)^2 + \beta\xi_n^\infty\sigma_{\nu_n^l}^2\right] \tag{6.6.9}$$

Using (6.6.2) with $\Omega = I$,

$$\begin{aligned} 2\xi_n^{\infty} + \gamma\left(\xi_n^{\infty}\right)^2 &= \mu Tr\left(\tilde{R}\right)\xi_n^{\infty} + \mu Tr\left(\tilde{R}\right)\sigma_{\nu_n^l}^2 + \mu\gamma Tr\left(\tilde{R}\right)\left(\xi_n^{\infty}\right)^2 + \mu\gamma Tr\left(\tilde{R}\right)\sigma_{\nu_n^l}^2\xi_n^{\infty} \\ &+\mu\gamma^2\left(\frac{1}{2-\beta}\right)\left(\frac{1-\beta}{2}\right)Tr\left(\tilde{R}\right)\left(\xi_n^{\infty}\right)^3 \\ &+\mu\gamma^2\left(\frac{1}{2-\beta}\right)\left(\frac{1-\beta}{2}\right)Tr\left(\tilde{R}\right) \\ &+\mu\beta Tr\left(\tilde{R}\right)\sigma_{\nu_n^l}^2\left(\xi_n^{\infty}\right)^2 + \mu\beta Tr\left(\tilde{R}\right)\sigma_{\nu_n^l}^2\xi_n^{\infty} \end{aligned} \tag{6.6.10}$$

(6.6.10) is cubic in terms of $\xi_n^{\infty}$and can be expressed as

$$A\left(\xi_n^{\infty}\right)^3 + B\left(\xi_n^{\infty}\right)^2 + C\xi_n^{\infty} + D = 0 \tag{6.6.11}$$

In 6.6.11above,

$$A = -\mu\gamma^2 Tr\left(\tilde{R}\right)\left(\frac{1}{2-\beta}\right)\left(\frac{1-\beta}{2}\right) \tag{6.6.12}$$

$$B = \gamma - \mu Tr\left(\tilde{R}\right)\left[\gamma + \sigma_{\nu_n^l}^2\left\{\left(\frac{1}{1-\beta}\right)\left(\frac{1-\beta}{2}\right) + \beta\right\}\right] \tag{6.6.13}$$

$$C = 2 - \mu Tr\left(\tilde{R}\right)\left[1 + \left(\gamma + \beta\sigma_{\nu_n^l}^2\right)\sigma_{\nu_n^l}^2\right] \tag{6.6.14}$$

And

$$D = -\mu Tr\left(\tilde{R}\right)\sigma_{\nu_n^l}^2 \tag{6.6.15}$$

Now assuming that at steady-state, $\mu Tr\left(\tilde{R}\right) \ll 1$ [131], it can be shown that at steady-state, the value of ξ_n^{∞} is close to zero meaning that higher powers of ξ_n^{∞} can be ignored. Consequently, (6.6.11) will become,

$$C\xi_n^{\infty} + D = 0 \tag{6.6.16}$$

or

$$\xi_n^{\infty} = \frac{-D}{C} \tag{6.6.17}$$

Hence, steady-state EMSE of the proposed MNCLMS algorithm in the presence of MAI and noise can be shown to be

$$\xi_{n(MNCLMS)}^{\infty} \approx \frac{\mu Tr\left(\tilde{R}\right)\sigma_{\nu_n^l}^2}{2-\mu Tr\left(\tilde{R}\right)\left[1+\left(\gamma+\beta\sigma_{\nu_n^l}^2\right)\sigma_{\nu_n^l}^2\right]} \tag{6.6.18}$$

By using the same procedure developed above, steady-state EMSE of the LMS, NCLMS, ZNCLMS, and MCLMS algorithms in the presence of MAI and noise can be shown, respectively to be

$$\xi_{n(LMS)}^{\infty} \approx \frac{\mu Tr\left(\tilde{R}\right)\sigma_{\nu_n^l}^2}{2} \tag{6.6.19}$$

$$\xi_{NCLMS}^{\infty} \approx \frac{-\left(2+\gamma\sigma_U^2\right)+2\mu Tr\left(\tilde{R}\right)\sigma_U^2\left[1+\gamma\sigma_U^4+\gamma^2\left(\frac{1-\beta}{2-\beta}\right)\left\{\sigma_U^2+\sigma_U^4\right\}\right]}{\left(2+\gamma\sigma_U^2\right)-2\mu Tr\left(\tilde{R}\right)} \tag{6.6.20}$$

$$\xi_{ZNCLMS}^{\infty} \approx \frac{-\left(2+\gamma\sigma_{\nu_n^l}^2\right)+2\mu Tr\left(\tilde{R}\right)\sigma_{\nu_n^l}^2\left[1+\gamma\sigma_{\nu_n^l}^4+\gamma^2\left(\frac{1-\beta}{2-\beta}\right)\left\{\sigma_{\nu_n^l}^2+\sigma_{\nu_n^l}^4\right\}\right]}{\left(2+\gamma\sigma_{\nu_n^l}^2\right)-2\mu Tr\left(\tilde{R}\right)} \tag{6.6.21}$$

$$\xi_{MCLMS}^{\infty} \approx \frac{-\left(2+\gamma\sigma_{\nu_n^l}^2\right)+2\mu Tr\left(\tilde{R}\right)\sigma_{\nu_n^l}^2\left[1+\gamma\sigma_{\nu_n^l}^4+\gamma^2\left(\frac{1-\beta}{2-\beta}\right)\left\{\sigma_{\nu_n^l}^2+\sigma_{\nu_n^l}^4\right\}\right]}{\left(2+\gamma\sigma_{\nu_n^l}^2\right)-2\mu Tr\left(\tilde{R}\right)} \tag{6.6.22}$$

6.6.1 Steady State Mean Square Deviation (MSD)

For the steady-state MSD, the weight matrix is chosen to be equal to the inverse of the input correlation matrix $\left(\Omega = \tilde{\mathbf{R}^{-1}}\right)$ so (6.6.2) will be reduced to

$$2\bar{\mu}_n^{\infty} MSD = \overline{(\mu_n^{\infty})^2} \lim_{l\to\infty} E\left[\left\|D_n^l\right\|^2_{\tilde{R^{-1}}}\right]\left(\xi_n^{\infty} + \sigma^2_{\bar{\nu_n^l}}\right) \tag{6.6.23}$$

Where $MSD = \lim_{l\to\infty} E\left[\left\|\mathbf{v}_n^l\right\|^2\right]$. By using diagonalization of $\tilde{\mathbf{R}^{-1}}$ it can shown that

$$\lim_{l\to\infty} E\left[\left\|D_n^l\right\|^2_{\tilde{R^{-1}}}\right] = L \tag{6.6.24}$$

Where L is the length of the adaptive filter. Now (6.6.23) can be solved for MSD by substituting the values of $\bar{\mu}_n^{\infty}$ and $\overline{(\mu_n^{\infty})^2}$ in it

$$2\bar{\mu}_n^{\infty} MSD = \overline{(\mu_n^{\infty})^2} L\left(\xi_n^{\infty} + \sigma^2_{\bar{\nu_n^l}}\right) \tag{6.6.25}$$

(6.6.25) can be expressed as

$$\begin{aligned} 2\left(1 + \frac{\mu_n^{\infty}}{2}\right) MSD &= \mu\left[1 + \gamma\xi_n^{\infty} + \gamma^2\left\{\left(\frac{1-\beta}{2\,(2-\beta)}\right)(\xi_n^{\infty})^2 + \beta\xi_n^{\infty}\sigma^2_{\bar{\nu_n^l}}\right\}\right] \\ &\quad \times L\left(\xi_n^{\infty} + \sigma^2_{\bar{\nu_n^l}}\right) \end{aligned} \tag{6.6.26}$$

$$\begin{aligned} MSD &= \frac{\mu}{2\left(1 + \frac{\mu_n^{\infty}}{2}\right)}\left[1 + \gamma\xi_n^{\infty} + \gamma^2\left\{\left(\frac{1-\beta}{2\,(2-\beta)}\right)(\xi_n^{\infty})^2 + \beta\xi_n^{\infty}\sigma^2_{\bar{\nu_n^l}}\right\}\right] \\ &\quad \times L\left(\xi_n^{\infty} + \sigma^2_{\bar{\nu_n^l}}\right) \end{aligned} \tag{6.6.27}$$

By putting the value of ξ_n^{∞} in (6.6.27), MSD can be found.

6.7 Tracking Analysis of the MNCLMS Algorithms for the Random Walk Channel in the Presence of MAI and Noise

Tracking analysis of an adaptive filter is performed to study its ability to track down the time variations in the channel. This is due to the fact that statistical properties of the weight vector and error signals are able to track the changes in the input signal variation by relying on instantaneous data [128]. In this section, tracking analysis of the proposed algorithm is performed for a random walk model.

6.7.1 Random Walk Model

This section deals with the tracking analysis of the MNCLMS algorithm performed for a random walk channel. A general framework for the tracking analysis of adaptive algorithms is used in this section which can handle random system nonstationarities [132] . This framework is based on an energy conservation relation and is valid for adaptive algorithms whose recursion is of the form

$$\mathbf{w}_n^{l+1} = \mathbf{w}_n^l + \mu_n^l D_n^l f\left(e_n^l\right) \tag{6.7.1}$$

Where $f\left(e_n^l\right)$ represents a general scalar function of the output estimation error e_n^l. For an LMS algorithm $f\left(e_n^l\right) = e_n^l$.

The random walk model for a channel is given by

$$\mathbf{w}_n^{l+1} = \mathbf{w}_{o,n}^l + q_n^l \tag{6.7.2}$$

q_n^l in (6.7.2) is assumed to be zero mean, i.i.d, with a positive definite co-variance matrix $E\left[q_n q_n^T\right] = Q$ and is also statistically independent of the input regressor and the MAI plus noise, whereas $\mathbf{w}_n^o$ is the unknown system to be tracked. For tracking

analysis of an adaptive algorithm, a very important measure is its steady-state tracking EMSE (ξ_n^{∞}) defined as

$$\xi_n^{\infty} = \lim_{l\to\infty} E\left[\left|e_{an}^{l}\right|^2\right] = E\left[\left\|\mathbf{v}_n^l\right\|_{\tilde{R}}^2\right] \tag{6.7.3}$$

Where $\mathbf{v}_n^l = \mathbf{w}_n^o - \mathbf{w}_n^l$ is the weight error vector for the random walk channel.

6.7.2 Fundamental Energy Relation for the Random Walk Channel

In this section, the fundamental energy conservation relation [128] is used to develop the framework for the tracking analysis of the proposed MNCLMS algorithm. By using (5.3.24) and (6.7.2), it can be shown that

$$\mathbf{v}_n^{l+1} = \mathbf{v}_n^l - \mu_n^l e_n^l D_n^l + q \tag{6.7.4}$$

Consider the (6.7.1) , which is given by

$$\mathbf{w}_n^{l+1} = \mathbf{w}_n^l + \mu_n^l D_n^l f\left(e_n^l\right) \tag{6.7.5}$$

Subtracting both sides of the (6.7.5) from $\mathbf{w}_{0,n}^{l+1}$

$$\left(\mathbf{w}_{o,n}^{l+1} - \mathbf{w}_n^{l+1}\right) = \left(\mathbf{w}_{o,n}^{l+1} - \mathbf{w}_n^l\right) - \mu_n^l D_n^l f\left(e_n^l\right) \tag{6.7.6}$$

In case of an LMS algorithm, $f\left(e_n^l\right) = e_n^l$, so (6.7.6) becomes

$$\mathbf{w}_{o,n}^{l+1} - \mathbf{w}_n^{l+1} = \left(\mathbf{w}_{o,n}^{l+1} - \mathbf{w}_n^l\right) - \mu_n^l D_n^l e_n^l \tag{6.7.7}$$

Now we transpose both sides of (6.7.7)

$$\left(\mathbf{w}_{o,n}^{l+1} - \mathbf{w}_n^{l+1}\right)^T = \left(\mathbf{w}_{o,n}^{l+1} - \mathbf{w}_n^l\right)^T - \mu_n^l e_n^l \left(D_n^l\right)^T \tag{6.7.8}$$

By multiplying both sides of (6.7.8) with D_n^l from left yields

$$\left(\mathbf{w}_{o,n}^{l+1} - \mathbf{w}_n^{l+1}\right)^T D_n^l = \left(\mathbf{w}_{o,n}^{l+1} - \mathbf{w}_n^l\right)^T D_n^l - \mu_n^l e_n^l \left(D_n^l\right)^T D_n^l \tag{6.7.9}$$

Equation (6.7.9) in terms of a priori error and a posteriori errors can be expressed as

$$e_{p,n}^l = e_{a,n}^l - \mu_n^l e_n^l \left\|D_n^l\right\|^2 \tag{6.7.10}$$

For the case when $\Omega = I$, 6.7.4 becomes

$$\mathbf{v}_n^{l+1} = \mathbf{v}_n^l - D_n^l \left[\frac{e_{an}^l - e_{pn}^l}{\left\|D_n^l\right\|^2}\right] + q_n^l \tag{6.7.11}$$

By evaluating the energies on both sides of (6.7.11) We get

$$\left\|\mathbf{v}_n^{l+1} - q_n^l\right\|^2 + \frac{1}{\left\|D_n^l\right\|^2}\left|e_{an}^l\right|^2 = \left\|\mathbf{v}_n^{l\,l}\right\|^2 + \frac{1}{\left\|D_n^l\right\|^2}\left|e_{pn}^l\right|^2 \tag{6.7.12}$$

Since q_n^l is a zero mean stationary random vector and is independent of the input regressor vector and the MAI plus noise, so (6.7.12) , can be expressed as

$$\left\|\mathbf{v}_n^{l+1}\right\|^2 - \left\|q_n^l\right\|^2 + \frac{1}{\left\|D_n^l\right\|^2}\left|e_{an}^l\right|^2 = \left\|\mathbf{v}_n^l\right\|^2 + \frac{1}{\left\|D_n^l\right\|^2}\left|e_{pn}^l\right|^2 \tag{6.7.13}$$

(6.7.13) is the random walk tracking model for MNCLMS algorithm. The energy relation is used to evaluate the excess mean-square error at steady state.

6.7.3 Tracking Steady-State EMSE of the MNCLMS Algorithms

A7): q_n is a zero-mean stationary random vector process with a positive definite covariance matrix Q and is statistically independent of the input regressor vector $\mathbf{x}_n^l$ and MAI plus noise Z_m^l sequence .

Taking expectation on both sides of equation (6.7.13) and using equation (6.5.7)

assumption A7) and the fact that at steady-state, $\mathbf{v}_n^{l+1} = \mathbf{v}_n^l$, the following equation can be obtained

$$2E\left[\mu_n^\infty \xi_n^\infty\right] = Tr\left(Q_n^\infty\right) + E\left[\left(\mu_n^\infty\right)^2 \left\|D_n^\infty\right\|^2 \left(e_n^\infty\right)^2\right] \tag{6.7.14}$$

Where $Tr\left(Q_n^\infty\right) = \left[q_n^\infty \left(q_n^\infty\right)^T\right]$. By using equation (6.7.14) together with assumption A4 yields

$$2\mu_n^\infty \xi_n^\infty = Tr\left(Q_n^\infty\right) + \overline{\left(\mu_n^\infty\right)^2} Tr\left(\tilde{R}\right)\left(\xi_n^\infty - \sigma^2_{\nu_n^l}\right) \tag{6.7.15}$$

By substituting the values of $\bar{\mu}_n^\infty$, $\bar{\lambda}_n^\infty$, $\overline{\left(\mu_n^\infty\right)}^2$and $\overline{\left(\lambda_n^\infty\right)^2}$ in equation (6.7.15) , we get the steady-state EMSE of the proposed algorithm.

$$\xi_n^\infty \approx \frac{\mu Tr\left(\tilde{R}\right)\sigma^2_{\nu_n^l}}{2 - \mu Tr\left(\tilde{R}\right)\left[1 + \left(\gamma + \beta\sigma^2_{\nu_n^l}\right)\sigma^2_{\nu_n^l}\right]} + Tr\left(\frac{Q_n^\infty}{2\mu}\right) \tag{6.7.16}$$

Since q is assumed to be an i.i.d, therefore $Tr\left(Q_n^\infty\right) = L\sigma_q^2$, so equation (6.7.16) will be reduced to

$$\xi_{n(MNCLMS)}^\infty \approx \frac{\mu Tr\left(\tilde{R}\right)\sigma^2_{\nu_n^l}}{2 - \mu Tr\left(\tilde{R}\right)\left[1 + \left(\gamma + \beta\sigma^2_{\nu_n^l}\right)\sigma^2_{\nu_n^l}\right]} + \frac{L\sigma_q^2}{2\mu} \tag{6.7.17}$$

Where L is the length of the decision feedback filter.

6.8 Simulation Results for MIMO-CDMA MNCLMS Algorithm (DFE)

In this section, simulation resulst are shown to assess the performance of the MNCLMS algorithm for the MIMO CDMA DFE case. The performance of the proposed MIMO-CDMA MNCLMS algorithm is compared with the standard LMS, MCLMS, noise constrained LMS and zero noise algorithms. The average MSE is the perfor-

mance measure through which the algorithms are assessed. A 2×2 MIMO system is considered here. Random signature sequences of length 31 and rectangular chip waveforms are used. SNR is kept at 10 dB and 20 dB for 4 and 20 subscribers respectively. Two channel environments have been used in the simulations i.e flat fading Rayleigh channel and AWGN channel. All simulations are performed using a MIMO DFE with feed forward filter of length 10 and feedback filter length of 5.

To compare the convergence rates of the algorithms, the usual way is to set the parameters such that all the algorithms have the same steady-state EMSE. To obtain this, the step-size of the LMS algorithm (μ_{LMS}) required to achieve a specified steady-state EMSE is found first and then the step sizes of the comparing algorithms are set to the step-size value of the LMS algorithm. In other words

$$\mu_{LMS} = \mu_{MCLMS} = \mu_{NCLMS} = \mu_{ZNCLMS} = \mu_{MNCLMS} \tag{6.8.1}$$

Now the tuning parameters μ, β and γ for LMS, ZNCLMS, MCLMS,NCLMS and MNCLMS algorithms are specified in such a way that

$$\xi^{\infty}_{n(MNCLMS)} = \xi^{\infty}_{n(ZNCLMS)} = \xi^{\infty}_{n(NCLMS)} = \xi^{\infty}_{n(MCLMS)} = \xi^{\infty}_{n(LMS)} \tag{6.8.2}$$

6.8.1 Interference Cancellation in an AWGN Channel

In an AWGN channel, μ, β and γ are selected according to the previously described method and are given in tables 6.1 and 6.2 for an SNR of 20 dB and 10 dB. As is evident from the tables, analytical EMSE is increasing with the increase in the value of γ. For a specific value of μ and a specific value of β the convergence behavior of the MNCLMS algorithm can be improved by increasing the value of γ but at the cost of an increased MSE as shown in figure 6.1.

Table 6.1: Tuning Parameters of MIMO-CDMA MNCLMS algorithm for DFE in the AWGN Environment at 20 dB SNR

$K = 4$		$K = 20$	
Tuning Parameters	EMSE	Tuning Parameters	EMSE
$\mu = 0.0005$ $\beta = 0.005$,$\gamma = 1$	0.0014966	$\mu = 0.0005$ $\beta = 0.005$,$\gamma = 1$	0.00984869
$\mu = 0.0005$ $\beta = 0.0005, \gamma = 50$	0.0016146	$\mu = 0.0005$ $\beta = 0.0005, \gamma = 50$	0.0190205
$\mu = 0.0005$ $\beta = 0.0005, \gamma = 100$	0.0017566	$\mu = 0.0005$ $\beta = 0.0005, \gamma = 100$	0.3923183

Table 6.2: Tuning Parameters of the Proposed MIMO-CDMA MNCLMS Algorithm for DFE in the AWGN Environment at 10 dB SNR

$K = 4$		$K = 20$	
Tuning Parameters	EMSE	Tuning Parameters	EMSE
$\mu = 0.0005$ $\beta = 0.005$,$\gamma = 1$	0.0011098	$\mu = 0.0005$, $\beta = 0.005$,$\gamma = 1$	0.0098486
$\mu = 0.0005$ $\beta = 0.0005, \gamma = 50$	0.0011709	$\mu = 0.0005$ $\beta = 0.0005, \gamma = 50$	0.0190205
$\mu = 0.0005$ $\beta = 0.0005, \gamma = 100$	0.0013024	$\mu = 0.0005$ $\beta = 0.0005, \gamma = 100$	0.3923183

It is also clear from the figure that a lower steady state MSE is achieved with a faster initial convergence, if the value of β is decreased and that of γ is increased. This led us to the conclusion that a faster convergence can be achieved by choosing a larger value of γ while keeping the value of β as low as possible.

The results of the comparison of the convergence speed of these algorithms for 4 and 20 subscribers, in an AWGN channel, are depicted, respectively, in Figs.6.4 and 6.3. In both cases, it can be seen that the MIMO-CDMA MNCLMS algorithm converges faster than the rest of the algorithms. Moreover, it is also obvious that MSE worsens as the number of subscribers is increased from 4 to 20. The degradation in MSE is because of the increase in MAI at the receiver. In the case of 4 subscribers,

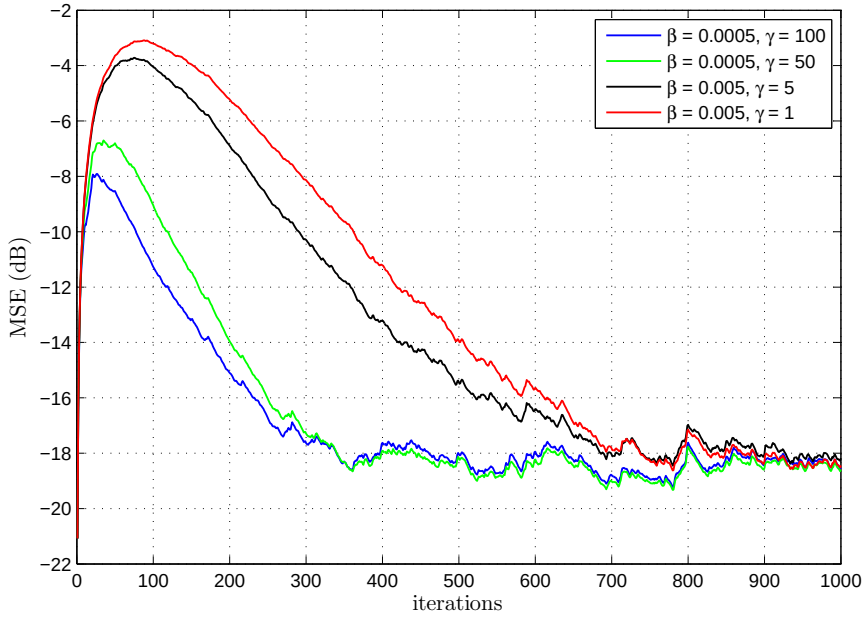

Figure 6.1: Effect of β and γ on MSE learning curves of the MNCLMS algorithm in an AWGN environment with $K = 4$ at 20 dB SNR

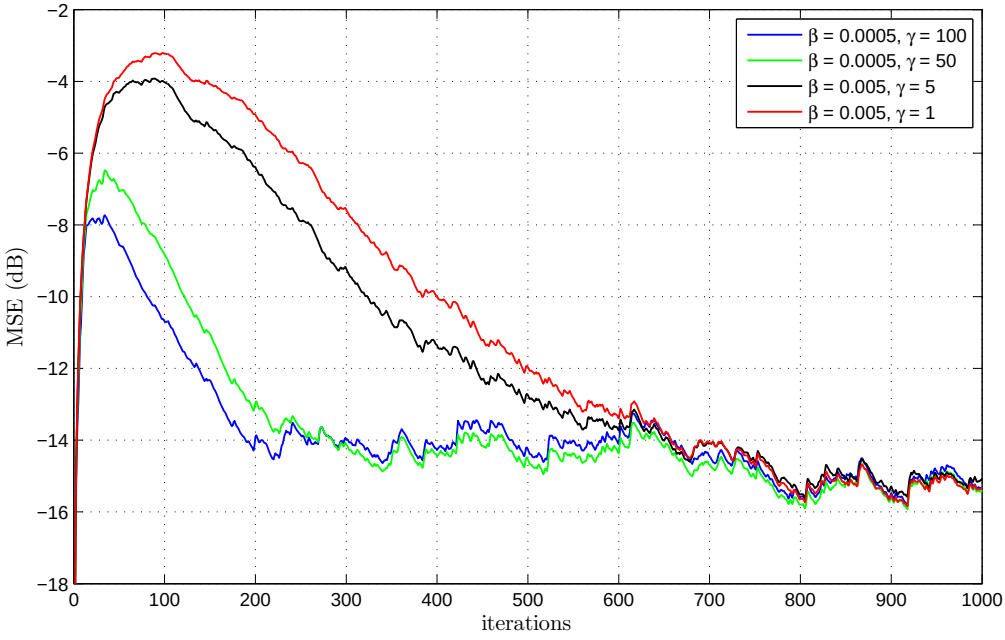

Figure 6.2: Effect of β and γ on MSE learning curves of the MNCLMS algorithm in an AWGN environment with $K = 4$ at 10 dB SNR

the proposed algorithm was able to achieve an MSE at around -10 dB at around 150 iterations while the first of the other algorithms converged at this same MSE value after 400 iterations. In case of 20 subscribers, the proposed MNCLMS algorithm was able to achieve MSE at -4 dB and in around 200 iteration. Hence it can be concluded that there is a two-fold gain in convergence speed. Similar behavior is obtained for the case when SNR is kept at 10 dB with 4 and 20 subscribers.

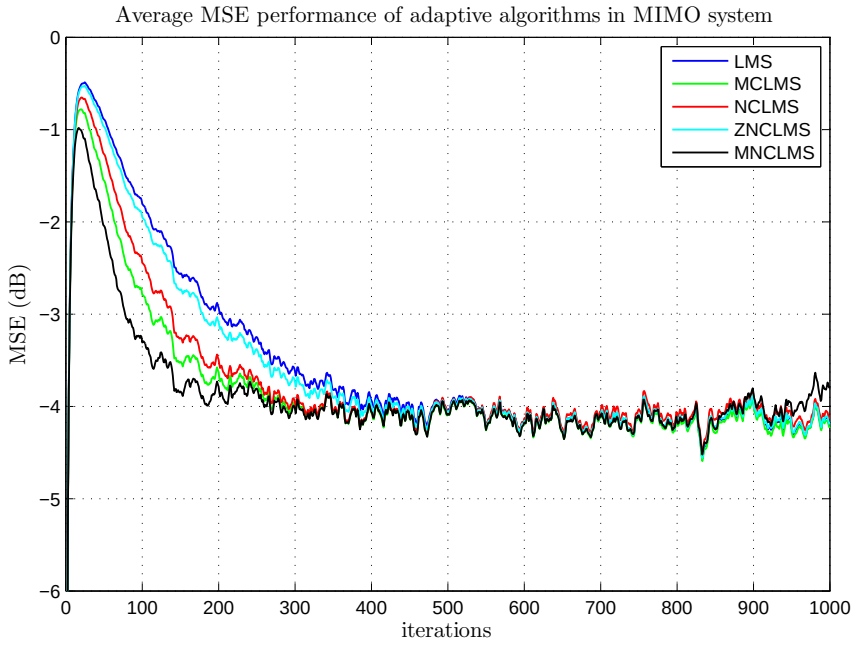

Figure 6.3: MSE behavior for different algorithms in an AWGN environment with $K = 20$

Behavior of the step size of the MIMO-CDMA MNCLMS algorithm is shown in figure 6.7 for 4 subscribers. As can be seen, in the transient state, the MIMO-CDMA MNCLMS algorithm has the largest step-size value when compared to the other algorithms and, thus, yields the fastest convergence. Also, in the steady state, the step-size parameter of the MNCLMS algorithm was reduced to the smallest value amongst all algorithms. The step-size parameter of the proposed algorithm behaves as what is called a "gear-shifting" mechanism. Same behavior is achieved for 4 subscribers when an SNR is kept at 10 dB.

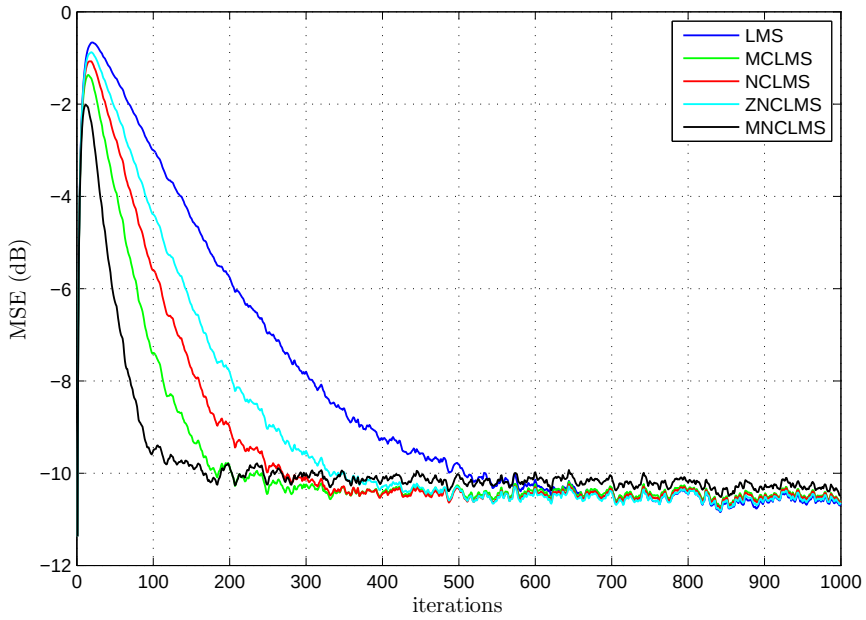

Figure 6.4: MSE behavior for different algorithms in an AWGN environment with $K = 4$ at 20dB

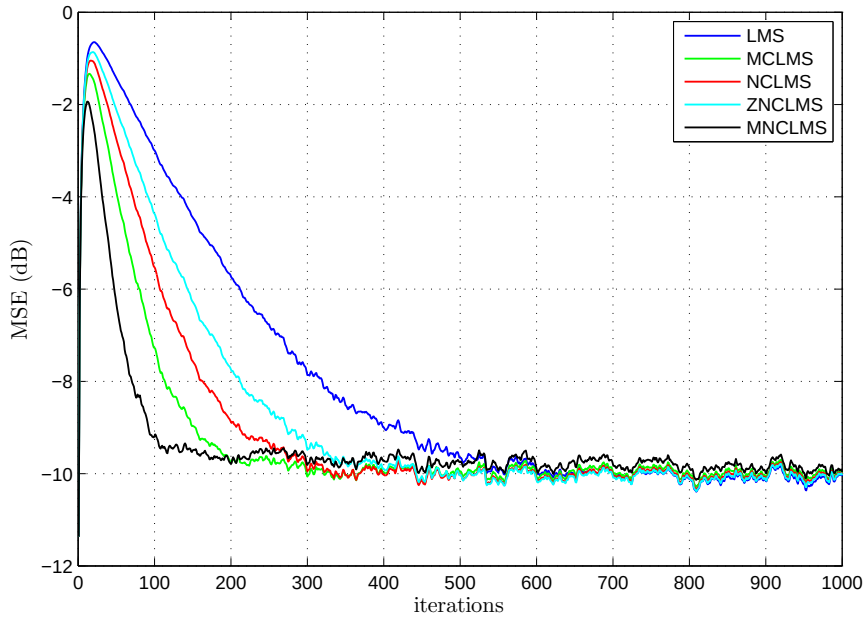

Figure 6.5: MSE behavior for different algorithms in an AWGN environment with $K = 4$ at 10dB

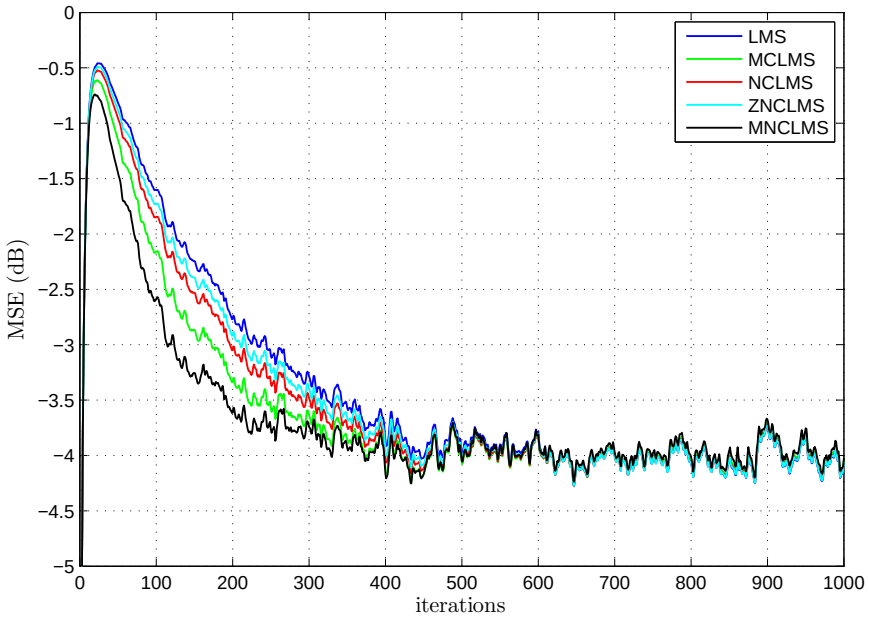

Figure 6.6: MSE behavior for different algorithms in an AWGN environment with $K = 20$ at 10dB

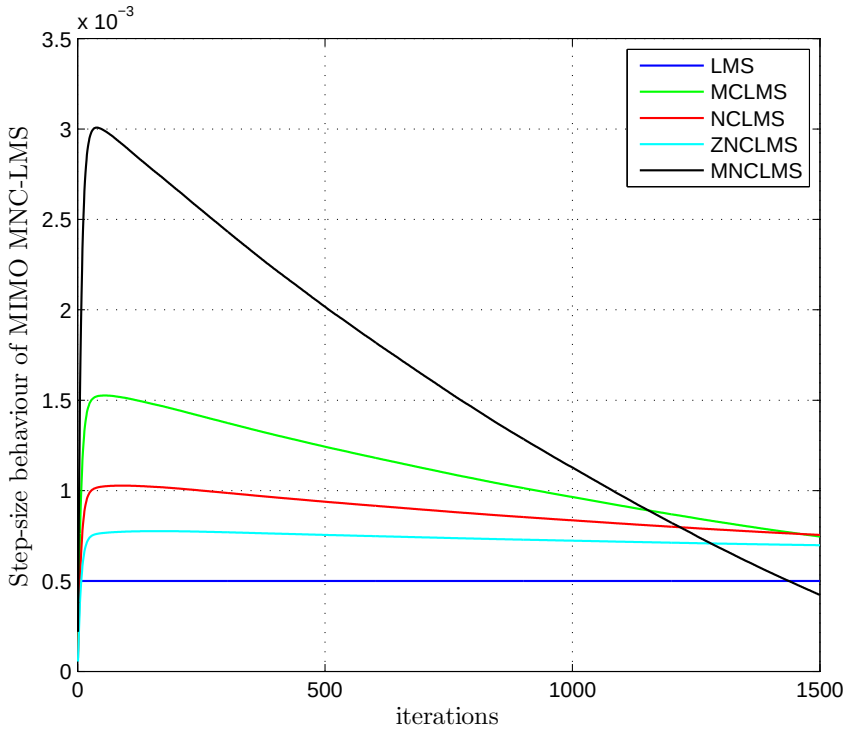

Figure 6.7: Behavior of time-varying step size of the MNCLMS algorithm for $K = 4$ at 20 dB SNR

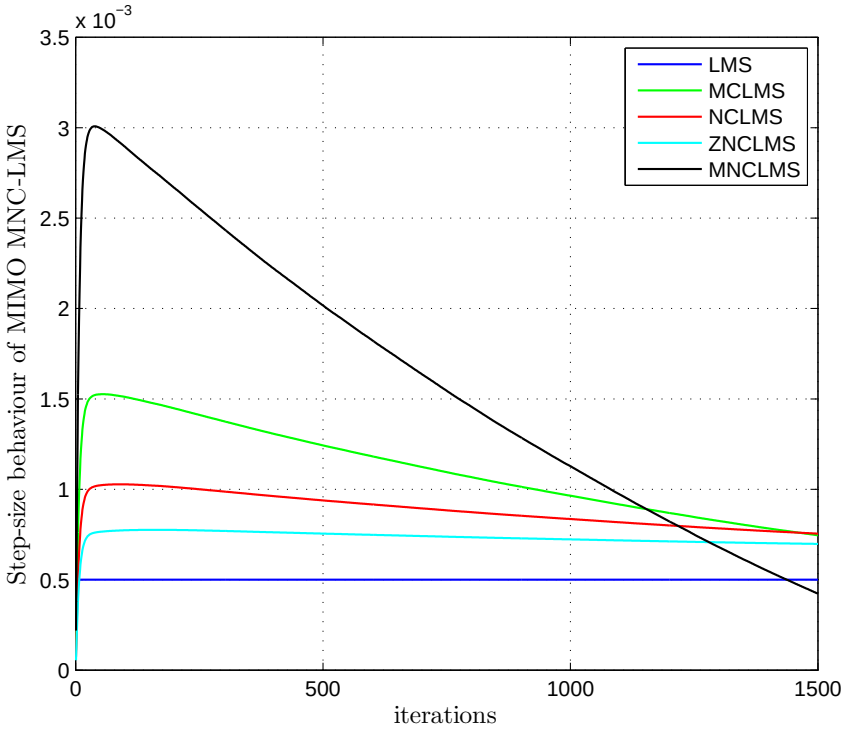

Figure 6.8: Behavior of time-varying step size of the MNCLMS algorithm for $K = 4$ at 10 dB SNR

Effect of the spreading sequence length N_c on the performance of the comparing algorithms is shown in table 6.3. It can be seen from the table that the proposed MIMO-CDMA MNCLMS algorithm required the lowest number of iterations to achieve the same steady-state MSE as compared to other algorithms. It is also evident from the table that the number of iterations is increasing as N_c is increasing.

Table 6.3: Effect of N_c on the convergence behavior, number of iteration, in the AWGN environment at 20 dB

Algorithm	$N_c = 31$	$N_c = 63$	$N_c = 127$	$N_c = 255$
LMS	443	588	739	792
$NCLMS$	237	290	400	398
$ZNCLMS$	291	382	511	527
$MCLMS$	163	236	273	286
$MNCLMS$	100	136	165	203

The effect of a sudden increase in the number of subscribers on the performance behavior of different algorithms is shown in figure 6.9. It is clear from the figure

that the proposed algorithm is able to recover faster than the rest of the algorithms as the number of subscribers is suddenly increased from four to ten which shows that a consistency in the performance of the proposed algorithm is maintained.

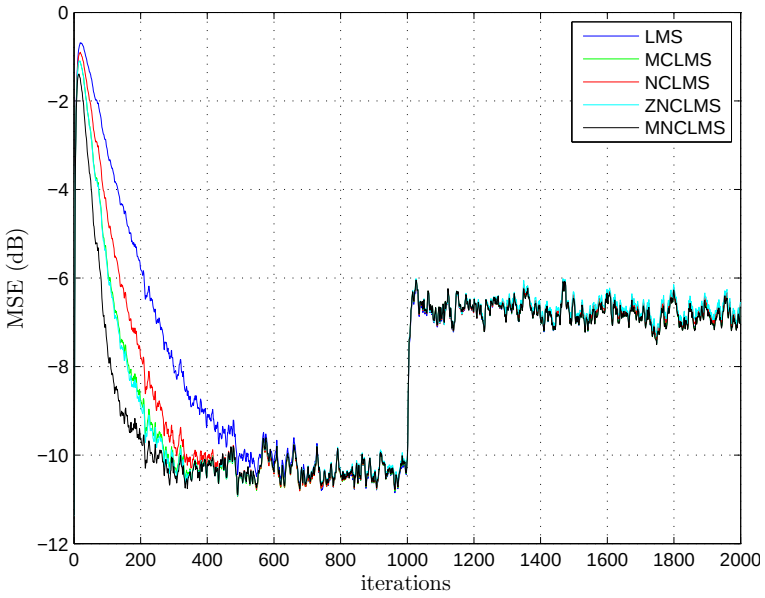

Figure 6.9: Effect of a sudden increase in the number of subscribers from 4 to 10 subscribers

In UTP case, subscriber of interest(subscriber one) has a transmitted power that is one; whereas, transmitted powers of the rest of the subscribers are uniformly distributed between zero and one. Figure 6.10 shows the comparison of the convergence speed for the algorithms under consideration. As can be seen, a consistency in performance of the proposed algorithm is sustained.

MIMO-CDMA MNCLMS algorithm was able to achieve an MSE of around -13dB at around 190 iterations while the first of the other algorithms converged at the same MSE value at around 310 iterations.The result for UTP, figure 6.10 is superior as compared to the ETP case, figure 6.4. This is due to fact that in an UTP , some subscribers may have transmitted powers of less than one (due to the uniform power assignment between zero and one) which reduces the effect of MAI in the system whereas in an ETP case, all subscribers have equal transmitted powers (one) which will increase MAI in the system.

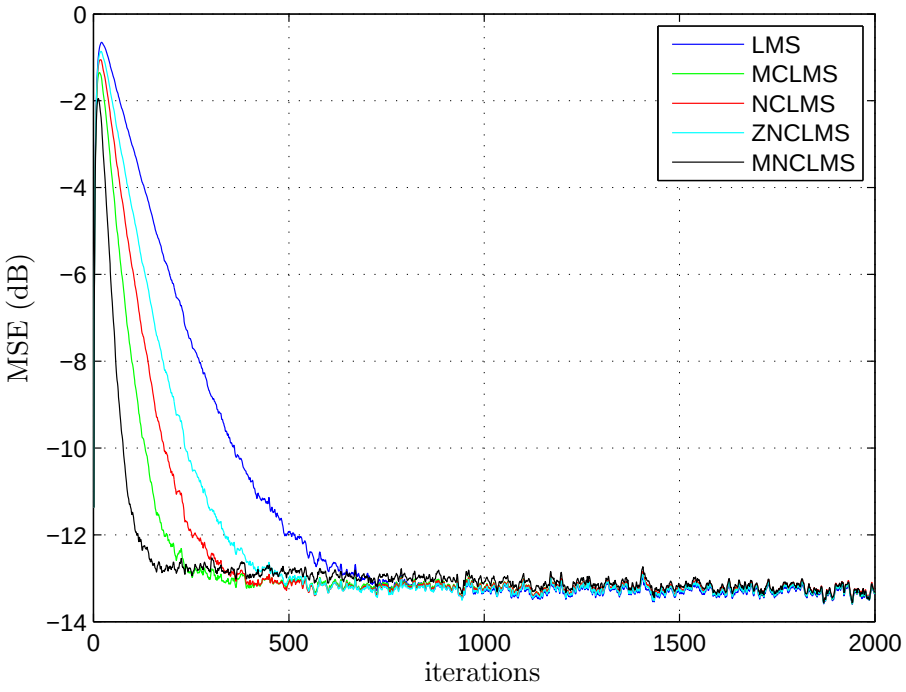

Figure 6.10: MSE behavior for different algorithms in an AWGN environment with $K = 4$ under the unequal transmitted powers scenario at 20 dB SNR

6.9 Interference Cancellation in Rayleigh Fading Channel

In this section the convergence speed of MIMO-CDMA MNCLMS algorithm is investigated for 4 and 20 subscribers and for this purpose, a flat Rayleigh fading channel is used with a Doppler frequency of $fd = 250Hz$ using BPSK modulation while SNR is kept at 20 dB. Figure 6.11 and figure 6.12 show the MSE learning curves for different algorithms. As can be seen, The MIMO-CDMA MNCLMS algorithm is outperforming rest of the algorithms in terms of faster convergence. It is also evident from the figures that when the number of subscribers is increased, there is a deterioration in the steady-state performance of all algorithms.This deterioration is attributed to a larger MAI produced by the increasing subscribers. Similar behavior is seen for the case when SNR was kept at 10dB. All algorithms reached at the same steady-state MSE value, but the proposed MIMO-CDMA MNCLMS

algorithm achieved this value first as it was specifically designed to do so.

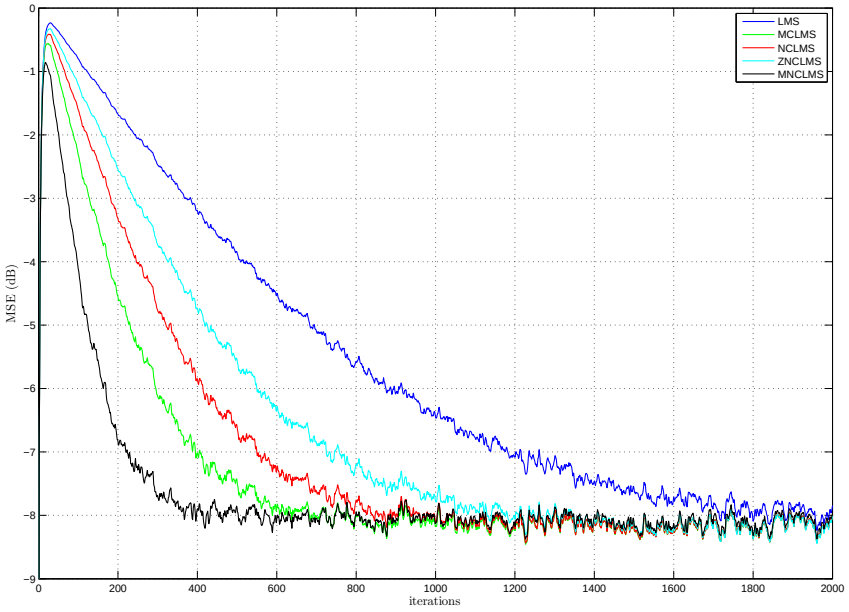

Figure 6.11: MSE in flat Rayleigh fading, $fd = 250Hz$, $K = 4$ at 20dB

6.10 Tracking Performance for Random Walk Channel in the Presence of MAI

Tracking performance in a random walk channel is investigated in this section. As was shown earlier, the selection of the adaptation parameters is of paramount importance to the performance behavior of the algorithms. A similar approach used in the previous section for the selection of these parameters is utilized here. First, the optimal step size for the LMS algorithm μ^o_{LMS} is obtained by differentiating its respective steady-state tracking EMSE given by (6.7.8) and then equating it to zero. This gives

$$\mu^o_{LMS} = \sqrt{\frac{N\sigma_q^2}{Tr\left(\tilde{R}\right)\sigma^2_{\nu_n^l}}} \tag{6.10.1}$$

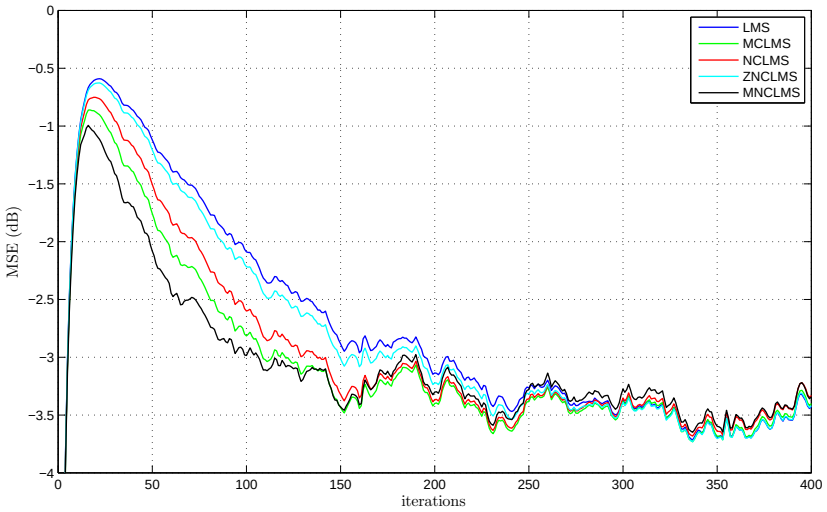

Figure 6.12: MSE in flat Rayleigh fading, $fd = 250Hz$, $K = 20$ at 20dB

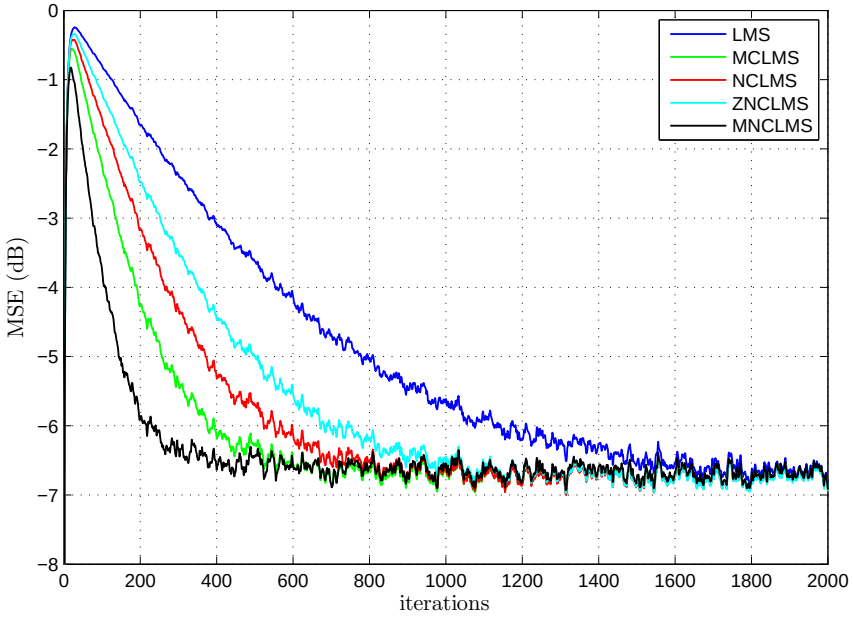

Figure 6.13: MSE in flat Rayleigh fading, $fd = 250Hz$, $K = 4$ at 10dB

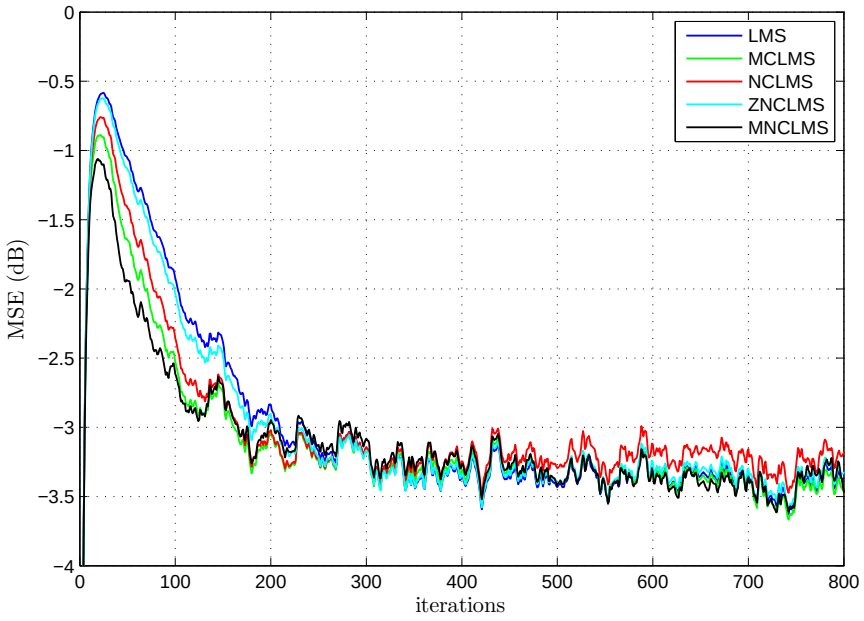

Figure 6.14: MSE in flat Rayleigh fading, $fd = 250Hz$, $K = 20$ at 10dB

And the corresponding optimal steady-state tracking EMSE of the LMS algorithm (ξ^o_{LMS}) is calculated and is found to be

$$\xi^o_{LMS} \cong \sqrt{NTr\left(\tilde{R}\right)\sigma^2_{\bar{\nu}^i_n}\sigma^2_q} \tag{6.10.2}$$

Step sizes of the other algorithms are then chosen to be equal to the optimal step size of the LMS algorithm defined by (6.10.1). After that values of β and γ are found in such a way that

$$\xi^\infty_{n(MNCLMS)} = \xi^\infty_{n(ZNCLMS)} = \xi^\infty_{n(NCLMS)} = \xi^\infty_{n(MCLMS)} = \xi^\infty_{n(LMS)} \tag{6.10.3}$$

Examples of the selection of the tuning parameters in a random walk channel using the aforementioned procedure are reported in table 6.4 for two different values of $\sigma^2_q(10^{-7}$ and $10^{-10})$ and $K = 20$.

Figure 6.15 shows the MSE learning curve for the considered algorithms in a

Table 6.4: Effect of Tuning Parameters of the Adaptive Algorithm in a Random Walk Channel on Analytical EMSE

$\sigma_q^2 = 10^{-10}$		$\sigma_q^2 = 10^{-7}$	
Tuning Parameters	EMSE	Tuning Parameters	EMSE
$\mu = 0.0005$ $\beta = 0.005$,$\gamma = 1$	0.0011098	$\mu = 0.0005$, $\beta = 0.005$,$\gamma = 5$	0.0098486
$\mu = 0.0005$ $\beta = 0.0005, \gamma = 5$	0.0011709	$\mu = 0.0005$ $\beta = 0.0005, \gamma = 50$	0.0190205
$\mu = 0.0005$ $\beta = 0.0005, \gamma = 50$	0.0013024	$\mu = 0.0005$ $\beta = 0.0005, \gamma = 100$	0.3923183

random walk channel for four subscribers with $\sigma_q = 10^{-10}$ and an SNR of 20dB. As can be seen in the figure, the proposed MIMO-CDMA MNCLMS algorithm is outperforming the other algorithms. Similar results are obtained with an SNR of 10 dB

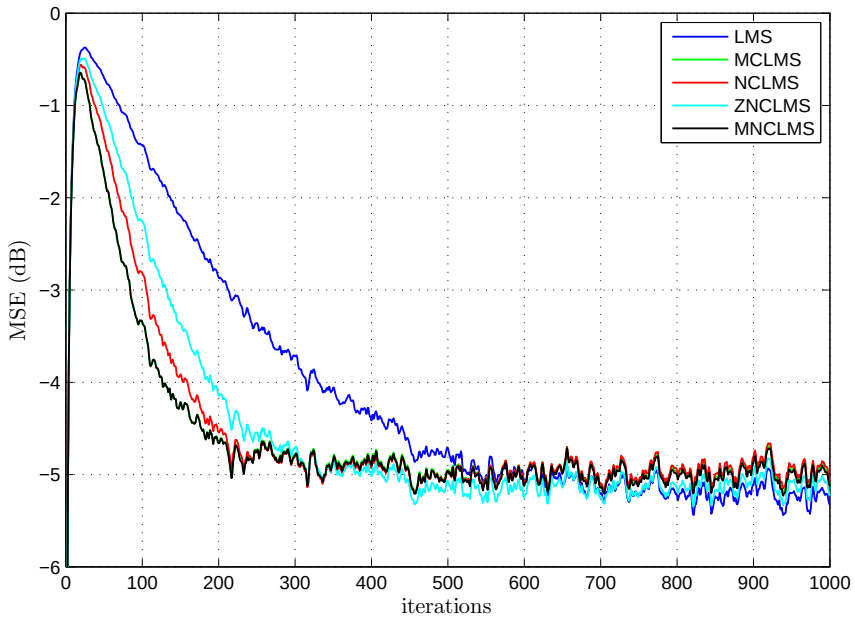

Figure 6.15: Tracking performance in a random walk channel with $\sigma_q = 10^{-10}$ and SNR of 20 dB

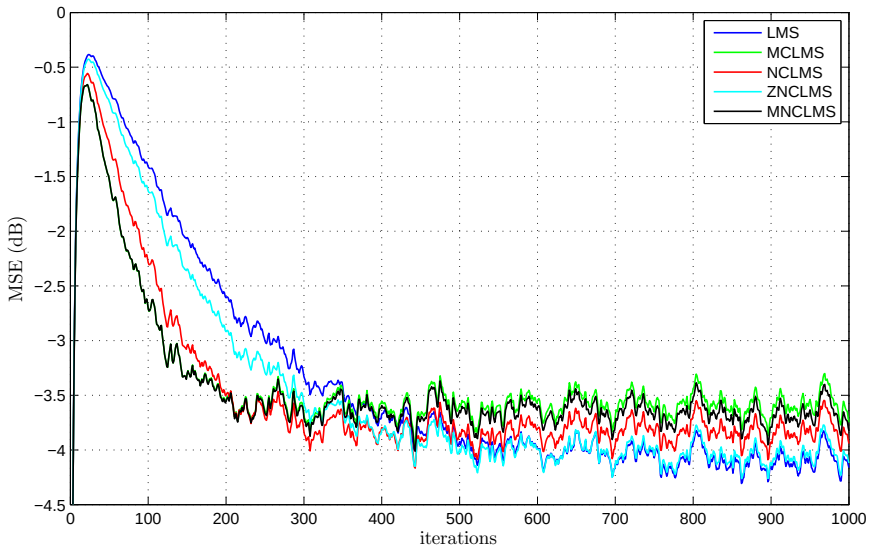

Figure 6.16: Tracking performance in a random walk channel with $\sigma_q = 10^{-10}$ and SNR of 10 dB

6.11 Simulation Results For MIMO-CDMA MN-CLMS Algorithm(LE)

6.11.1 Interference Cancellation in an AWGN Channel

In this section, we present simulation results to assess the performance of the MN-CLMS algorithm for the MIMO CDMA LE case. The performance of the proposed MIMO-CDMA MNCLMS algorithm is compared with the standard LMS, MCLMS noise constrained LMS and zero noise algorithms. The average mean square error is the performance measure through which the algorithms are assessed. A 2×2 MIMO system is considered in this section. Random signature sequences of length 31 and rectangular chip waveforms are used. SNR is kept at 20 dB for 10 and 20 subscribers.

The results of the comparison of the convergence speed of these algorithms for 10 and 20 subscribers, in an AWGN channel, are depicted, respectively, in Figs.6.17 and 6.18. In both cases, it can be seen that the MIMO-CDMA MNCLMS algorithm converges faster than the rest of the algorithms. Moreover, it is also obvious that

MSE worsens as the number of subscribers is increased from 10 to 20. The degradation in MSE is because of the increase in MAI at the receiver. In the case of 10 subscribers, the proposed algorithm was able to achieve an MSE at around -6 dB at around 120 iterations while the first of the other algorithms converged at this same MSE value after 140 iterations. In case of 20 subscribers, the proposed MNCLMS algorithm was able to achieve MSE at around -2.6 dB and in around 140 iterations.

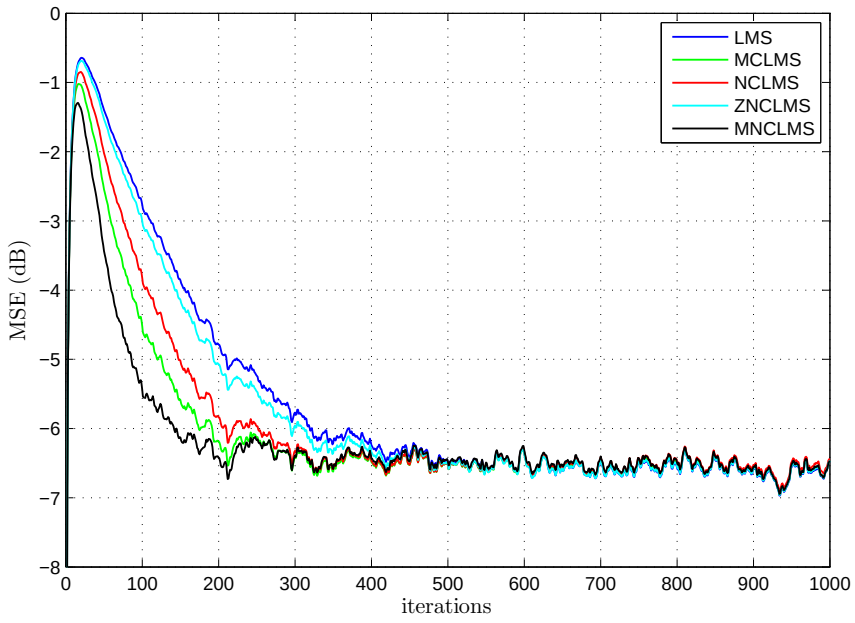

Figure 6.17: MSE behavior for different algorithms in an AWGN environment with $K = 10$ at 20dB

Behavior of the step size of the MIMO-CDMA MNCLMS algorithm is shown in figure 6.19 for 10 subscribers. As can be seen, in the transient state, the MIMO-CDMA MNCLMS algorithm has the largest step-size value when compared to the other algorithms and, thus, yields the fastest convergence. Also, in the steady state, the step-size parameter of the MNCLMS algorithm was reduced to the smallest value amongst all algorithms. Same behavior is achieved for 20 subscribers as shown in figure 6.20

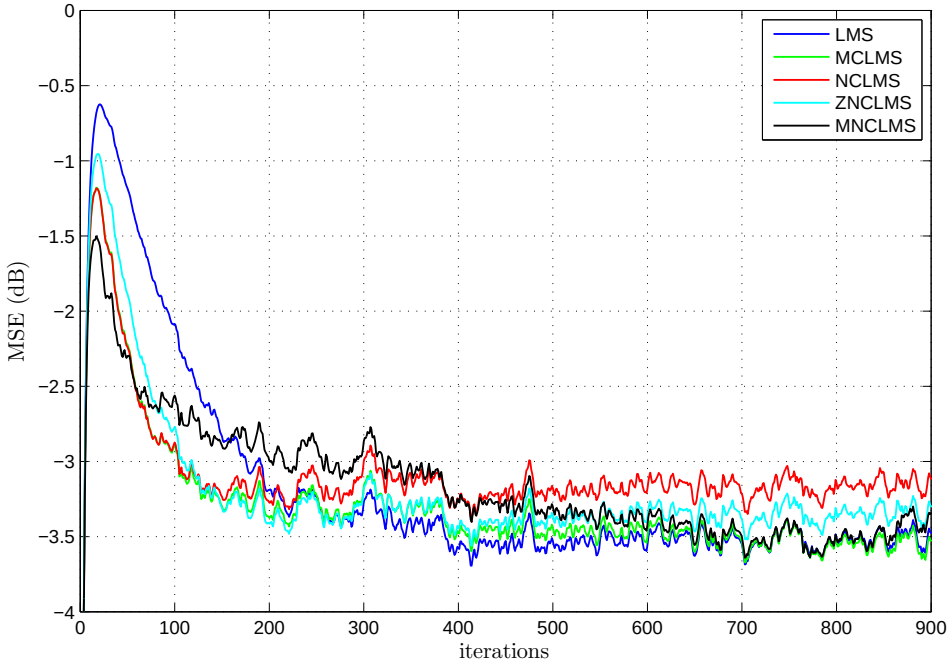

Figure 6.18: MSE behavior for different algorithms in an AWGN environment with $K = 20$ at 20dB

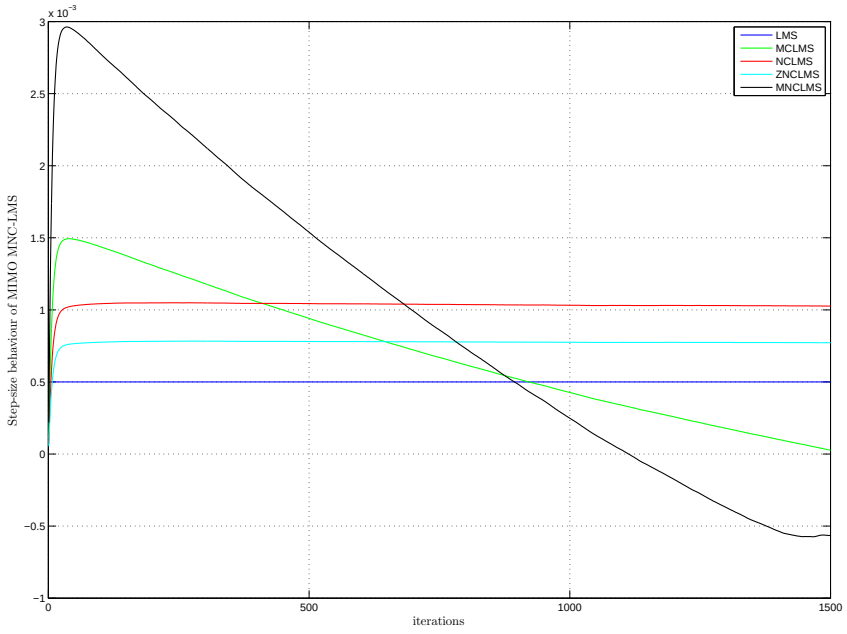

Figure 6.19: Behavior of time-varying step size of the MNCLMS algorithm for $K = 10$ at 20 dB SNR

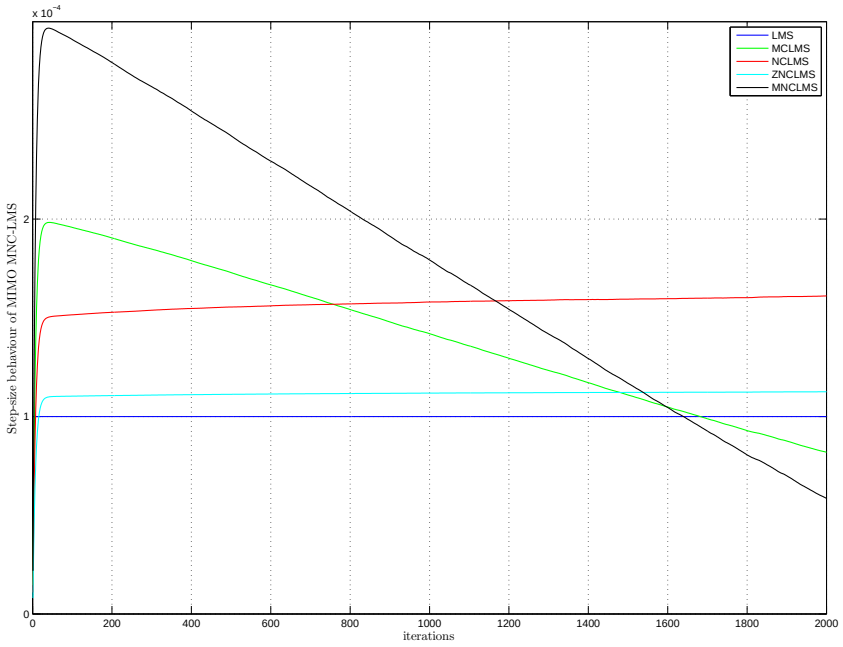

Figure 6.20: Behavior of time-varying step size of the MNCLMS algorithm for $K = 25$ at 20 dB SNR

6.12 Interference Cancellation in Rayleigh Fading Channel

In this section, simulation results are presented to assess the performance of the MNCLMS algorithm for the MIMO CDMA LE case. The performance of the proposed MIMO-CDMA MNCLMS algorithm is compared with the standard LMS, MCLMS noise constrained LMS and zero noise algorithms. The average MSE is the performance measure through which the algorithms are assessed. A 2×2 MIMO system is considered here. Random signature sequences of length 31 and rectangular chip waveforms are used. The SNR is kept at 10 dB and 20 dB respectively.

The results of the comparison of the convergence speed of these algorithms for 10 and 25 subscribers, in a Rayleigh fading channel, are depicted, respectively, in Figure.6.21 and figure 6.22. In both cases, it can be seen that the MIMO-CDMA

MNCLMS algorithm converges faster than the rest of the algorithms. In the case of 10 subscribers, the proposed algorithm was able to achieve an MSE at around -4.8 dB at around 200 iterations . In case of 25 subscribers, the proposed MNCLMS algorithm was able to achieve MSE at -5.2 dB and in around 240 iterations.

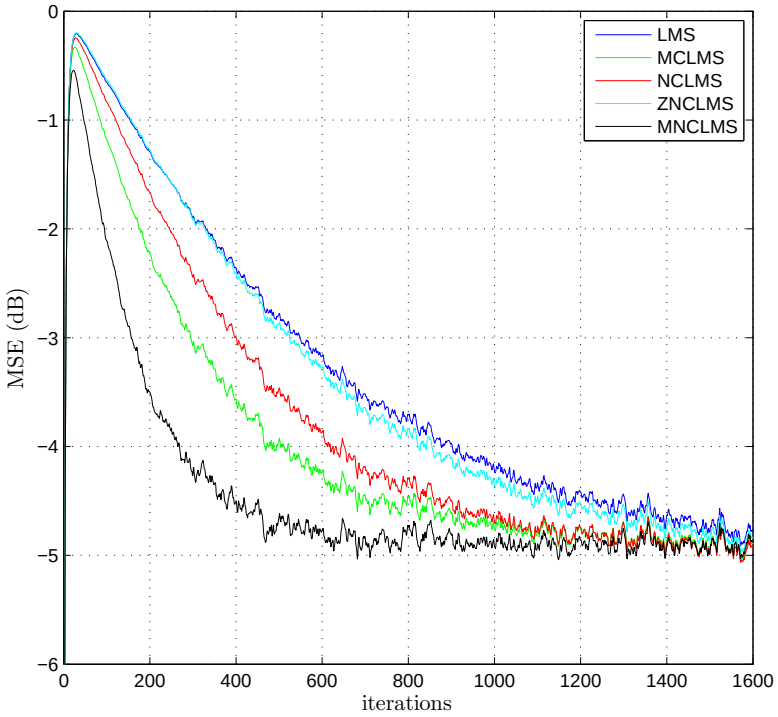

Figure 6.21: MSE behavior for different algorithms in Rayleigh Fading environment with for $K = 10$ at 10 dB SNR

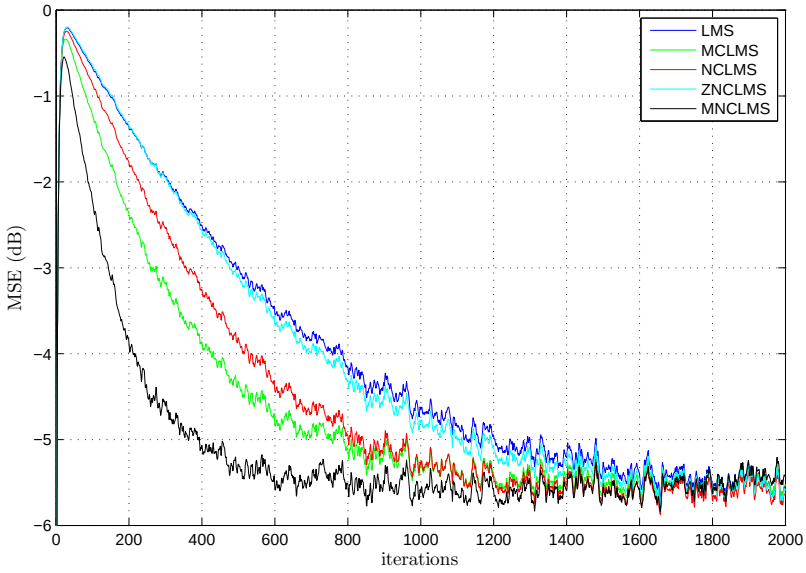

Figure 6.22: MSE behavior for different algorithms in Rayleigh Fading environment for $K = 20$ at 20 dB SNR

Chapter 7

Dissertation Contribution, Conclusion and Recommendation for Future Work

7.1 Dissertation Contribution and Conclusion

Statistical analysis of MAI in Synchronous MIMO - CDMA system for BPSK signals with random signature sequence is performed in the fading environment (Rayleigh). The derivation of the pdf of MAI and noise has been used to design an LMS based algorithm. Major contributions of this dissertation are

1. Statistical analysis of MAI in Synchronous MIMO - CDMA system for BPSK signals with random signature sequence is performed in the fading environment (Rayleigh) and a closed form expression for the pdf of MAI together with noise for a MIMO-CDMA system is derived.

2. Optimum coherent reception with MAI is investigated for BER and a closed form expression is derived.

3. The closed form expression for the pdf of MAI and noise has been used to

design an LMS based algorithm. In this approach, a Robbins - Monroe algorithm is used to minimize the conventional MSE criterion incorporating MAI and noise as a constraint. This scheme resulted in MAI and noise constrained LMS (MNCLMS) algorithm in the MIMO-CDMA scenario.The proposed algorithm is a variable step size algorithm as the step size rule is applicable placing the constraint on MAI and noise.

4. Convergence analysis is performed in the mean and mean square sense.

5. Tracking ability of the algorithm is tested in the presence of MAI and for this task, random walk channel is used. A closed form expression for the steady state MSE is also derived.

7.2 Recommendations for Future Work

A closed from expression for MAI in MIMO-CDMA synchronous system in flat fading channel such as Rayleigh is derived and and based on that, a MNCLMS algorithm has been developed for linear as well as decision feedback equalization. This work can be extended to frequency selective fading channels and asynchronous CDMA systems.

Appendix A

Probability Density Function of $f_P(p)$

Evaluation of $\frac{1}{2\pi}\int_{-\infty}^{\infty}\frac{\exp(-\mathbf{i}\omega\mathbf{z})}{\prod_{\mathbf{n=1}}^{\mathbf{N}}(\omega^{\mathbf{2}}\sigma^{\mathbf{2}}_{\mathbf{p_n^l}}+\mathbf{1})}\mathbf{d}\omega$

Before evaluating the inverse Fourier transform, a partial fraction expansion of the product in equation (2.3.2) is performed as follows:

$$\prod_{n=1}^{N}\frac{1}{\omega^2\sigma^2_{p_n^l}+1}=\sum_{n=1}^{N}\frac{C_n}{\omega^2\sigma^2_{p_n^l}+1} \tag{A.1}$$

where constant C_n in the numerator is given by

$$C_n=\frac{\left(\sigma^2_{p_n^l}\right)^{N-1}}{\prod_{j=1,j\neq n}^{N}\left(\sigma^2_{p_j^l}-\sigma^2_{p_i^l}\right)} \tag{A.2}$$

Thus, the inverse Fourier transform can be set up as

$$\begin{aligned} f_Z(z) &= \mathcal{F}^{-1}\left[\Phi_Z(\omega)\right] \\ &= \frac{1}{2\pi}\int_{-\infty}^{\infty}\exp(-i\omega z)\sum_{n=1}^{N}\frac{C_n}{\omega^2\sigma^2_{P_n^l}+1}d\omega \\ &= \sum_{n=1}^{N}\frac{C_n}{2\pi}\int_{-\infty}^{\infty}\frac{\exp(-i\omega z)}{\omega^2\sigma^2_{P_n^l}+1}d\omega \end{aligned} \tag{A.3}$$

which is a sum of N inverse Fourier transforms. The inner integral can be easily evaluated using the residue theory [73] as

$$\frac{1}{2\pi}\int_{-\infty}^{\infty}\frac{e^{-i\omega z}}{\omega^2\sigma_{P_n^l}^2+1}d\omega=\frac{e^{-\frac{z}{\sigma_{P_n^l}}}}{2\sigma_{P_n^l}}\left(e^{\frac{2z}{\sigma_{P_n^l}}\theta(-z)+\theta(z)}\right) \tag{A.4}$$

where $\theta(z)$ is the unit step function. The result in equation (A.4) can be simplified as

$$\frac{1}{2\pi}\int_{-\infty}^{\infty}\frac{e^{-i\omega z}}{\omega^2\sigma_{P_n^l}^2+1}d\omega=\frac{1}{2}\frac{e^{-\frac{|z|}{\sigma_{P_n^l}}}}{\sigma_{P_n^l}} \tag{A.5}$$

Finally, after substituting the result for the above integral in equation (A.3), the pdf of the MAI is found to be given in equation (2.3.4).

Appendix B

Evaluation of Pdf of MAI-plus-noise and the BER

The pdf of Mai-plus-noise can be setup as follows:

$$
\begin{aligned}
f_{\gamma_z}(\gamma_z) &= \frac{\left(\frac{2}{N}\sqrt{\frac{\gamma_z\sigma_I^2\sigma_\alpha^2 t}{E_b}}\right)^{2N-1}\exp\left(-\frac{\left(\frac{2}{N}\sqrt{\frac{\gamma_z\sigma_I^2\sigma_\alpha^2 t}{E_b}}\right)^2}{2b}\right)}{2^{N-1}b^N(N-1)!\left(\frac{2}{N}\sqrt{\frac{\gamma_z\sigma_I^2\sigma_\alpha^2 t}{E_b}}\times\frac{N^2E_b}{2\sigma_I^2\sigma_\alpha^2 t}\right)} \\
&= \frac{\left(\frac{4\gamma_z\sigma_I^2\sigma_\alpha^2 t}{N^2E_b}\right)^{N-1}\exp\left(-\frac{2\gamma_z\sigma_I^2\sigma_\alpha^2 t}{N^2bE_b}\right)}{2^{N-2}b^N(N-1)!\frac{N^2E_b}{\sigma_I^2\sigma_\alpha^2 t}} \qquad \text{(B.1)} \\
f_{\gamma_z}(\gamma_z) &= \frac{2^N\gamma_z^{N-1}\left(\frac{\sigma_I^2\sigma_\alpha^2 t}{N^2bE_b}\right)^N\exp\left(-\frac{2\gamma_z\sigma_I^2\sigma_\alpha^2 t}{N^2bE_b}\right)}{(N-1)!} = \frac{2^N\gamma_z^{N-1}\left(\frac{N}{2\overline{\gamma_z}}\right)^N\exp\left(-\frac{N\gamma_z}{\overline{\gamma_z}}\right)}{(N-1)!} \\
f_{\gamma_z}(\gamma_z) &= \frac{\gamma_z^{N-1}\left(\frac{N}{\overline{\gamma_z}}\right)^N\exp\left(-\frac{N\gamma_z}{\overline{\gamma_z}}\right)}{(N-1)!} \qquad \text{(B.2)}
\end{aligned}
$$

For $N=1$, the pdf of γ_z reduces to

$$
f_{\gamma_z}(\gamma_z) = \frac{1}{\overline{\gamma_z}}e^{-\gamma_z/\overline{\gamma_z}} \qquad \text{(B.3)}
$$

which is consistent with [33]. So the conditional probability of error can be

written as

$$P\left(e|w_{i,1}\right) = \frac{1}{2}\sum_{j=1}^{N} C_j \exp\left(\frac{\sigma_\eta^2}{2\sigma_I^2\sigma_\alpha^2}\right)\int_{\sigma_\eta^2/2\sigma_I^2\sigma_\alpha^2}^{\infty} e^{-t}\mathrm{erfc}\left(\sqrt{\gamma_z}\right)dt \tag{B.4}$$

As the channel attenuation is taken to be deterministic then γ_z is also deterministic. If α_i is taken to be random then the above conditional pdf will have to be averaged over the pdf of γ_z. So the average probability of error in BPSK symbols can be obtained as

$$\begin{aligned} P\left(e\right) &= \int_0^\infty P\left(e|w_{i,1}\right)p\left(\gamma_z\right)d\gamma_z \\ &= \frac{1}{2}\sum_{j=1}^{N} C_j \exp\left(\frac{\sigma_\eta^2}{2\sigma_I^2\sigma_\alpha^2}\right)\int_0^\infty \left[\int_{\sigma_\eta^2/2\sigma_I^2\sigma_\alpha^2}^{\infty} e^{-t}\mathrm{erfc}\left(\sqrt{\gamma_z}\right)dt\right] \\ &\quad \times\frac{\gamma_z^{N-1}\left(\frac{N}{\overline{\gamma_z}}\right)^N \exp\left(-\frac{N\gamma_z}{\overline{\gamma_z}}\right)}{(N-1)!}d\gamma_z \end{aligned} \tag{B.5}$$

Rearranging the above, following is obtained

$$\begin{aligned} P\left(e\right) &= \frac{1}{2}\sum_{j=1}^{N} C_j \exp\left(\frac{\sigma_\eta^2}{2\sigma_I^2\sigma_\alpha^2}\right)\int_{\sigma_\eta^2/2\sigma_I^2\sigma_\alpha^2}^{\infty} e^{-t}\left(\frac{N}{\overline{\gamma_z}}\right)^N \\ &\quad \times\left[\int_0^\infty \gamma_z^{N-1}\exp\left(-\frac{N\gamma_z}{\overline{\gamma_z}}\right)\mathrm{erfc}\left(\sqrt{\gamma_z}\right)d\gamma_z\right]dt \end{aligned} \tag{B.6}$$

The inner integral can be evaluated as

$$\begin{aligned} I_{\gamma_z} &= \int_0^\infty \gamma_z^{N-1}\exp\left(-\frac{N\gamma_z}{\overline{\gamma_z}}\right)\mathrm{erfc}\left(\sqrt{\gamma_z}\right)d\gamma_z \\ I_{\gamma_z} &= 2^{1-2N}\Gamma\left(2N\right){}_2F_1\left(N, N+\frac{1}{2}; N+1, -\frac{N}{\overline{\gamma_z}}\right)/\Gamma\left(N+1\right) \end{aligned}$$

The above result is again consistent with [33] for $N = 1$ which yields $I_{\gamma_z} = \overline{\gamma_z}\left(1-\sqrt{\frac{\overline{\gamma_z}}{1+\overline{\gamma_z}}}\right)$. Replacing in the above integral we get

$$
\begin{aligned}
P(e) &= \frac{1}{2}\sum_{j=1}^{N} C_j \exp\left(\frac{\sigma_\eta^2}{2\sigma_I^2\sigma_\alpha^2}\right)\int_{\sigma_\eta^2/2\sigma_I^2\sigma_\alpha^2}^{\infty} e^{-t}\left(\frac{N}{\overline{\gamma_z}}\right)^N \\
&\quad \times\left[2^{1-2N}\Gamma(2N)\,{}_2F_1\left(N, N+\frac{1}{2}; N+1, -\frac{N}{\overline{\gamma_z}}\right)/\Gamma(N+1)\right]dt \qquad \text{(B.7)} \\
&= \frac{1}{2}\sum_{j=1}^{N} C_j \exp\left(\frac{\sigma_\eta^2}{2\sigma_I^2\sigma_\alpha^2}\right)2^{1-2N}\frac{\Gamma(2N)}{\Gamma(N+1)}N^N\int_{\sigma_\eta^2/2\sigma_I^2\sigma_\alpha^2}^{\infty} e^{-t}\left(\frac{1}{\overline{\gamma_z}}\right)^N \\
&\quad \times\left[{}_2F_1\left(N, N+\frac{1}{2}; N+1, -\frac{N}{\overline{\gamma_z}}\right)\right]dt \qquad \text{(B.8)} \\
&= \frac{1}{2}\sum_{j=1}^{N} C_j \exp\left(\frac{\sigma_\eta^2}{2\sigma_I^2\sigma_\alpha^2}\right)2^{1-2N}\frac{\Gamma(2N)}{\Gamma(N+1)}N^N\int_{\sigma_\eta^2/2\sigma_I^2\sigma_\alpha^2}^{\infty} e^{-t}\left(\frac{2\sigma_I^2\sigma_\alpha^2 t}{bN^3E_b}\right)^N \\
&\quad \times\left[{}_2F_1\left(N, N+\frac{1}{2}; N+1, -\frac{2\sigma_I^2\sigma_\alpha^2 t}{bN^2E_b}\right)\right]dt \qquad \text{(B.9)} \\
P(e) &= \frac{1}{2}\sum_{j=1}^{N} C_j 2^{1-N}\exp\left(\frac{\sigma_\eta^2}{2\sigma_I^2\sigma_\alpha^2}\right)\left(\frac{\sigma_I^2\sigma_\alpha^2}{bN^2E_b}\right)^N\frac{\Gamma(2N)}{\Gamma(N+1)} \\
&\quad \times\int_{\sigma_\eta^2/2\sigma_I^2\sigma_\alpha^2}^{\infty} e^{-t}t^N\,{}_2F_1\left(N, N+\frac{1}{2}; N+1, -\frac{2\sigma_I^2\sigma_\alpha^2 t}{bN^2E_b}\right)dt \qquad \text{(B.10)}
\end{aligned}
$$

The integral in (B.10) is given by

$$
\int_{\sigma_\eta^2/2\sigma_I^2\sigma_\alpha^2}^{\infty} e^{-t}t^N\,{}_2F_1\left(N, N+\frac{1}{2}; N+1, -\frac{2\sigma_I^2\sigma_\alpha^2 t}{bN^2E_b}\right)dt \qquad \text{(B.11)}
$$

Appendix C

EMSE of the LMS NCLMS, ZNCLMS and the MCLMS Algorithms in the Presence of Both MAI and Noise

EMSE of LMS Algorithm

In LMS algorithm for $\Omega = I$ equation (6.6.18) will be reduce to the following equation

$$2\xi^{\infty}_{LMS} = \mu^{\infty}_{n} Tr(\tilde{R}) \left(\xi^{\infty}_{LMS} + \sigma^{2}_{\nu^{l}_{n}} \right) \tag{C.1}$$

EMSE of the LMS algorithm can be shown to be

$$\xi^{\infty}_{n(LMS)} \approx \frac{\mu Tr\left(\tilde{R}\right) \sigma^{2}_{\nu^{l}_{n}}}{2 - \mu Tr\left(\tilde{R}\right)} \tag{C.2}$$

By using the small step size assumption, EMSE of the LMS algorithm can be written as

$$\xi^{\infty}_{n(LMS)} \approx \frac{\mu Tr\left(\tilde{R}\right) \sigma^{2}_{\nu^{l}_{n}}}{2} \tag{C.3}$$

EMSE of NCLMS Algorithm

In case of NCLMS algorithm, equations (6.6.6), (6.6.7) and (6.6.9) are modified as below

$$\bar{\lambda_n^{\infty}} = \frac{\xi_{NCLMS}^{\infty} + \sigma_U^2}{2} \tag{C.4}$$

$$\bar{\mu_n^{\infty}} = \mu \left[1 + \frac{\gamma}{2}\left(\xi_{NCLMS}^{\infty} + \sigma_U^2\right)\right] \tag{C.5}$$

$$\overline{(\lambda_n^{\infty})^2} = \frac{1}{(2-\beta)}\left[\frac{(1-\beta)}{2}\left(\xi_{NCLMS}^{\infty} + \sigma_U^2\right)^2 + \beta\left(\xi_{NCLMS}^{\infty} + \sigma_U^2\right)\sigma_U^2\right]$$

$$\begin{aligned}\overline{(\lambda_n^{\infty})^2} &= \frac{1}{(2-\beta)}\left[\frac{(1-\beta)}{2}\left((\xi_{NCLMS}^{\infty})^2 + \sigma_U^2 + 2\xi_{NCLMS}^{\infty}\sigma_U^2\right)\right. \\ &\left. +\beta\left(\xi_{NCLMS}^{\infty} + \sigma_U^2\right)\sigma_U^2\right]\end{aligned} \tag{C.6}$$

Using the criteria mentioned in section 6.4, EMSE of the MCLMS algorithm in presence of MAI and noise can be written as

Constants A, B , C and D can be shown to be

$$A = -\mu\gamma^2 Tr\left(\tilde{R}\right)\left[\frac{1-\beta}{2\,(2-\beta)}\right] \tag{C.7}$$

$$B = \gamma - \mu Tr\left(\tilde{R}\right)\left[\gamma + \beta\sigma_U^2 + \gamma^2\left(\frac{1-\beta}{2-\beta}\right)\right]\sigma_U^2 \tag{C.8}$$

$$C = \left(2 + \gamma\sigma_U^2\right) - \mu Tr\left(\tilde{R}\right)\left[1 + 3\gamma\sigma_U^2 + 3\beta\sigma_U^4 + \gamma\left\{\frac{1-\beta}{2(2-\beta)}\right\}\sigma_U^2\right] \tag{C.9}$$

$$D = \left(2 + \gamma\sigma_{\bar{\nu_n^l}}^2\right) - 2\mu Tr\left(\tilde{R}\right)\sigma_U^2\left[1 + \gamma\sigma_U^4 + \gamma^2\left(\frac{1-\beta}{2-\beta}\right)\left\{\sigma_U^2 + \sigma_U^4\right\}\right] \quad \text{(C.10)}$$

Using the criteria mentioned in section 6.4, EMSE of the MCLMS algorithm in presence of MAI and noise can be written as

$$\xi_{NCLMS}^{\infty} \approx \frac{-\left(2 + \gamma\sigma_U^2\right) + 2\mu Tr\left(\tilde{R}\right)\sigma_U^2\left[1 + \gamma\sigma_U^4 + \gamma^2\left(\frac{1-\beta}{2-\beta}\right)\left\{\sigma_U^2 + \sigma_U^4\right\}\right]}{\left(2 + \gamma\sigma_U^2\right) - 2\mu Tr\left(\tilde{R}\right)} \quad \text{(C.11)}$$

EMSE of ZNCLMS Algorithm

In case of ZNCLMS algorithm, equations (6.6.6), (6.6.7) and (6.6.9) are modified as below

$$\bar{\lambda_n^{\infty}} = \frac{\xi_{ZNCLMS}^{\infty} + \sigma_{\bar{\nu_n^l}}^2}{2} \quad \text{(C.12)}$$

$$\bar{\mu_n^{\infty}} = \mu\left[1 + \frac{\gamma}{2}\left(\xi_{ZNCLMS}^{\infty} + \sigma_{\bar{\nu_n^l}}^2\right)\right] \quad \text{(C.13)}$$

$$\overline{\left(\lambda_n^{\infty}\right)^2} = \frac{1}{(2-\beta)}\left[\frac{(1-\beta)}{2}\left(\xi_{ZNCLMS}^{\infty} + \sigma_{\bar{\nu_n^l}}^2\right)^2 + \beta\left(\xi_{ZNCLMS}^{\infty} + \sigma_{\bar{\nu_n^l}}^2\right)\sigma_{\bar{\nu_n^l}}^2\right]$$

$$\begin{aligned}\overline{\left(\lambda_n^{\infty}\right)^2} &= \frac{1}{(2-\beta)}\left[\frac{(1-\beta)}{2}\left(\left(\xi_{ZNCLMS}^{\infty}\right)^2 + \sigma_{\bar{\nu_n^l}}^4 + 2\xi_{ZNCLMS}^{\infty}\sigma_{\bar{\nu_n^l}}^2\right)\right. \\ &\quad \left. +\beta\left(\xi_{ZNCLMS}^{\infty} + \sigma_{\bar{\nu_n^l}}^2\right)\sigma_{\bar{\nu_n^l}}^2\right] \quad \text{(C.14)}\end{aligned}$$

Constants A, B , C and D can be shown to be

$$A = -\mu\gamma^2 Tr\left(\tilde{R}\right)\left[\frac{1-\beta}{2\left(2-\beta\right)}\right] \tag{C.15}$$

$$B = \gamma - \mu Tr\left(\tilde{R}\right)\left[\gamma + \beta\sigma^2_{\bar{\nu^l_n}} + \gamma^2\left(\frac{1-\beta}{2-\beta}\right)\right]\sigma^2_{\bar{\nu^l_n}} \tag{C.16}$$

$$C = \left(2 + \gamma\sigma^2_{\bar{\nu^l_n}}\right) - \mu Tr\left(\tilde{R}\right)\left[1 + 3\gamma\sigma^2_{\bar{\nu^l_n}} + 3\beta\sigma^4_{\bar{\nu^l_n}} + \gamma\left\{\frac{1-\beta}{2(2-\beta)}\right\}\sigma^2_{\bar{\nu^l_n}}\right] \tag{C.17}$$

$$D = \left(2 + \gamma\sigma^2_{\bar{\nu^l_n}}\right) - 2\mu Tr\left(\tilde{R}\right)\left[1 + \gamma\sigma^4_{\bar{\nu^l_n}} + \gamma^2\left(\frac{1-\beta}{2-\beta}\right)\left\{\sigma^2_{\bar{\nu^l_n}} + \sigma^4_{\bar{\nu^l_n}}\right\}\sigma^2_{\bar{\nu^l_n}}\right] \tag{C.18}$$

Using the criteria mentioned in section 6.4, EMSE of the MCLMS algorithm in presence of MAI and noise can be written as

$$\xi^{\infty}_{ZNCLMS} \approx \frac{-\left(2 + \gamma\sigma^2_{\bar{\nu^l_n}}\right) + 2\mu Tr\left(\tilde{R}\sigma^2_{\bar{\nu^l_n}}\right)\left[1 + \gamma\sigma^4_{\bar{\nu^l_n}} + \gamma^2\left(\frac{1-\beta}{2-\beta}\right)\left\{\sigma^2_{\bar{\nu^l_n}} + \sigma^4_{\bar{\nu^l_n}}\right\}\right]}{\left(2 + \gamma\sigma^2_{\bar{\nu^l_n}}\right) - 2\mu Tr\left(\tilde{R}\right)} \tag{C.19}$$

EMSE of MCLMS Algorithm

In case of MCLMS algorithm, equations (6.6.6), (6.6.7) and (6.6.9) are modified as below

$$\bar{\lambda^{\infty}_n} = \frac{\xi^{\infty}_{MCLMS} + \sigma^2_{\bar{\nu^l_n}}}{2} \tag{C.20}$$

$$\bar{\mu^{\infty}_n} = \mu\left[1 + \frac{\gamma}{2}\left(\xi^{\infty}_{MCLMS} + \sigma^2_{\bar{\nu^l_n}}\right)\right] \tag{C.21}$$

$$\overline{(\lambda_n^\infty)^2} = \frac{1}{(2-\beta)}\left[\frac{(1-\beta)}{2}\left(\xi_{MCLMS}^\infty + \sigma_{\nu_n^l}^2\right)^2 + \beta\left(\xi_{MCLMS}^\infty + \sigma_{\nu_n^l}^2\right)\sigma_{\nu_n^l}^2\right]$$

$$\begin{aligned}\overline{(\lambda_n^\infty)^2} &= \frac{1}{(2-\beta)}\Big[\frac{(1-\beta)}{2}\left(\left(\xi_{MCLMS}^\infty\right)^2 + \sigma_{\nu_n^l}^4 + 2\xi_{MCLMS}^\infty\sigma_{\nu_n^l}^2\right) \\ &\quad +\beta\left(\xi_{MCLMS}^\infty + \sigma_{\nu_n^l}^2\right)\sigma_{\nu_n^l}^2\Big] \end{aligned} \tag{C.22}$$

Constants A, B , C and D can be shown to be

$$A = -\mu\gamma^2 Tr\left(\tilde{R}\right)\left[\frac{1-\beta}{2\,(2-\beta)}\right] \tag{C.23}$$

$$B = \gamma - \mu Tr\left(\tilde{R}\right)\left[\gamma + \beta\sigma_{\nu_n^l}^2 + \gamma^2\left(\frac{1-\beta}{2-\beta}\right)\right]\sigma_{\nu_n^l}^2 \tag{C.24}$$

$$C = \left(2 + \gamma\sigma_{\nu_n^l}^2\right) - \mu Tr\left(\tilde{R}\right)\left[1 + 3\gamma\sigma_{\nu_n^l}^2 + 3\beta\sigma_{\nu_n^l}^4 + \gamma\left\{\frac{1-\beta}{2(2-\beta)}\right\}\sigma_{\nu_n^l}^2\right] \tag{C.25}$$

$$D = \left(2 + \gamma\sigma_{\nu_n^l}^2\right) - 2\mu Tr\left(\tilde{R}\right)\left[1 + \gamma\sigma_{\nu_n^l}^4 + \gamma^2\left(\frac{1-\beta}{2-\beta}\right)\left\{\sigma_{\nu_n^l}^2 + \sigma_{\nu_n^l}^4\right\}\right] \tag{C.26}$$

Using the criteria mentioned in section 6.4, EMSE of the MCLMS algorithm in presence of MAI and noise can be written as

$$\xi_{MCLMS}^\infty \approx \frac{-\left(2 + \gamma\sigma_{\nu_n^l}^2\right) + 2\mu Tr\left(\tilde{R}\right)\sigma_{\nu_n^l}^2\left[1 + \gamma\sigma_{\nu_n^l}^4 + \gamma^2\left(\frac{1-\beta}{2-\beta}\right)\left\{\sigma_{\nu_n^l}^2 + \sigma_{\nu_n^l}^4\right\}\right]}{\left(2 + \gamma\sigma_{\nu_n^l}^2\right) - 2\mu Tr\left(\tilde{R}\right)} \tag{C.27}$$

References

[1] E. T. Ar and I. E. Telatar, "Capacity of multi-antenna gaussian channels," *European Transactions on Telecommunications*, vol. 10, pp. 585–595, Nov-Dec 1999.

[2] T. Rappaport and S. B. O. (Firme), *Wireless communications: principles and practice*, vol. 2. Prentice Hall PTR Upper Saddle River (New Jersey), 1996.

[3] S. Verdu, *Multiuser detection*. Cambridge Univ Pr, 1998.

[4] K. Deng, Q. Yin, L. Ding, and Z. Zhao, "Blind channel estimator for v-blast coded ds-cdma system in frequency-selective fading environment," in *Vehicular Technology Conference, 2003. VTC 2003-Fall. 2003 IEEE 58th*, vol. 1, pp. 458 – 462 Vol.1, Oct. 2003.

[5] S. Sfar and K. Ben Letaief, "Transactions letters - layered group detection for multiuser mimo wireless cdma systems," *Wireless Communications, IEEE Transactions on*, vol. 5, pp. 2305 –2311, Sep 2006.

[6] S.-M. Tseng, "Sequential detection for multiuser mimo cdma systems with single spreading code per user," *Wireless Communications, IEEE Transactions on*, vol. 8, pp. 3492 –3497, Jul 2009.

[7] W. Choi and J. Andrews, "Spatial multiplexing in cellular mimo-cdma systems with linear receivers: Outage probability and capacity," *Wireless Communications, IEEE Transactions on*, vol. 6, pp. 2612 –2621, Jul 2007.

[8] M. Dohler, S. McLaughlin, and A. Aghvami, "Implementable wireless access for b3g networks. ii. mimo receiver architectures [topics in radio communications]," *Communications Magazine, IEEE*, vol. 45, pp. 93 –97, Mar 2007.

[9] J. Winters, "On the capacity of radio communication systems with diversity in a rayleigh fading environment," *Selected Areas in Communications, IEEE Journal on*, vol. 5, pp. 871 – 878, Jun 1987.

[10] M. Simon, B. Levitt, J. Omura, and R. Scholtz, "Spread spectrum communications. volume 1, 2 & 3," *NASA STI/Recon Technical Report A*, vol. 87, p. 10096, 1985.

[11] G. J. Foschini and M. J. Gans, "On limits of wireless communications in a fading environment when using multiple antennas," *Wireless personal communications*, vol. 6, pp. 311–335, Mar 1998.

[12] H. Huang, H. Viswanathan, and G. Foschini, "Achieving high data rates in cdma systems using blast techniques," in *Global Telecommunications Conference, 1999. GLOBECOM '99*, vol. 5, pp. 2316 – 2320 vol.5, Dec 1999.

[13] C. Belfiore and J. Park Jr, "Decision feedback equalization," *Proceedings of the IEEE*, vol. 67, no. 8, pp. 1143–1156, 1979.

[14] A. H. Sayed, *Adaptive Filters*. IEEE Press, Wiley-Interscience, 2008.

[15] C. Belfiore and J. Park Jr, "Decision feedback equalization," *Proceedings of the IEEE*, vol. 67, pp. 1143–1156, Aug 1979.

[16] M. Pursley and D. Sarwate, "Performance evaluation for phase-coded spread-spectrum multiple-access communication–part ii: Code sequence analysis," *Communications, IEEE Transactions on*, vol. 25, pp. 800 – 803, Aug 1977.

[17] J. Morrow, R.K. and J. Lehnert, "Bit-to-bit error dependence in slotted ds/ssma packet systems with random signature sequences," *Communications, IEEE Transactions on*, vol. 37, pp. 1052 –1061, Oct 1989.

[18] J. Holtzman, "A simple, accurate method to calculate spread spectrum multiple access error probabilities," in *Communications, 1991. ICC '91, Conference Record. IEEE International Conference on*, pp. 1633 –1636 vol.3, Jun 1991.

[19] B. Long, J. Hu, and P. Zhang, "Method to improve gaussian approximation accuracy for calculation of spread-spectrum multiple-access error probabilities," *Electronics Letters*, vol. 31, pp. 529 –531, Mar 1995.

[20] J. Lehnert and M. Pursley, "Error probabilities for binary direct-sequence spread-spectrum communications with random signature sequences," *Communications, IEEE Transactions on*, vol. 35, pp. 87 – 98, Jan 1987.

[21] K. Ho and P.-C. Ching, "Performance analysis of a split-path lms adaptive filter for ar modeling," *Signal Processing, IEEE Transactions on*, vol. 40, pp. 1375–1382, Mar 1992.

[22] K. Yao, "Error probability of asynchronous spread spectrum multiple access communication systems," *Communications, IEEE Transactions on*, vol. 25, pp. 803–809, Aug 1977.

[23] E. Geraniotis and M. Pursley, "Error probability for direct-sequence spread-spectrum multiple-access communications–part ii: Approximations," *Communications, IEEE Transactions on*, vol. 30, pp. 985–995, Jun 1982.

[24] M. Kavehrad, "Performance of nondiversity receivers for spread spectrum in indoor wireless communications," *AT&T technical journal*, vol. 64, pp. 1181–1210, Aug 1985.

[25] M. O. Sunay and P. J. McLane, "Calculating error probabilities for ds-cdma systems: When not to use the gaussian approximation," in *Global Telecommunications Conference, 1996. GLOBECOM'96.'Communications: The Key to Global Prosperity*, vol. 3, pp. 1744–1749, IEEE, Nov 1996.

[26] D. Borth and M. Pursley, "Analysis of direct-sequence spread-spectrum multiple-access communication over rician fading channels," *Communications, IEEE Transactions on*, vol. 27, pp. 1566–1577, Oct 1979.

[27] C. Gardner and J. Orr, "Fading effects on the performance of a spread spectrum multiple access communication system," *Communications, IEEE Transactions on*, vol. 27, pp. 143–149, Jan 1979.

[28] E. Geraniotis, "Direct-sequence spread-spectrum multiple-access communications over nonselective and frequency-selective rician fading channels," *Communications, IEEE Transactions on*, vol. 34, pp. 756–764, Aug 1986.

[29] M. O. Sunay and P. J. McLane, "Probability of error for diversity combining in ds cdma systems with synchronization errors," *European transactions on telecommunications*, vol. 9, pp. 449–463, Sep 1998.

[30] J. Cheng and N. C. Beaulieu, "Accurate ds-cdma bit-error probability calculation in rayleigh fading," *Wireless Communications, IEEE Transactions on*, vol. 1, pp. 3–15, Jan 2002.

[31] J. Lehnert and M. Pursley, "Error probabilities for binary direct-sequence spread-spectrum communications with random signature sequences," *Communications, IEEE Transactions on*, vol. 35, pp. 87–98, Jan 1987.

[32] W. M. Jang, L. Nguyen, and P. Bidarkar, "Mai and ici of synchronous downlink mc-cdma with frequency offset," *Wireless Communications, IEEE Transactions on*, vol. 5, pp. 693–703, Mar 2006.

[33] M. Moinuddin, a. U. H. Sheikh, A. Zerguine, and M. Deriche, "A Unified Approach to BER Analysis of Synchronous Downlink CDMA Systems with Random Signature Sequences in Fading Channels with Known Channel Phase," *EURASIP Journal on Advances in Signal Processing*, vol. 2008, pp. 1–13, Mar 2008.

[34] J. O. Mark, M. N. M. Saad, and B. Samir, "Average ber perfomance and spectral efficiency for mimo orthogonal mc ds-cdma system over nakagami-m fading channels," in *National Postgraduate Conference (NPC), 2011*, pp. 1–6, IEEE, Sep 2011.

[35] P. Li, R. C. de Lamare, and R. Fa, "Multiple feedback successive interference cancellation detection for multiuser mimo systems," *Wireless Communications, IEEE Transactions on*, vol. 10, pp. 2434–2439, Aug 2011.

[36] G. Kaddoum, M. Coulon, D. Roviras, and P. Chargé, "Theoretical performance for asynchronous multi-user chaos-based communication systems on fading channels," *Signal Processing*, vol. 90, pp. 2923–2933, Nov 2010.

[37] G. Stuber, J. Barry, S. Mclaughlin, Y. Li, M. Ingram, and T. Pratt, "Broadband mimo-ofdm wireless communications," *Proceedings of the IEEE*, vol. 92, pp. 271–294, Feb 2004.

[38] X. Zhu and R. Murch, "Layered space-frequency equalization in a single-carrier mimo system for frequency-selective channels," *Wireless Communications, IEEE Transactions on*, vol. 3, pp. 701–708, May 2004.

[39] X. Zhu and R. Murch, "Layered space-frequency equalization in a single-carrier mimo system for frequency-selective channels," *Wireless Communications, IEEE Transactions on*, vol. 3, pp. 701–708, May 2004.

[40] R. Dinis, R. Kalbasi, D. Falconer, and A. Banihashemi, "Iterative layered space-time receivers for single-carrier transmission over severe time-dispersive channels," *Communications Letters, IEEE*, vol. 8, pp. 579–581, May 2004.

[41] N. Al-Dhahir and A. Sayed, "The finite-length multi-input multi-output mmse-dfe," *Signal Processing, IEEE Transactions on*, vol. 48, pp. 2921–2936, Oct 2000.

[42] S. Chen, L. Hanzo, and A. Livingstone, "MBER space-time decision feedback equalization assisted multiuser detection for multiple antenna aided SDMA systems," *Signal Processing, IEEE Transactions on*, vol. 54, pp. 3090–3098, Mar 2006.

[43] R. C. de Lamare and R. Sampaio-Neto, "Adaptive MBER decision feedback multiuser receivers in frequency selective fading channels," *Communications Letters, IEEE*, vol. 7, pp. 73–75, Feb 2003.

[44] A. Maleki-Tehrani, B. Hassibi, and J. M. Cioffi, "Adaptive equalization of multiple-input multiple-output (MIMO) channels," in *Communications, 2000. ICC 2000. 2000 IEEE International Conference on*, vol. 3, pp. 1670–1674, IEEE, Jun 2000.

[45] V. Kekatos, A. Rontogiannis, and K. Berberidis, "Cholesky factorization-based adaptive blast dfe for wideband mimo channels," *EURASIP Journal on Applied Signal Processing*, vol. 2007, pp. 132–132, Jan 2007.

[46] V. Kekatos, K. Berberidis, and A. A. Rontogiannis, "A block adaptive frequency domain MIMO DFE for wideband channels," vol. 3, pp. 197–200, IEEE, Apr 2007.

[47] A. S. Lalos, V. Kekatos, and K. Berberidis, "Adaptive conjugate gradient DFEs for wideband MIMO systems," *Signal Processing, IEEE Transactions on*, vol. 57, pp. 2406–2412, Jun 2009.

[48] D. P. Palomar, J. M. Cioffi, and M. A. Lagunas, "Joint Tx-Rx beamforming design for multicarrier MIMO channels: A unified framework for convex optimization," *Signal Processing, IEEE Transactions on*, vol. 51, pp. 2381–2401, Sep 2003.

[49] Y. Jiang, D. Palomar, and M. Varanasi, "Precoder optimization for nonlinear mimo transceiver based on arbitrary cost function," in *Information Sciences and Systems, 2007. CISS'07. 41st Annual Conference on*, pp. 119–124, IEEE, Mar 2007.

[50] D. Palomar and Y. Jiang, "Mimo transceiver design via majorization theory," *Foundations and Trends in Communications and Information Theory*, vol. 3, pp. 331–551, Nov 2006.

[51] M. Shenouda and T. Davidson, "A design framework for limited feedback MIMO systems with zero-forcing DFE," *IEEE Journal on Selected Areas in Communications*, vol. 26, pp. 1578–1587, Oct 2008.

[52] D. Love, R. Heath Jr, W. Santipach, and M. Honig, "What is the value of limited feedback for mimo channels?," *Communications Magazine, IEEE*, vol. 42, pp. 54–59, Oct 2004.

[53] A. Narula, M. Lopez, M. Trott, and G. Wornell, "Efficient use of side information in multiple-antenna data transmission over fading channels," *Selected Areas in Communications, IEEE Journal on*, vol. 16, pp. 1423–1436, Oct 1998.

[54] D. Love, R. Heath Jr, and T. Strohmer, "Grassmannian beamforming for multiple-input multiple-output wireless systems," *Information Theory, IEEE Transactions on*, vol. 49, pp. 2735–2747, Oct 2003.

[55] W. Santipach and M. L. Honig, "Asymptotic performance of mimo wireless channels with limited feedback," in *Military Communications Conference, 2003. MILCOM'03. 2003 IEEE*, vol. 1, pp. 141–146, IEEE, Oct 2003.

[56] J. Roh and B. Rao, "Transmit beamforming in multiple-antenna systems with finite rate feedback: A vq-based approach," *Information Theory, IEEE Transactions on*, vol. 52, pp. 1101–1112, Mar 2006.

[57] D. J. Love and R. W. Heath, "Limited feedback unitary precoding for spatial multiplexing systems," *Information Theory, IEEE Transactions on*, vol. 51, pp. 2967–2976, Aug 2005.

[58] D. Love and R. Heath Jr, "Limited feedback unitary precoding for orthogonal space-time block codes," *Signal Processing, IEEE Transactions on*, vol. 53, pp. 64–73, Jan 2005.

[59] G. Jongren and M. Skoglund, "Quantized feedback information in orthogonal space-time block coding," *Information Theory, IEEE Transactions on*, vol. 50, pp. 2473–2486, Oct 2004.

[60] Y. Bae and J. Lee, "Antenna selection for mimo systems with sequential nulling and cancellation," in *Information Sciences and Systems, 2006 40th Annual Conference on*, pp. 745–749, IEEE, Mar 2006.

[61] Y. Jiang and M. K. Varanasi, "A novel spatial multiplexing architecture with finite rate feedback," in *Information Sciences and Systems, 2006 40th Annual Conference on*, pp. 755–760, IEEE, Nar 2006.

[62] J. Nagumo and A. Noda, "A learning method for system identification," *Automatic Control, IEEE Transactions on*, vol. 12, pp. 282–287, Mar 1967.

[63] A. Zerguine, "Convergence behavior of the normalized least mean fourth algorithm," *Signals, Systems and Computers, 2000. Conference Record of the Thirty-Fourth Asilomar Conference on*, vol. 1, Nov 2000.

[64] Y. Wei, S. B. Gelfand, and J. V. Krogmeier, "Noise-constrained least mean squares algorithm," *Signal Processing, IEEE Transactions on*, vol. 49, pp. 1961–1970, Apr 2001.

[65] M. Moinuddin, A. Zerguine, and A. U. H. Sheikh, "Multiple-Access Interference Plus Noise-Constrained Least Mean Square (MNCLMS) Algorithm for CDMA Systems," *IEEE Transactions on Circuits and Systems I: Regular Papers*, vol. 55, pp. 2870–2883, Oct 2008.

[66] S. Chen, B. Mulgrew, E. Chng, and G. Gibson, "Space translation properties and the minimum-ber linear-combiner dfe," in *Communications, IEE Proceedings-*, vol. 145, pp. 316–322, IET, Oct 1998.

[67] E. Telatar, "Capacity of multi-antenna Gaussian channels," *European Transactions on Telecommunications*, vol. 10, pp. 585–595, Nov-Dec 1999.

[68] A. Burr, "Capacity bounds and estimates for the finite scatterers MIMO wireless channel," *IEEE Journal on Selected Areas in Communications*, vol. 21, pp. 812–818, Jun 2003.

[69] B. B. S. J. O. Mark and M. Naufal, "Average channel capacity for MIMO orthogonal MC DS-CDMA system in Nakagami-m fading environment," in *IEEE 13th International Conference on Communication Technology (ICCT)*, pp. 445–450, Sep 2011.

[70] M. N. J. O. Mark and B. B. Samir, "Average BER perfomance and spectral efficiency for MIMO orthogonal MC DS-CDMA system over Nakagami-m fading channels," in *National Postgraduate Conference (NPC), 2011*, pp. 1–6, Sep 2011.

[71] R. C. D. L. P. Li and R. Fa, "Multiple Feedback Successive Interference Cancellation Detection for Multiuser MIMO Systems," *IEEE Transactions on Wireless Communications*, vol. 10, pp. 2434 – 2439, Aug 2011.

[72] P. T. C. W. Huang and C. Huang, "A Novel Message Passing Based MIMO-OFDM Data Detector with a Progressive Parallel ICI Canceller," *IEEE Transactions on Wireless Communications*, vol. 10, pp. 1260 – 1268, Apr 2011.

[73] Gradshteyn and Ryzhik, *Table of Integrals, Series, and Products*. Alan Jeffrey and Daniel Zwillinger (eds.), Seventh edition, Feb, 2007.

[74] Chaudhry, M. Aslam, Zubair, Syed M, *On A Class Of Incomplete Gamma Functions with Applications*. Chapman & Hall\CRC, 2002.

[75] C. D'Amours and A. O. Dahmane, "Bit error rate performance of a mimo-cdma system employing parity-bit-selected spreading in frequency nonselective rayleigh fading," *International Journal of Antennas and Propagation*, vol. 2011, Jun 2011.

[76] J. Hu, S. Member, and N. C. Beaulieu, "Accurate Simple Closed-Form Approximations to Rayleigh Sum Distributions and Densities," vol. 9, pp. 109–111, Feb 2005.

[77] A. U. H. Sheikh and F. Hendessi, "FRESH-DFE: A New Structure for Interference Cancellation," *Wireless Personal Communications*, vol. 44, pp. 101–118, Sep 2007.

[78] M. Abdulrahman and D. D. Falconer, "Cyclostationary crosstalk suppression by decision feedback equalization on digital subscriber loops," *Selected Areas in Communications, IEEE Journal on*, vol. 10, pp. 640–649, Apr 1992.

[79] J. G. Proakis, *Intersymbol Interference in Digital Communication Systems*. Wiley Online Library, 1995.

[80] W. A. Brown, "On the theory of cyclostationary signals," *Signal Processing*, vol. 18, p. 229, Jan 1989.

[81] R. M. Buehrer, A. Kaul, S. Striglis, and B. D. Woerner, "Analysis of ds-cdma parallel interference cancellation with phase and timing errors," *Selected Areas in Communications, IEEE Journal on*, vol. 14, pp. 1522–1535, Oct 1996.

[82] M. Abdulrahman, A. U. Sheikh, and D. D. Falconer, "Decision feedback equalization for cdma in indoor wireless communications," *Selected Areas in Communications, IEEE Journal on*, vol. 12, pp. 698–706, May 1994.

[83] F. Hendessi, H. Hafez, and a.U.H. Sheikh, "The structure and performance of FRESH-decision feedback equalizer in the presence of adjacent channel interference," *IEEE 43rd Vehicular Technology Conference*, pp. 641–644, May 1993.

[84] J. Cui, D. D. Falconer, and A. U. Sheikh, "Performance evaluation of optimum combining and maximal ratio combining in the presence of co-channel interference and channel correlation for wireless communication systems," *Mobile Networks and Applications*, vol. 2, pp. 315–324, Dec 1997.

[85] J. Cui, D. D. Falconer, and A. U. Sheikh, "Sinr of antenna array with a large number of interfering users," in *Vehicular Technology Conference, 1996.'Mobile Technology for the Human Race'., IEEE 46th*, vol. 3, pp. 1486–1490, IEEE, May 1996.

[86] R. Lucky, *Techniques for adaptive equalization of digital communication systems*. American Telephone and Telegraph Company, Jul 1966.

[87] P. Monsen, "Feedback equalization for fading dispersive channels," *Information Theory, IEEE Transactions on*, vol. 17, pp. 56–64, Jan 1971.

[88] P. Monsen, "Adaptive equalization of the slow fading channel," *Communications, IEEE Transactions on*, vol. 22, pp. 1064–1075, Aug 1974.

[89] A. Bentrcia, A. Sheikh, and A. Zerguine, "A new ordering and grouping algorithm for the linear weighted group matched filter successive interference cancellation detector," *Vehicular Technology, IEEE Transactions on*, vol. 55, pp. 704–709, Mar 2006.

[90] J. Cui, D. D. Falconer, and A. U. Sheikh, "Blind adaptation of antenna arrays using a simple algorithm based on small frequency offsets," *Communications, IEEE Transactions on*, vol. 46, pp. 61–70, Jul 1998.

[91] W. A. Gardner, *Introduction to Random Processes: with applications to signals and systems*, vol. 31. McGraw-Hill New York, 1990.

[92] B. W. Kozminchuk and A. U. Sheikh, "A kalman filter-based architecture for interference excision," *Communications, IEEE Transactions on*, vol. 43, pp. 574–580, Feb 1995.

[93] W. A. Gardner, "Cyclic wiener filtering: theory and method," *Communications, IEEE Transactions on*, vol. 41, pp. 151–163, Jan 1993.

[94] J. Cui, D. D. Falconer, and A. U. Sheikh, "A phase algorithm for blind adaptive optimum diversity combining," in *Vehicular Technology Conference, 1995 IEEE 45th*, vol. 1, pp. 414–418, IEEE, Jul 1995.

[95] K. Ho and P.-C. Ching, "Performance analysis of a split-path lms adaptive filter for ar modeling," *Signal Processing, IEEE Transactions on*, vol. 40, pp. 1375–1382, Mar 1992.

[96] P. C. Ching and K. Wan, "A unified approach to split structure adaptive filtering," in *Circuits and Systems, 1995. ISCAS'95., 1995 IEEE International Symposium on*, vol. 3, pp. 1604–1607, IEEE, Apr 1995.

[97] L. S. Resende, J. M. T. Romano, and M. G. Bellanger, "Adaptive split transversal filtering: a linearly-constrained approach," in *Adaptive Systems for Signal*

Processing, Communications, and Control Symposium 2000. AS-SPCC. The IEEE 2000, pp. 213–217, IEEE, Oct 2000.

[98] W. Saif, A. Zerguine, A. Sheikh, and M. Bellanger, "Performance of multi-split decision feedback equalizer," in *Personal, Indoor and Mobile Radio Communications, 2002. The 13th IEEE International Symposium on*, vol. 4, pp. 1703–1707, IEEE, Sep 2002.

[99] M. Shenouda and T. Davidson, "A framework for designing mimo systems with decision feedback equalization or tomlinson-harashima precoding," in *Acoustics, Speech and Signal Processing Conference*, vol. 3, pp. III–209, IEEE, Feb 2007.

[100] E. Visotsky and U. Madhow, "Space-time transmit precoding with imperfect feedback," *Information Theory, IEEE Transactions on*, vol. 47, pp. 2632–2639, Sep 2001.

[101] K. Mukkavilli, A. Sabharwal, E. Erkip, and B. Aazhang, "On beamforming with finite rate feedback in multiple-antenna systems," *Information Theory, IEEE Transactions on*, vol. 49, pp. 2562–2579, Oct 2003.

[102] P. Xia and G. Giannakis, "Design and analysis of transmit-beamforming based on limited-rate feedback," *Signal Processing, IEEE Transactions on*, vol. 54, pp. 1853–1863, May 2006.

[103] Y. Wei, S. B. Gelfand, and J. V. Krogmeier, "Noise constrained lms algorithm," in *Acoustics, Speech, and Signal Processing, 1997. ICASSP-97., 1997 IEEE International Conference on*, vol. 3, pp. 2353–2356, IEEE, Apr 1997.

[104] R. C. Bilcu, P. Kuosmanen, and C. Rusu, "A noise constrained vs-lms algorithm," in *EUROCOMM 2000. Information Systems for Enhanced Public Safety and Security. IEEE/AFCEA*, pp. 29–33, IEEE, Apr 2000.

[105] S. Woo-Jin, "A complementary pair lms algorithm for adaptive filtering," *IEICE TRANSACTIONS on Fundamentals of Electronics, Communications and Computer Sciences*, vol. 81, pp. 1493–1497, Jul 1998.

[106] S. Woo-Jin, "A complementary pair lms algorithm for adaptive filtering," *IEICE TRANSACTIONS on Fundamentals of Electronics, Communications and Computer Sciences*, vol. 81, pp. 1493–1497, Jul 1998.

[107] D. G. Luenberger, *Linear and nonlinear programming*. Springer, 2003.

[108] X. H. Nguyen and J. Choi, "On the constrained MMSE decision feedback equalization for MIMO wireless systems," *Communications, 2005 Asia-Pacific Conference on*, pp. 329–333, Oct 2005.

[109] G. Latouche, D. Pirez, and P. Vila, "MMSE Cyclic Equalization," *Military Communications Conference, 1998. MILCOM 98. Proceedings., IEEE*, vol. 1, pp. 150–154, Oct 2002.

[110] Y. Lee and W. R. Wu, "Adaptive channel aided decision feedback equalisation for SISO and MIMO systems," *Communications, IEE Proceedings-*, vol. 153, pp. 657–663, Jul 2006.

[111] A. J. Paulraj and B. C. Ng, "Space-time modems for wireless personal communications," *Personal Communications, IEEE*, vol. 5, pp. 36–48, Feb 1998.

[112] S. Chen, L. Hanzo, and B. Mulgrew, "Adaptive minimum symbol-error-rate decision feedback equalization for multilevel pulse-amplitude modulation," *Signal Processing, IEEE Transactions on*, vol. 52, pp. 2092–2101, Jul 2004.

[113] B.-s. Chen, C.-l. Tsai, and C.-s. Hsu, "Robust adaptive MMSE/DFE multiuser detection in multipath fading channel with impulse noise," *IEEE Transactions on Signal Processing*, vol. 53, pp. 306–317, Jan 2005.

[114] R. Irmer, R. Habendorf, W. Rave, and G. Fettweis, "Overloaded tdd-cdma cells with multiuser transmission," in *Smart Antennas, 2004. ITG Workshop on*, pp. 235–242, IEEE, Mar 2004.

[115] J. Wehinger, V. Anreddy, C. Mecklenbrauker, S. Paul, and C. Antón-Haro, "Adaptive minimum bit error rate space-time rake receiver for the uplink of umts frequency division duplex mode," in *Signal Processing and Information Technology, 2003. ISSPIT 2003. Proceedings of the 3rd IEEE International Symposium on*, pp. 294–297, IEEE, Dec 2003.

[116] N. Al-dhahir, S. Member, and A. H. Sayed, "The Finite-Length Multi-Input Multi-Output," *October*, vol. 48, pp. 2921–2936, Oct 2000.

[117] N. Al-Dhahir and J. M. Cioffi, "Fast computation of channel-estimate based equalizers in packet data transmission," *Signal Processing, IEEE Transactions on*, vol. 43, pp. 2462–2473, Nov 1995.

[118] H. Lev-Ari and T. Kailath, "Triangular factorization of structured hermitian matrices," *Operator Theory: Advances and Applications*, vol. 18, pp. 301–324, Mar 1986.

[119] R. Merched and N. R. Yousef, "Fast techniques for computing finite-length mimo mmse decision feedback equalizers," *Signal Processing, IEEE Transactions on*, vol. 54, pp. 701–711, Feb 2006.

[120] A. Sayed and T. Kailath, "A state-space approach to adaptive rls filtering," *Signal Processing Magazine, IEEE*, vol. 11, pp. 18–60, Jul 1994.

[121] M. Moinuddin, A. Zerguine, and A. Sheikh, "Multiple-access interference plus noise-constrained least mean square (mnclms) algorithm for cdma systems," *Circuits and Systems I: Regular Papers, IEEE Transactions on*, vol. 55, pp. 2870–2883, Oct 2008.

[122] S. Haykin, "Adaptive filter theory-3/e.," 1996.

[123] M. B. Pursley, "Performance evaluation for phase-coded spread-spectrum multiple-access communication. i-system analysis," *IEEE Transactions on communications*, vol. 25, pp. 795–799, Aug 1977.

[124] L. Horowitz and K. Senne, "Performance advantage of complex lms for controlling narrow-band adaptive arrays," *Circuits and Systems, IEEE Transactions on*, vol. 28, pp. 562–576, Jun 1981.

[125] R. H. Kwong and E. W. Johnston, "A variable step size LMS algorithm," *Signal Processing, IEEE Transactions on [see also Acoustics, Speech, and Signal Processing, IEEE Transactions on]*, vol. 40, pp. 1633–1642, Jul 1992.

[126] A. Dembo, "Bounds on the extreme eigenvalues of positive-definite toeplitz matrices," *Information Theory, IEEE Transactions on*, vol. 34, pp. 352–355, Mar 1988.

[127] F. Riera-Palou, J. M. Noras, and D. G. Cruickshank, "Analysis of the decision delay effect on the convergence of gradient recursive decision feedback equalizers," in *Acoustics, Speech, and Signal Processing (ICASSP), 2002 IEEE International Conference on*, vol. 3, pp. III–2665, IEEE, May 2002.

[128] A. H. Sayed, *Adaptive filters*. Wiley. com, 2008.

[129] N. J. Bershad, "On error-saturation nonlinearities in lms adaptation," *Acoustics, Speech and Signal Processing, IEEE Transactions on*, vol. 36, pp. 440–452, Apr 1988.

[130] N. J. Bershad and M. Bonnet, "Saturation effects in lms adaptive echo cancellation for binary data," *Acoustics, Speech and Signal Processing, IEEE Transactions on*, vol. 38, pp. 1687–1696, Oct 1990.

[131] B. Widrow, J. M. McCool, M. G. Larimore, and C. R. Johnson Jr, "Stationary and nonstationary learning characteristics of the lms adaptive filter," *Proceedings of the IEEE*, vol. 64, pp. 1151–1162, Aug 1976.

[132] N. R. Yousef and A. H. Sayed, "A unified approach to the steady-state and tracking analyses of adaptive filters," *Signal Processing, IEEE Transactions on*, vol. 49, pp. 314–324, Feb 2001.